

---

# Investigation of loading techniques to create thoracolumbar burst fractures

Joseph Mwiseneza

Masters thesis (18 - units)

October 2018

Supervisor

A/Professor John Costi

Submitted to College of Science and Engineering in partial fulfilment of the requirements for the degree of Bachelor of Engineering Mechanical (Honours)/Master of Engineering Biomedical at Flinders University - Adelaide Australia.

---

## DECLARATION

I certify that this work does not incorporate without acknowledgment any material previously submitted for a degree or diploma in any university; and that to the best of my knowledge and belief it does not contain any material previously published or written by another person except where due reference is made in the text.

Signed 23 October 2018

By Joseph Mwiseneza

### **ACKNOWLEDGEMENTS:**

I would like to thank my family particularly my wife Gisele for her support and encouragement and my children Joshua and Jessica for their patients and understanding during the long hours spent away working on this thesis.

I would also like to extend my Sincere thanks to my supervisor A/Professor John Costi for his guidance and support using x-ray and mentorship during the whole process of this project, Dr Saulo Martelli for allowing me to use his load cell, Dr Reza Oskouei for loaning me his drop tower, Surgeon Rob Kuru for his input dissecting some of the specimen during the analysis of pilot tests. would also like to thank Ms Dhara for her help with x-ray, Michael and Daniel's assistance during the testing stage and PhD student Marco Palanca for his great input during the pilot testing and helping to use a high-speed camera during the pilot tests.

I would also like to thank the Engineering Services team for their great help during the testing process, Richard Stanley for helping to cut my specimens with a bandsaw and making sure the drop tower was in good condition and Fiona Cramer and Craig Dawson helping to set up Labview software.

Finally, I would like to give many thanks to Stephen Keen for his mentorship, encouragement and his great work of proof reading my thesis report.

---

## ABSTRACT

Thoracolumbar burst fracture is one of the spine fractures that is mainly found in people falling from high heights, especially young active people aged between 14 and 24 years who participate in activities requiring to jump from a height of more than 2 m and landing on their feet or buttocks. These fractures often lead to problems including medical conditions, inability to participate in social activities or cessation of employment leading to financial crisis. Many studies have been performed to investigate a proper treatment method; however, there is no consensus yet. The present study was directed with the first aim of investigating loading techniques to create reproducible thoracolumbar burst fractures and with a second aim of comparing the results with clinical cases examined in the literature review. Twenty-four sheep specimens were divided into three groups of eight, where each group represented different spinal levels (T12-L1, T12-L2, and T13-L2). The T12-L1 and T13-L2 groups had a single unconstrained vertebra while the T12-L2 group had two unconstrained vertebrae. All the specimens were struck axially by a high-speed impact drop tower. The results were analysed by observing the nature of the fractures produced and matching them with their x-ray images, to determine where the fractures initiated, and the energy and forces used for their production. The results were validated by comparing with the findings from the literature. The maximum energy used was 140 joules while the fracture force across all groups varied between 2369 N and 6506 N. The results from the T12-L2 group showed six burst fractures at T13 and two burst fractures at L1. The group of T12-L1 showed six burst fractures at T13, while the T13-L2 group produced five burst fractures only. The rest of specimens in the single unconstrained vertebrae groups had some fractures, but these were not classified as the burst fractures. A univariate ANOVA revealed no significant difference in fracture load between each group ( $p = 0.194$ ). To gain further insight into the results, the fracture load was normalised by the impact energy, and the impact energy and disc area, both of which were not significantly different ( $p > 0.205$ ). Some of the limitations of this experiment include the height of the drop tower, the loadcell that was only designed for axial impact, the sheep specimens grew up in different environments and had an unknown age, and no human specimens were available for this study to compare the results with.

---

This study has shown that by testing multilevel FSU (T13-L1), the chance of fracture is higher in T13 than L1 and by comparing with the literature, the required force to create Thoracolumbar burst fracture was found to be higher in sheep than human spines. This study should be developed further using human specimens with an increased height of the drop tower, using a 6DOF loadcell and a camera to observe the motion of bone fragments in the spinal canal.

---

## Table of Contents

<b>DECLARATION</b> .....	<b>ii</b>
<b>ACKNOWLEDGEMENTS:</b> .....	<b>iii</b>
<b>ABSTRACT</b> .....	<b>iv</b>
<b>Notation</b> .....	<b>xiii</b>
<b>1. Introduction</b> .....	<b>1</b>
1.1 <i>Background</i> .....	1
1.2 <i>Scope</i> .....	2
1.3 <i>Outline of the study</i> .....	2
<b>2. Literature review</b> .....	<b>4</b>
2.1 <i>The anatomy of thoracolumbar burst fracture</i> .....	4
2.1.1 Structural composition of both thoracic and lumbar vertebrae .....	5
2.1.2 Vertebral body.....	8
2.1.3 Intervertebral disc .....	8
2.2 <i>Thoracolumbar Burst Fracture</i> .....	11
2.2.1 Cause of thoracolumbar burst fracture .....	11
2.2.2 Problems and clinical significance of thoracolumbar burst fractures.....	12
2.3 <i>Previous methods and testing equipment</i> .....	13
2.3.1 Method of drop tower .....	14
2.3.2 Gravitational and hammer impact method .....	16
2.3.3 Pendulum method .....	17
2.3.4 Hybrid cadaveric simulation .....	19
2.3.5 Flinders Hexapod .....	22
2.3.6 Flinders drop tower .....	24
<b>3. Aims</b> .....	<b>24</b>
3.1 <i>Updated aims</i> .....	25
<b>4. Current testing methods</b> .....	<b>26</b>
4.1 <i>Sheep specimens</i> .....	26
4.2 <i>Specimen preparation</i> .....	26
4.3 <i>Specimen potting</i> .....	31
4.4 <i>Testing procedure</i> .....	33
4.4.1 <i>Pilot testing</i> .....	34

---

4.4.2 Final tests.....	35
4.4.3 X-ray imaging.....	36
4.4.4 Statistical analysis.....	36
<b>5. Results.....</b>	<b>36</b>
5.1 Geometrical measurement results of all three specimen groups.....	36
5.2 Force and energy required to produce burst fractures.....	38
5.3 Impact of free vertebrae's geometry on fracture forces.....	40
5.4 Fracture results of all FSUs and observation.....	40
5.4.1 Fracture results of T12-L1.....	42
5.4.2 Fractures of T13-L2.....	42
5.4.3 Group of multilevel free vertebrae (T12-L2).....	43
5.4.4 Visual examination of fractures.....	43
5.4.5 Classification of burst fractures based on the observation and X-ray images.....	44
5.5 Comparison of the result in all three groups and the literature.....	44
5.5.1 Forces comparison.....	44
5.5.2 Statistical comparison.....	47
<b>6. Discussion.....</b>	<b>48</b>
6.1.1 Comparison of the results with the Literature.....	48
6.2 Limitations.....	50
6.3 Recommendation for future research.....	51
<b>7. Conclusion.....</b>	<b>51</b>
<b>8. References.....</b>	<b>53</b>
<b>Appendices.....</b>	<b>57</b>
Appendix A.....	57
Appendix B.....	71
Appendix C.....	80
Appendix D.....	104

---

FIGURE

2-1: IMAGE OF THE ENTIRE HUMAN SPINE SHOWING ALL ITS SEGMENTS: CERVICAL (ORANGE), THORACIC (BLUE) AND LUMBAR (YELLOW). THE THORACOLUMBAR SEGMENT IS SHOWN BY THE EXTERNAL CURLY BRACKET AND THE THORACOLUMBAR JUNCTION BY INTERNAL CURLY BRACKET (THE VERTEBRAL COLUMN | BOUNDLESS ANATOMY AND PHYSIOLOGY, 2017). ..... 5

FIGURE 2-2: STRUCTURAL COMPOSITION OF VERTEBRAL IN BOTH TRANSVERSE AND SAGITTAL VIEW. THIS PICTURE SHOWS THE LOCATION OF ALL PARTS AS DESCRIBED ABOVE (ADAM 2013). ..... 6

FIGURE 2-3: STRUCTURAL COMPOSITION OF THE LUMBAR REGION IN LATERAL ANTEROPOSTERIOR AND ANTERIOR AND POSTERIOR VIEW (ADAM 2013). ..... 7

FIGURE 2-4 - SIDE VIEW OF THE VERTEBRAL BODY (A) AND SEMI COLUMNAR FROM TOP VIEW OF THE VERTEBRAL (B). THEIR STRUCTURAL COMPOSITION ASSISTS IN RESISTING THE AXIAL COMPRESSION (ADAM 2013). ..... 8

FIGURE 2-5: THE STRUCTURE OF THE INTERVERTEBRAL DISC BETWEEN TWO VERTEBRAL BODIES. IT IS SURROUNDED BY LIGAMENTS THAT CONNECT THE END PLATES OF BOTH THE ADJACENT VERTEBRAL BODIES (ADAMS 2013). ..... 9

FIGURE 2-6: THE ANNULUS FIBRES OF INTERVERTEBRAL DISC AND ITS STRUCTURAL COMPOSITION. THE DISC INDICATES THE COMPRESSIVE FORCES (DOWNWARDS ARROWS(C)) AND A RESTRAINING STRESS OR TENSION BY THE RED ARROWS(T) (ADAMS 2013). ..... 10

FIGURE 2-7 BURST FRACTURE OF L1 (OBERKIRCHER ET AL. 2016) ..... 11

FIGURE 2-8: DROP TOWER TESTING APPARATUS SHOWING THE IMPACTOR, GUIDED MASS, FLEXION CONSTRAINT AND LATERAL CONSTRAINT. THIS DROP TOWER WAS USED MULTIPLE TIMES TO CREATE BURST FRACTURE WITHOUT CHANGING ITS MASS (JONES ET AL. 2011). ..... 15

FIGURE 2-9: TESTING APPARATUS CONTAINING A GUIDED TUBE, BRACING PIECE, CYLINDRICAL BARRIER BLOCK, LIMITING ROD, DENTAL PLASTER CUP BASE PLATE AND A MANIPULATOR (ZHANG ET AL. 2017) ..... 17

FIGURE 2-10: METHOD OF TESTING USING A HAMMER, HIGH SPEED CAMERA AND IMPACTOR (GERMANEAU ET AL. 2017) ..... 18

FIGURE 2-11: TESTING TECHNIQUE THAT UTILIZES A DUMMY SIMULATING A REAL-LIFE FALL FROM A



---

FIGURE

HEIGHT. IT POSSESSES LOAD CELLS, SPECIMEN, AND WIRES TO HOLD THE PIECES TOGETHER,  
TRUNK AND PELVIS (IVANCIC, PAUL C 2013). ..... 21

FIGURE 2-12: FLINDERS HEXAPOD 6 DOF ROBOT. IT IS USED TO TEST SPECIMENS IN SIX DEGREES  
OF FREEDOM. IT CAN APPLY COMPRESSIVE OR EXTENSIVE FORCES (BOYIN ET AL. 2011). .... 25

FIGURE 4-1 - FRESH UNCLEAN THORACOLUMBAR WITH THREE THORACIC AND THREE LUMBAR  
VERTEBRAE. .... 28

vii

4-2 - EQUIPMENT USED TO CLEAN THE SPECIMENS. .... 29

FIGURE 4-3 - SPECIMENS WITH REMOVED SOFT TISSUES, WRAPPED IN PAPER TOWELS, SPRAYED  
WITH NORMAL SALINE AND THEN ZIPPED IN PLASTIC BAGS. .... 30

FIGURE 4-4 - SHEEP SPECIMEN WITH REMOVED SOFT TISSUES AND CUT AT T12 L1 USING A  
BANDSAW. .... 31

FIGURE 4-5 - MEASURING THE HEIGHTS AND DISCS OF THE SPECIMEN WITH A CALLIPER ..... 32

FIGURE 4-6 - SPECIMEN IN THE GROUP OF T13-L1 THAT IS READY TO BE POTTED. IT IS HELD IN THE  
CENTRE OF THE CUP BY THREE SCREWS..... 33

FIGURE 4-7 - L2 OF THE SPECIMEN POTTED IN THE BOTTOM CUP USING PMMA AND MONOMER  
LIQUID. .... 33

FIGURE 4-8 - SPECIMEN MOUNT ON THE BASE OF THE DROP TOWER AND ALIGNED WITH THE  
IMPACTOR LOAD CELL. .... 34

FIGURE 4-9 - VARIATION IN PILOT TESTING AND THE OUTCOME. AN IMPACT MASS OF 28.5KG  
SHOWED A HIGHER CHANCE OF PRODUCING A REPRODUCIBLE BURST FRACTURE. .... 36

FIGURE 4-10 - TOTAL NUMBER OF REQUIRED SPECIMENS AND ITS SUBDIVISION. .... 36

FIGURE 5-1 A) REPRESENTS THE BURST FRACTURE X-RAY IMAGE OF T12-L1, B) THE BURST  
FRACTURE AND C) THE MATLAB PLOT SHOWING THE CORRESPONDING FORCES APPLIED ON  
IMPACT..... 43

FIGURE 5-2 COMPARISON OF MEAN VALUE FORCES BASED ON EIGHT SPECIMENS IN EACH GROUP.

---

FIGURE

F

..... 47

FIGURE 5-3 COMPARISON OF FORCES BY DIVIDING THE MEAN VALUES OF FORCES BY MEAN VALUES OF ENERGIES. .... 48

FIGURE 5-4 COMPARISON OF T13, T13-L1 AND L1 BASED ON THE MEAN VALUES OF STRESSES DIVIDED BY THE MEAN VALUES OF ENERGIES ..... 49

FIGURE 8-1: SPECIMEN AND TOOLS USED TO REMOVE SOFT TISSUES ..... 59

FIGURE 8-2: BANDSAW USED TO CUT THE SPECIMENS TO THE REQUIRED SIZES ..... 60

FIGURE 8-3: SPECIMENS SPRAYED WITH NORMAL SALINE, WRAPPED IN PAPER TOWELS IN A ZIPPED BAG. .... 60

FIGURE 8-4: POTTING CUP WITH THE HOLES TAPPED WITH KAPTON TAPE FROM INSIDE. .... 61

FIGURE 8-5: POTTING CUP WITH SCREWS INSERTED IN THREE HOLES FROM ITS SIDES ..... 62

FIGURE 8-6: MOLYBOND LUBRICANT USED TO GREASE THE SCREWS BEFORE POURING THE MIXED PMMA IN THE POTTING CUPS. .... 62

FIGURE 8-7: BOTTOM CUP ATTACHED TO THE ALIGNMENT PLATE ..... 63

8-8: ALIGNMENT RIG DISPLAYING THE LOCATION WHERE THE ALIGNMENT PLATE IS ATTACHED ON ITS BASE. NOTE THAT THE ATTACHMENT SCREWS ARE LOCATED AT THE BACK OF THE VISIBLE SIDE. .... 63

FIGURE 8-9: PICTURE SHOWING HOW THE SPECIMEN SHOULD BE POSITIONED IN THE POTTING CUP. .... 64

FIGURE 8-10: THIS PICTURE INDICATES THE LEVEL OF PMMA IN THE POTTING CUP. .... 65

FIGURE 8-11: THIS PICTURE INDICATES THE ADAPTOR PLATE ATTACHED ON THE SMALL RAIL. .... 66

FIGURE 8-12: THIS PICTURE INDICATES THE RELEASE MECHANISM WITH THE LOCKING SCREW ATTACHED ON THE LEFT SIDE OF THE DROP TOWER. .... 66

FIGURE 8-13: LOCKING SCREW WITH A RELEASE MECHANISM. THE LOCKING SCREW PREVENTS THE UNWANTED RELEASE OF THE WEGHT THAT COULD RESULT IN INJURIES OR DAMAGE OF THE

---

FIGURE

SPECIMENS. ....	67
FIGURE 8-14: LONG RAIL ATTACHED ON THE BASE OF THE DROP TOWER, XY TABLE AND CLAMP THAT STOPS THE XY TABLE FROM FALLING OFF THE RAIL. ....	67
FIGURE 8-15: SMALL RAIL WITH THE ADAPTOR PLATE INSERTED INTO THE TOP OF XY TABLE ....	68
FIGURE 8-16: PICTURE DISPLAYING THE CLAMPS THAT STOP THE SLIDING MOTION OF THE CUPS THEREFORE STOPPING THEM FROM FALLING OFF THE RAILS. ....	69
FIGURE 8-17: THIS FIGURE ILLUSTRATES THE LOCATION WHERE THE MASS IS LOADED, THE CYLINDRICAL LOAD ADAPTOR, THE SAMPLE OF MASS AND THE NUT THAT SECURES THE WEIGHT ON THE TOP OF THE BOTTOM MALLET. ....	70
FIGURE 8-18: THIS PICTURE INDICATES THE LOCKING SCREW THAT PREVENT AN UNWANTED RELEASE OF THE WEIGHT THAT CAN RESULTS IN CAUSING INJURY OR DAMAGING THE SPECIMEN. ....	71
FIGURE 8-19: THIS PICTURE INDICATES THE COMPONENTS AND AREA THAT NEED TO BE CLEANED WITH ALCOHOL AT THE END OF TESTS. ....	72
FIGURE 8-20 - FIGURES A, B, AND B REPRESENT THE BURST FRACTURE, X-RAY IMAGE AND THE FORCE THAT PRODUCE THE BURST FRACTURE. ....	82
FIGURE 8-21 - A REPRESENT NO BURST FRACTURE, B SHOWS THE IMAGE FROM X-RAY AND C THE FORCE GENERATED TO CREATE THE FRACTURE. ....	83
FIGURE 8-22 - BURST FRACTURE OF THE VERTEBRA, X-RAY IMAGE AND FORCE TO CREATE THE FRACTURE REPRESENTED BY A, B, AND C RESPECTIVELY. ....	84
FIGURE 8-23 - BURST FRACTURE, X-RAY IMAGE OF THE FRACTURE AND THE FORCE THAT CREATED TO PRODUCE THE BURST FRACTURE ARE REPRESENTED BY A, B, AND C RESPECTIVELY. ....	85

---

FIGURE

F

8-24 - THE IMAGES IN A, B AND C REPRESENT THE PICTURE OF THE FRACTURE, THE X-RAY TO CONFIRM IT AND THE FORCE THAT WAS PRODUCED DURING THIS FRACTURE. THERE WAS A FRACTURE AT THE UPPER ENDPLATE OF L1 AND A SMALL PART OF T13 THAT WAS ..... 86

FIGURE 8-25 - A, B, AND C REPRESENT THE BURST FRACTURE OF L1 WITH THE DISC REMAINING INTACT, THE X-RAY IMAGE THAT CONFIRMS THIS FRACTURE, AND THE FORCE OF LESS THAN 300 N TO CREATE THIS BURST FRACTURE RESPECTIVELY. .... 87

FIGURE 8-26 - A, B, AND C REPRESENT THE BURST FRACTURE INITIATED AT LOWER ENDPLATE OF L1, THE X-RAY IMAGE OF THE BURST FRACTURED VERTEBRA AND FORCE OF LESS THAN 600 N THAT PRODUCED THIS FRACTURE. .... 88

FIGURE 8-27 - A, B, AND C REPRESENT THE FRACTURE OF THE TOP END PLATE OF L1, THE CONFIRMATION OF THIS FRACTURE BY X-RAY IMAGE AND FORCE OF LESS THAN 300 N TO CREATE THE FRACTURE. .... 89

FIGURE 8-28 - BURST FRACTURE OF THE SPINOUS PROCESS AND SHEAR FRACTURE OF L1 VERTEBRA, X-RAY IMAGE IN B CONFIRMS THE FRACTURE AND SHOWS THE FORCE THAT PRODUCED THE FRACTURE. .... 90

FIGURE 8-29 - A, B, AND C REPRESENT THE FRACTURE OF THE LOWER ENDPLATE OF T13, X-RAY IMAGE CONFIRMING THIS FRACTURE AND THE FORCE OF 700 N RESPECTIVELY ..... 91

FIGURE 8-30 - A, B, AND C REPRESENT A COMPLETE BURST FRACTURE OF L1 AND SPINOUS PROCESS, THE X-RAY IMAGE CONFIRMING THIS FRACTURE AND SHOWING A SPLIT OF THE VERTEBRA BODY AND A FORCE OF ABOUT 400 N THAT LED TO THIS FRACTURE RESPECTIVELY. .... 92

FIGURE 8-31 - A AND B REPRESENT THE BURST FRACTURE OF L1 INITIATED AT ITS UPPER ENDPLATE AND SPLIT THROUGH THE SPINOUS PROCESS AND THE VERTEBRA BODY, AND THE FORCE OF ABOUT 400 N TO CREATE THE BURST FRACTURE. .... 93

---

FIGURE 8-32 - IMAGE A REPRESENT THE FRACTURE OF T13 WITH A SPLIT IN THE LATERAL VIEW, THE AP X-RAY IMAGE IN B DOESN'T SEEM TO SHOW THE LATERAL VIEW FRACTURE AND FIGURE C REPRESENT THE FORCE GENERATED DURING THE FRACTURE OF VERTEBRA. .... 94

FIGURE 8-33 - A, B, AND C REPRESENT THE BURST FRACTURE OF T13, ITS X-RAY IMAGE AND THE FORCE GENERATED TO CREATE THE FRACTURE RESPECTIVELY. THE AP OF THE X-RAY DOES NOT APEAR TO SHOW THE FRACTURE OF THE VERTEBRA BODY. .... 95

FIGURE 8-34 - A, B, AND C REPRESENT A COMPLETE BURST FRACTURE OF THE VERTEBRAL BODY AND SPINOUS PROCESS, X-RAY IMAGE THAT AGREES WITH THE FRACTURE PICTURE AND THE FORCE OF ABOUT 3956 N GENERATED TO CREATE THIS FRACTURE RESPECTIVELY. .... 96

8-35 - IN THIS FIGURE, A, B, AND C REPRESENT RESPECTIVELY THE FRACTURE OF THE VERTEBRA BODY AND SPINOUS PROCESS AT T13, X-RAY IMAGE CONFIRMING THIS FRACTURE AND THE FORCE OF ABOUT 3956 N THAT CREATED THE FRACTURE. .... 97

FIGURE 8-36 - A, B, AND C REPRESENT RESPECTIVELY THE BURST FRACTURE OF T13 INITIATED AT ITS LOWER ENDPLATE, IT'S X-RAY IMAGE AND A FORCE OF JUST LESS THAN 2621 N THAT CREATED THE BURST FRACTURE. .... 98

FIGURE 8-37 - A, B, AND C INDICATE THE BURST FRACTURE OF T13 AND HERNIATION OF T13-L1, X-RAY IMAGE OF THE FRACTURE AND A FORCE OF AROUND 6506 N RESPECTIVELY. .... 99

FIGURE 8-38 - IMAGE A REPRESENT THE BURST FRACTURE OF L1 CONFIRMED BY THE X-RAY IMAGE B. THE FORCE OF AROUND 6502 N IN GRAPH C GENERATED THE BURST FRACTURE. .... 100

FIGURE 8-39 - BURST FRACTURE OF L1 REPRESENTED BY A, B REPRESENTS THE X-RAY IMAGE OF THE FRACTURE AND C REPRESENT THE FORCE OF AROUND 5506 N THAT CREATED THE FRACTURE. .... 101

FIGURE 8-40 IMAGE OF MATLAB WORKSPACE INDICATING THE MAXIMUM FORCE, THE FORCE WHEN THE SPECIMENS STARTED TO FAIL, THE THRESHOLD AND THE ACTUAL FORCES THAT CREATED THE FRACTURES ..... 102

### Notation

1. FSU: Functional Spine Unit
2. SD: Standard Deviation
3. BF: Burst Fracture
4. T12: twelfth vertebra of thoracic segment

---

FIGURE

F

5. T13: thirteenth vertebra of thoracic segment
6. L1: First vertebra of Lumbar segment

---

## 1. Introduction

### 1.1 Background

In modern times, there is an increased involvement in daring sporting activities ranging from ground activities like car racing, skating, scooting to heights of more than 2 m (including flips on scooters), ninja warriors, jumping from airplanes and more. All these activities have various benefit in terms of fitness, fun and financial value. However, there are several problems when these activities do not go according to plan, resulting in severe health conditions like disability, financial crisis and difficulties participating in social activities.

The literature has shown that there have been cases of patients presenting to clinics with fractured spines, because of falling or car accidents. All these cases had different patterns and levels of severities of fractures leading to unclear methods of their treatments. These dissimilarities and varied, complex nature of the burst fractures and their treatments pushed researchers to study their occurrence with a purpose of producing a method that could be ideal to repair these spines. The research methodology used in previous research involved reviewing statistics of patients that presented to clinics and the nature of conditions they presented and reproducing burst fractures like those presented to clinics. This encompassed axial high impact drop towers on intact specimens, using a pendulum hammer or dropping dummies from a height. There has also been evaluation of the performance of axial high impact testing on the specimens after inducing injuries on them. The specimens that were used for the high-speed impact included human cadavers, sheep, pigs and bovine. The results from these researches indicated that around 90% of all the spine fractures arise at the thoracolumbar section with about 20% of them being burst fractures (Alpantaki et al. 2010). Also, these studies discussed that the combination of vertical compression of the anterior column, fracture of the middle column and retropulsion of the fragments in the spinal canal are the main characteristics of burst fractures (Baker 2014).

These numbers of burst fractures have a significant impact on the community and get even worse when there is a burst fracture leading to some bone fragments that get pushed in the spinal canal compressing the spinal cord, which in turn results in neurological impairment causing patients to be paralysed. Also, the research has indicated that most of these cases appear in young people aged under 24 years who are very active.

---

Regardless of specimens' type, most, researchers tried to reproduce the thoracolumbar burst fractures like those seen clinically by axially impacting a segment made of three vertebrae with a drop weight at high speed. All papers reviewed indicated that this nature of fracture occurs at the Thoracolumbar junction especially at T12 and it is believed that it is because of the transitional biomechanical properties in this area. Even if previous studies indicated that the Thoracolumbar Burst Fracture occurs mostly at T12, the literature indicated that only the segments of three vertebrae were used during reproduction of burst fractures. However, both vertebrae at the end of the segments were being potted into two cups using resin to secure the specimens. These cups are the ones that would be impacted as well during the testing. This leaves the option of one vertebra that is exposed for fracture.

## 1.2 Scope

Current study sought to create a reproducible thoracolumbar burst fracture on sheep specimens using a drop tower but limited to using segments that range from T12 to L1, T13 to L2, and multiple segments from T12 to L2. At the end of the tests, the results from all three groups are compared with previous research to determine whether they emphasize or contradict previous findings. An assessment of the type of fractures, the point of initiation, and the fractured vertebrae is performed, and analysis is conducted to determine if there has been retropulsion of the bone fragments in the spinal canal. The results are also evaluated against geometrical measurement of the vertebra and disc of each specimen.

Based on the results from testing, a recommendation of a new direction of spine studies at Flinders University is given and possibly a new approach on how to treat the burst fracture provided to guide surgeons.

## 1.3 Outline of the study

To suitably inform this study, research on previous studies was conducted by reviewing papers on work done reproducing thoracolumbar burst fractures and clinical cases of patients with actual burst fractures. Furthermore, sheep specimens were obtained from a butcher shop (Austral meat) and prepared for potting and testing using a drop tower. The test regime would include collect data with labview data acquisition and doing a visual inspection of the tested specimens to assess the fractured vertebra and determine where



---

the fractures initiate. An X-ray of each specimen was taken to analyse the extent of fractures.

After the X-ray, the specimens would be dissected to investigate potential existence of the bone fragments in the spinal canal. Once the observation is finished, the results would be analysed against previous studies, discussing the limitations and concluding the study with a recommendation. At the completion of the project, the study would determine the required forces to create a thoracolumbar burst fracture in sheep models, the vertebrae that are more vulnerable to fracture based on the tested segment and relate the results with the human model.

---

## 2. Literature review

This literature review will investigate the study that has been done on thoracolumbar burst fractures, the nature of these fractures, their causes, their impact on people's lives and their communities and previous testing methodology.

### 2.1 The anatomy of thoracolumbar burst fracture

Thoracolumbar is one of the three main curves forming both the thoracic and lumbar regions of the spine. It is composed of a chain of vertebra bodies, endplates and intervertebral discs (discs) and whose labels range from T9 to L4. The junction of both thoracic and lumbar is located at T12 and L1 as illustrated in Figure 2-1. This junction is biomechanically considered to be the weakest due to its transitional properties.

As for all other vertebrae of the spine, the thoracolumbar region's vertebrae end with endplates at both extremities which are in turn connected to intervertebral bodies. This region interacts with the other spinal segments to maintain the rigidity of human spine with the junctions at the intervertebral bodies facilitating its mobility in either bending, twisting or smooth sliding of the vertebral bodies (Adams, 2013).

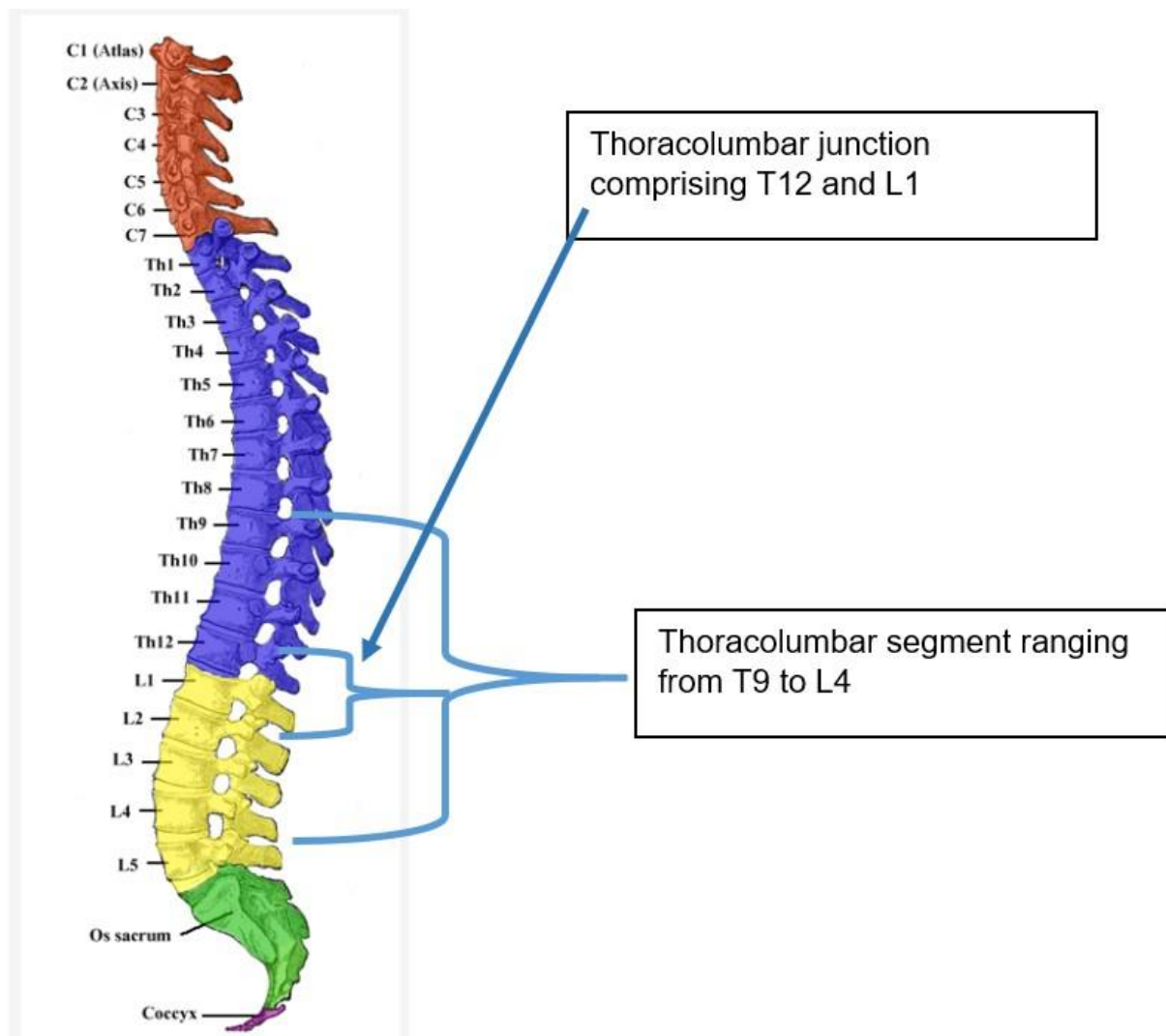


**Figure 2-1: Image of the entire human spine showing all its segments: cervical (orange), thoracic (blue) and lumbar (yellow). The thoracolumbar segment is shown by the external curly bracket and the thoracolumbar junction by internal curly bracket (The Vertebral Column | Boundless Anatomy and Physiology, 2017).**

### 2.1.1 Structural composition of both thoracic and lumbar vertebrae

Each vertebra in the thoracic region is composed of a vertebral body, vertebral foramen, facet for the rib, pedicle, lamina and transverse process (Figure 2-2).

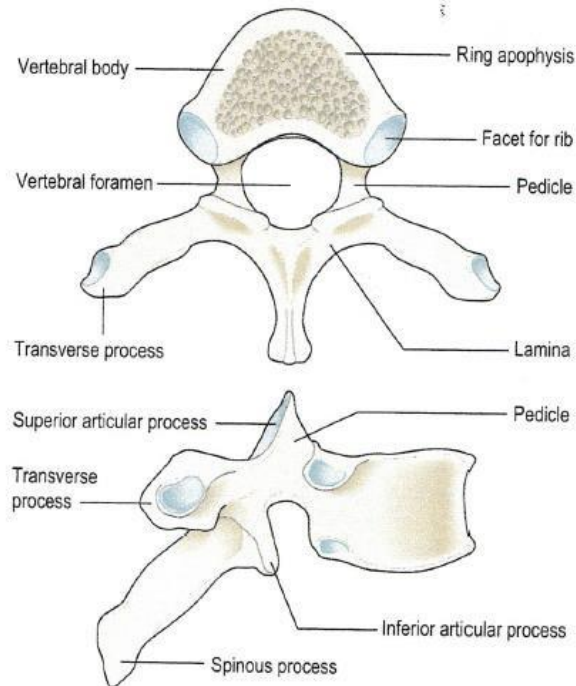


**Figure 2-2: Structural composition of vertebral in both transverse and sagittal view. This picture shows the location of all parts as described above (Adam 2013).**

The picture displayed in Figure 2-2 indicates the structural composition of thoracic vertebra in both transverse and sagittal view. It is structured in the way that it doesn't rotate in the axial direction at the lower thoracic level, however, allows rotation at middle and upper level.

The lumbar vertebrae are differentiated from the thoracic vertebrae by the fact that they don't have ribs while Thoracic vertebrae do, as shown in Figure 2-3.

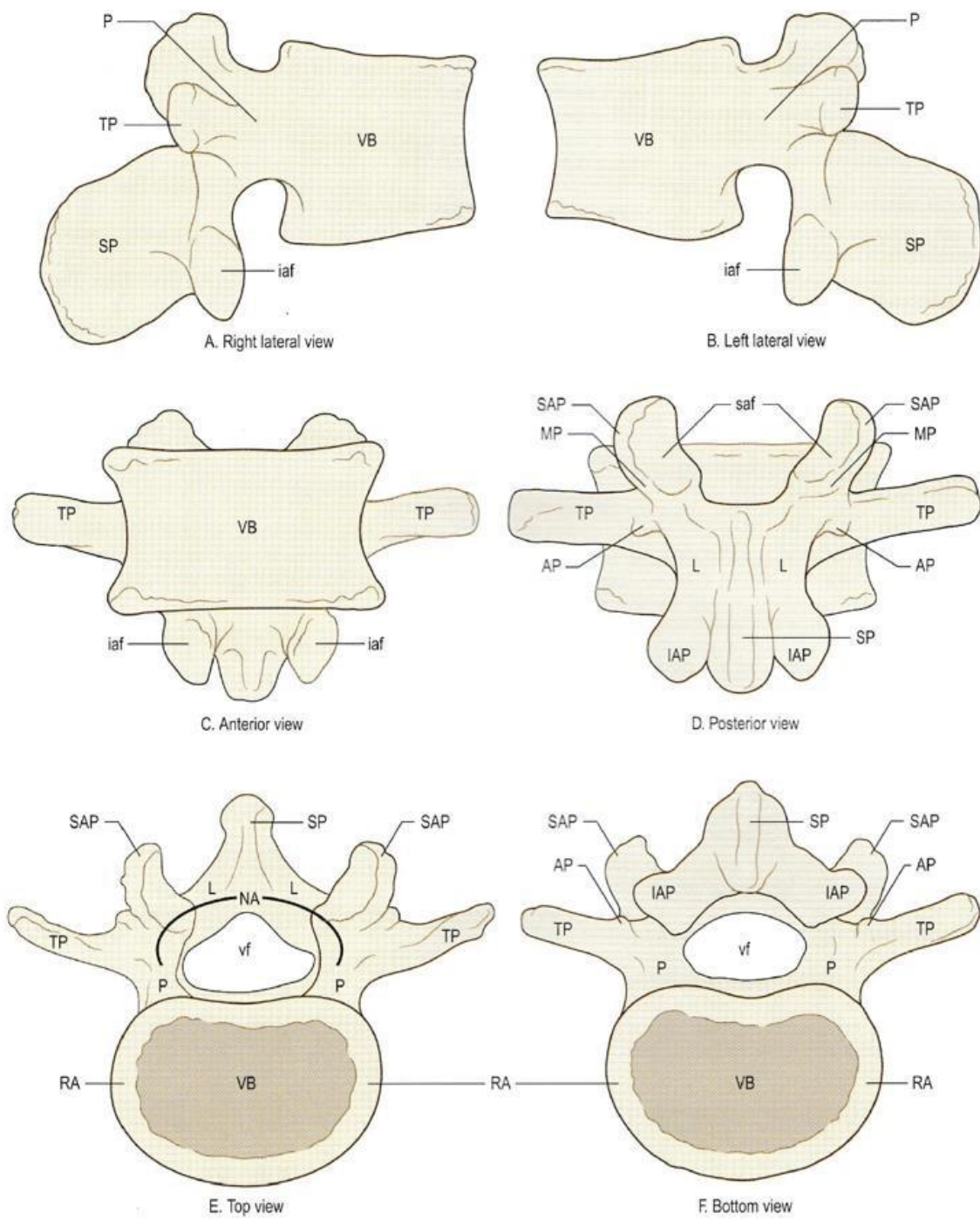


**Figure 2-3: Structural composition of the lumbar region in lateral anteroposterior and anterior and posterior view (Adam 2013).**

---

### 2.1.2 Vertebral body

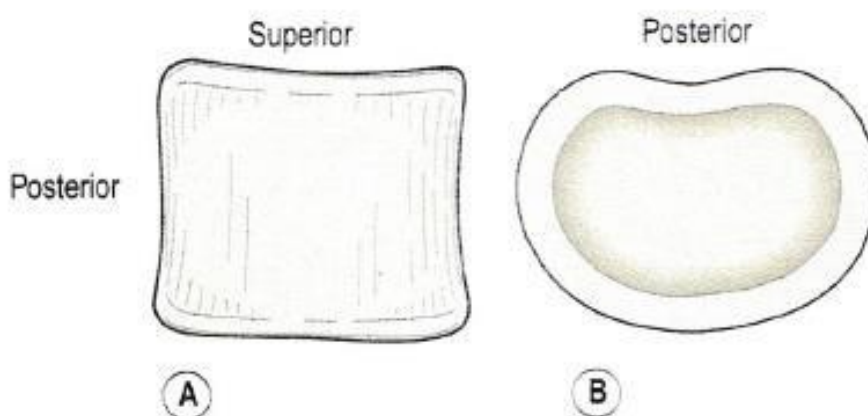


**Figure 2-4 - Side view of the vertebral body (A) and semi columnar from top view of the vertebral (B). Their structural composition assists in resisting the axial compression (Adam 2013).**

The structural composition of vertebra body and semi columnar, pictured in (Figure 2-4) maintain the rigidity of vertebral bodies by resisting compression and supporting the upper body (Adams, 2013). The vertebral body's strength is enhanced by the trabeculae that are organized in a horizontal and vertical array. This arrangement prevents sideways sliding under a high axial compression therefore giving support that prevents the vertebral body from crushing under compressive load (Adams, 2013). According to Adam (2013), the vertebral and intervertebral body resist up to 1 kN of compression of the spine in the standing position and most of this force is accumulated in the inferior of the joint surface. Even though this structure prevents the burst fracture, with a high-speed impact it can be fractured especially toward the inferior endplate.

### 2.1.3 Intervertebral disc

As discussed before, intervertebral discs separate vertebral bodies and play an important role in allowing the transfer of compressive forces between them with minimal movement. Adams (2013) has discussed that the intervertebral disc cannot absorb shock, resist bending, twisting or shearing forces on the spine due to its stiffness. However, the nucleus pulposus that is in the middle of the intervertebral disc facilitate an even distribution of compressive forces on the vertebral bodies, due to the resistance of the hydrostatic

---

properties (Costi, Hearn & Fazzalari 2002; Nachemson 1981). The intervertebral disc has three layers which are the nucleus pulposus (the innermost portion), the inner fibres constituting the capsular surrounding the nucleus pulposus and tracing through the vertebral end plates, and the outer fibres that are made of the ligamentous and tensile connected to both ends of the vertebral bodies (Figure 2-5). The annulus fibres are made of different concentric layers of lamellae that are arranged in an alternating structure forming an angle of about  $\alpha = 65^\circ$  to each other as shown in Figure 2-6. This angled structural formation of the lamellae assists in strengthening the outer of the intervertebral disc in different directions (Adams 2013). Even though the structure prevents the sideways or twisting of the vertebral bodies as it was discussed early, it doesn't resist the compressive loading as this is a job of hydrostatic property of the nucleus pulposus.

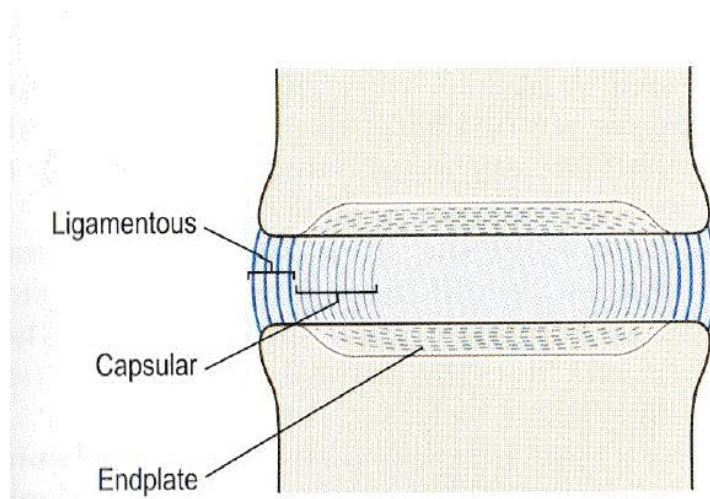


**Figure 2-5: The structure of the intervertebral disc between two vertebral bodies. It is surrounded by ligaments that connect the end plates of both the adjacent vertebral bodies (Adams 2013).**



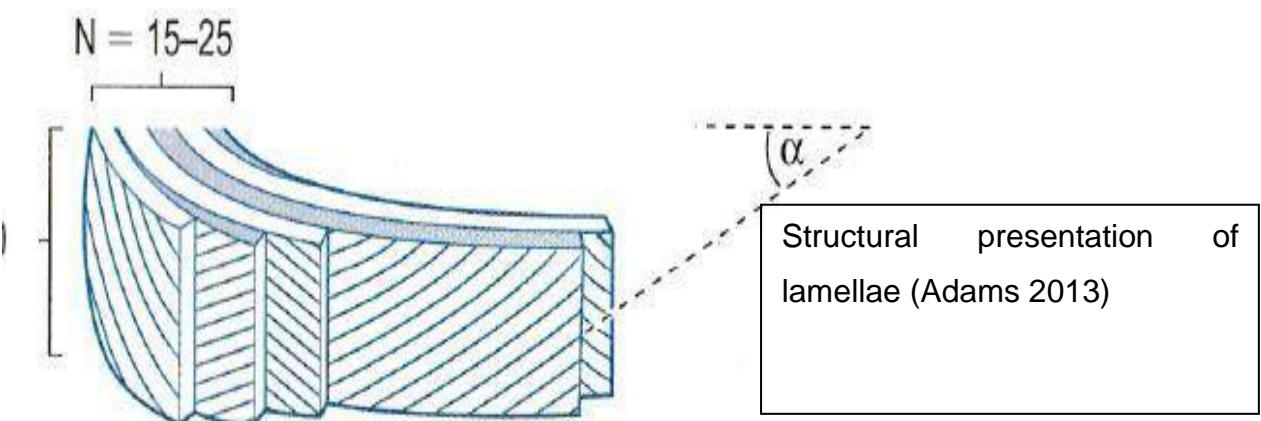
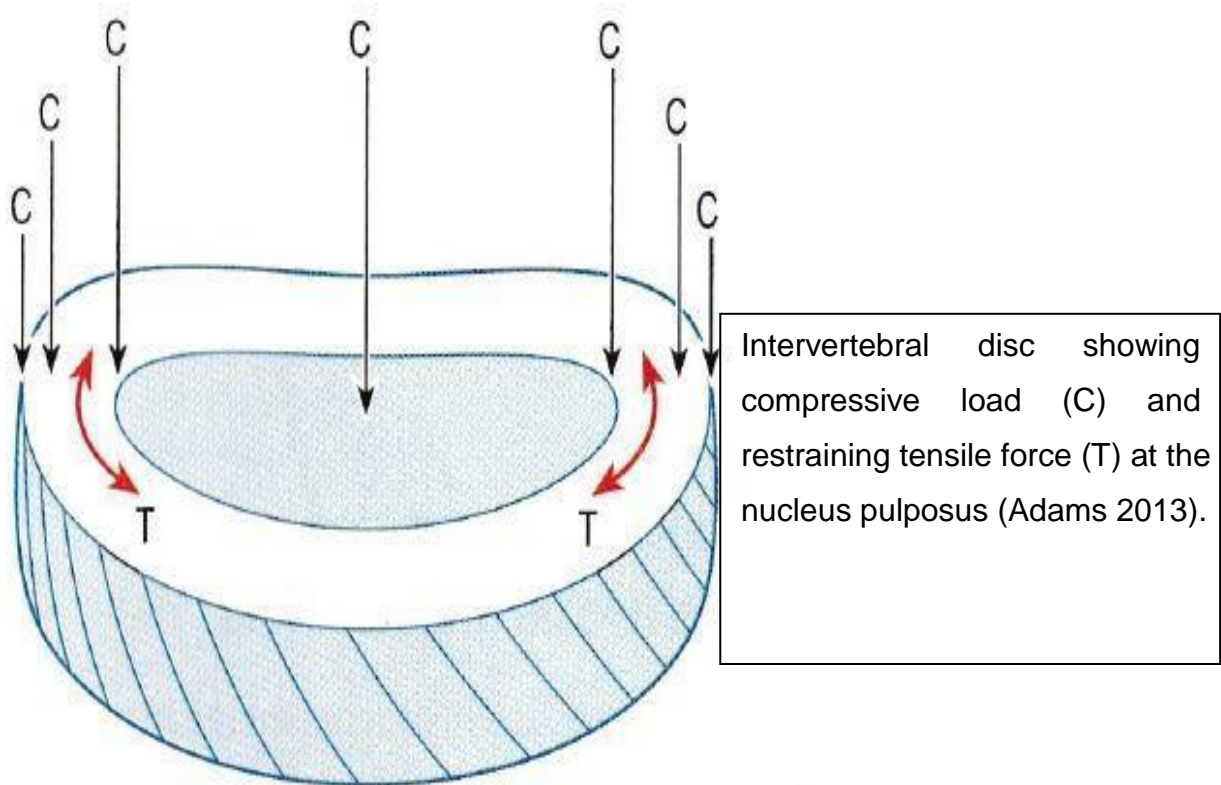


**Figure 2-6: the annulus fibres of intervertebral disc and its structural composition. The disc indicates the compressive forces (downwards arrows(C)) and a restraining stress or tension by the red arrows(T) (Adams 2013).**



---

According to Adams (2013), the intervertebral disc has height of 5 to 10 mm and contribute to about 25% of the total height of the spine.

## 2.2 Thoracolumbar Burst Fracture

### 2.2.1 Cause of thoracolumbar burst fracture

As indicated in the Introduction, thoracolumbar Burst Fracture occurs mainly in young people especially active males aged between 14 and 24 who participate in sports requiring high energy or involving jumping from heights of more than 2 m (Marco, Russell & Masters 2003). These strenuous physical activities include jumping from airplanes, diving, and parachuting. When these people fall or land on their feet or buttocks at a high speed there is a potential of creation of burst fractures of thoracolumbar like fracture in Figure 2-7 caused by a fast deceleration of the ground.

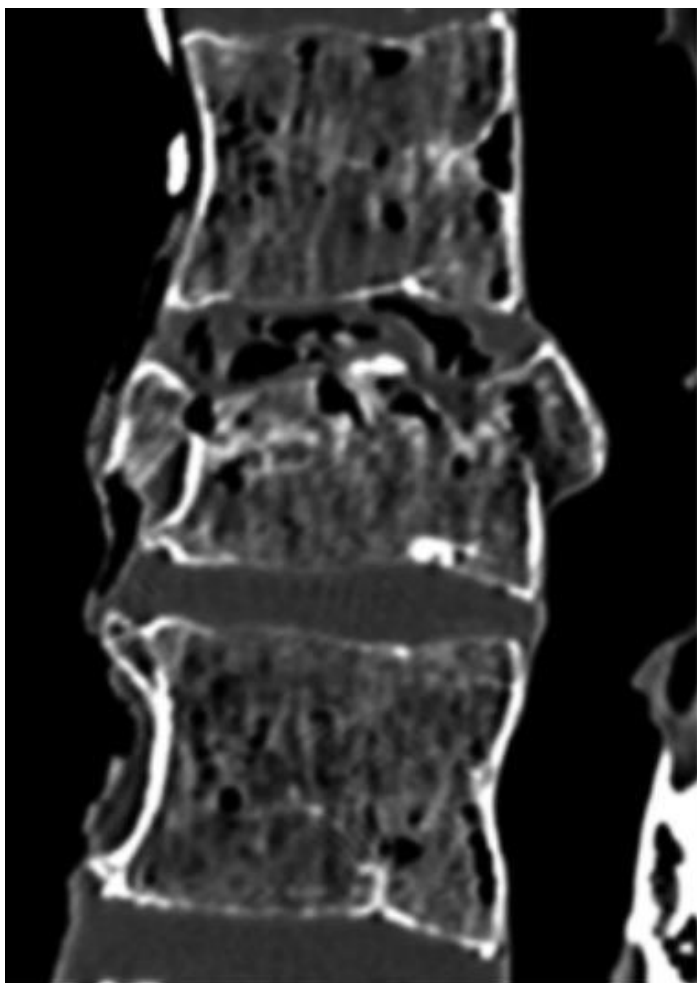


**Figure 2-7 Burst fracture of L1 (Oberkircher et al. 2016)**

---

The thoracolumbar burst fracture can also result from car accidents (Pintar et al. 2012; Yoganandan et al. 2013). Fast braking of cars or high impact during car crashes or a rotation of more than 0.5°/ ms at a high speed can trigger a burst fracture (El-Rich et al. 2009). Literature has shown that thoracolumbar burst fractures from car accidents are mainly due to the restraint of shoulder and lap belts during a fast deceleration or high impact (Ivancic, P. C. 2014; Ivancic, Paul C 2014; Pintar et al. 2012). Different studies have been conducted to investigating burst fractures of the spine, and they have shown that most of the severe ones occur at Thoracolumbar region (Fakurnejad et al. 2014), however, there is debate about how it happens. Some researchers have suggested that a burst fracture is initiated by a compressive force on top of the head of the vertebral endplates which is pushed into the vertebral body leading to its burst fracture (Fredrickson, B et al. 1992; Tran et al. 1995) while other studies have indicated that the cause of burst fracture is the difference in the rate of entrance of materials in the vertebral body compared to the rate of exit of fat and marrow (Tran et al. 1995). This region is believed to be vulnerable to this sort of fracture because of its transitional biomechanical properties. Based on the research, 90% of all spine fractures occur in thoracolumbar region with 10% to 20% of them being burst fractures (Panjabi et al. 1994; Fakurnejad et al. 2014; Park et al. 2009). Several studies have been and are still being conducted using different methods either by creating the burst fracture through testing or analysing clinical cases of patients presenting at the clinics with the above type of fracture. The main purpose was to understand how these disastrous injuries occur and investigate different techniques to treat them. Despite these tremendous efforts from different researchers, there is still a lack of consensus around its cause (Fakurnejad et al. 2014). As a result, there are difficulties deciding how it can be treated properly (Panjabi et al. 1994).

### 2.2.2 Problems and clinical significance of thoracolumbar burst fractures

The thoracolumbar burst fracture causes vertebra bone fragments to be pushed back into the spinal canal resulting in neurological complications such as paraplegia, backpain, dysfunction of the bowel, loss of movement of the legs and more other health issues (Willen et al. 1990). As discussed earlier, this is a critical challenge that requires a good knowledge to fix it, however a poor understanding of its occurrence leads to its inefficient treatment and implications of complex management that would inhibit a quick recovery allowing patients to go back to work and resume their daily activities (Alpantaki et al. 2010). Current

---

studies have shown that 60 percent of all thoracolumbar burst fractures developed a neurological deficit (Oxland, Panjabi & Lin 1994). An investigation conducted in Australia has indicated that at least 243 Australians develop severe spinal cord injury every year because of spinal fractures (Marco, Russell & Masters 2003) and in the USA there are at least 150 thousand spine fractures, annually (Jones et al. 2011). Therefore, there are an increasing number of people who would then rely on using wheelchairs to mobilize, socialize and participate in the community activities or sporting (Di Marco, Russell & Masters 2003; Shen et al. 2011) in addition to the financial burden from unemployment, medical and surgical treatment and everyday expenses (Aras et al. 2016). Even though several studies have been conducted to find a treatment, the absence of a deep understanding of its root cause (Fakurnejad et al. 2014) triggers complications when providing its proper treatment (Panjabi et al. 1994; Jones et al. 2011).

Another point of contention of the burst fracture results from its condition. According to the research of Panjabi et al. 1994, researchers agree that the burst fractures with a neurological deficit are unstable. However, a major disagreement is on the burst fractures with no sign of neurological issues, where some believe that these types of fractures are unstable, while others state that they should be considered unstable if they occur at the posterior element like facet, lamina and pedicles. Another group believes that if there is an angular deformity, the fracture should be considered unstable regardless. However, some clinicians say that in the absence of neurological deformity, the fracture should be diagnosed as stable.

### 2.3 Previous methods and testing equipment

Different researchers have used various testing methods and equipment in order to create thoracolumbar burst fractures that would resemble the fractures seen clinically, whilst analysing their consequences. The selection of each method, specimen and equipment was based on the aim of the test and the availability of both the equipment and specimen. The specimens used included bovine, sheep, and human cadavers (Jones et al. 2011) while other researchers used clinical cases to analyse the injuries of people who had fractured their spines (Zhang et al. 2017), and one of the papers indicated the test that used pig specimens (Germaneau et al. 2017). The elements that were considered during testing

---

were height, weight and speed of testing. The speed varied depending on the type of specimen being used. The testing speed for human specimen was around 5 m/s compared to other specimen speeds that were relatively low. The pig specimen used even lower speed of impact that ranged from 0.01 mm/s to 500 mm/s. A study by Germaneau et al. 2017 has indicated that the application of an angle of deflection can have an influence on the burst fracture. Their research has proven that the usage of an angulation of 15° halved the number of specimens that burst fractured.

### 2.3.1 Method of drop tower

Some researchers used a method of dropping weight from various heights ranging from 1 m to 2 m striking the top of the specimen at high speed and collected the data using personal computers (Jones et al. 2011; Oxland, Panjabi & Lin 1994). To gain a better understanding of different ways this fracture could occur, various impact techniques have been employed, which include grouping the specimens and performing different tests for the groups while ensuring the specimens in the same group were tested under the same conditions. For example, Oxland, Panjabi and Lin (1994) employed three different methods of testing where from a total number of 13 human spines, five of them were tested by dropping an initial weight of 8.3 kg on a flat plate interface with the specimen. This type of interface was used with the intention of avoiding bending the top vertebra in the vertical planes. The second technique used two specimens with a cylindrical impact interface aiming to facilitate sagittal rotation by applying a small mass of 2.3 kg. The last six specimens were tested by using a flat interface, and an applied mass of 4.3 kg. As many other papers commented, this procedure of testing lacked a knowledge on the exact load that would produce the thoracolumbar burst fracture which caused a need of performing multiple tests by varying the mass in 2 kg increment until the fracture occurred. According to the findings of Oxland, Panjabi and Lin (1994), more than three quarters of the specimen used, presented burst fractures like those found clinically but there was no influence from the type of interface used on the nature of fracture. Normally an access on transaxial CT scan helps to analyse the level and direction of fracture. Some of the drop towers were used multiple times to create the burst fracture without varying the weight (Figure 2-8).

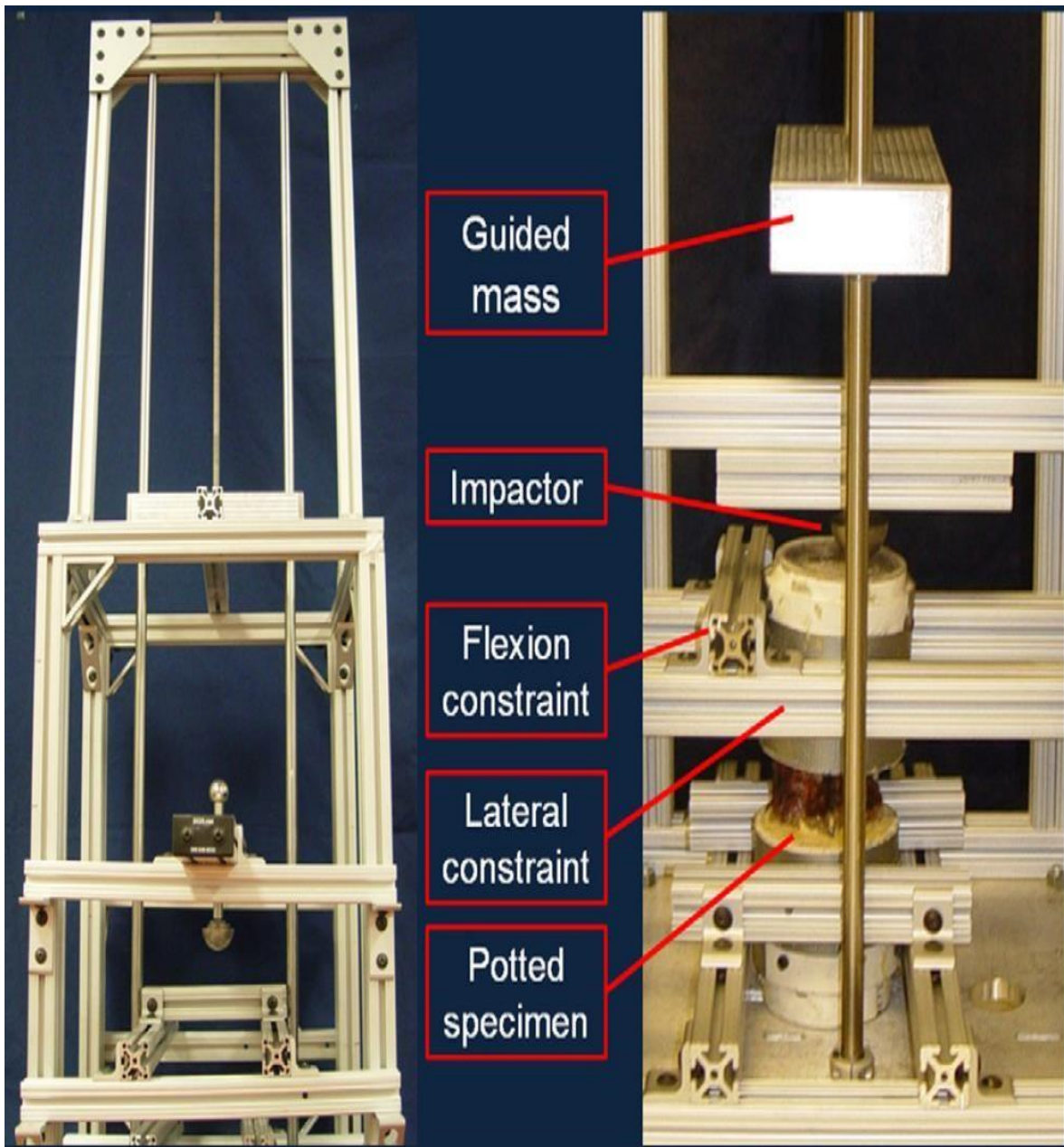


**Figure 2-8: Drop tower testing apparatus showing the impactor, guided mass, flexion constraint and lateral constraint . This drop tower was used multiple times to create burst fracture without changing its mass (Jones et al. 2011).**

The testing machine (Figure 2-8) used a drop tower with a guided weight during a free fall where a mass of 25 kg was dropped from a 1 m height striking the impactor (Jones et al. 2011). The study that used this method indicated that the specimens were pre-injured before they were burst fractured and the level of fractured specimens were analysed using x-ray, computed tomography and dissection. With this mode of testing, there was a measurement of the areas of the specimen before and after the actual test using geometric parameters where the height of each vertebra and disc, their interior and posterior areas



were measured. Imaging comparison and the variation in distance provided the percentage of the canal compromised. This paper concluded that the study's experiment was successful, however, the usage of the same mass multiple times may suggest that the burst fracture happened due to fatigue. In addition, there is no clear information if there couldn't be a smaller or larger mass that could produce a similar burst fracture by only testing once. Others use high speed impact machine like a hammer as discussed next. (Figure 2-9).

### 2.3.2 Gravitational and hammer impact method

The testing machine shown in Figure 2-9 is a gravitational impact machine that used a 5 kg hammer and impact from a height of 1.4 m. It had a limiting rod that would be utilized to push the specimen away to prevent multiple impacts, the guiding tube which guided the impactor onto the specimen, cylindrical barrier block, bracing piece and susceptor. The author has determined that the results in this paper were analysed using a CT scan and based on the information provided and the data presented, the corresponding impact speed was around 5.24 m/s.

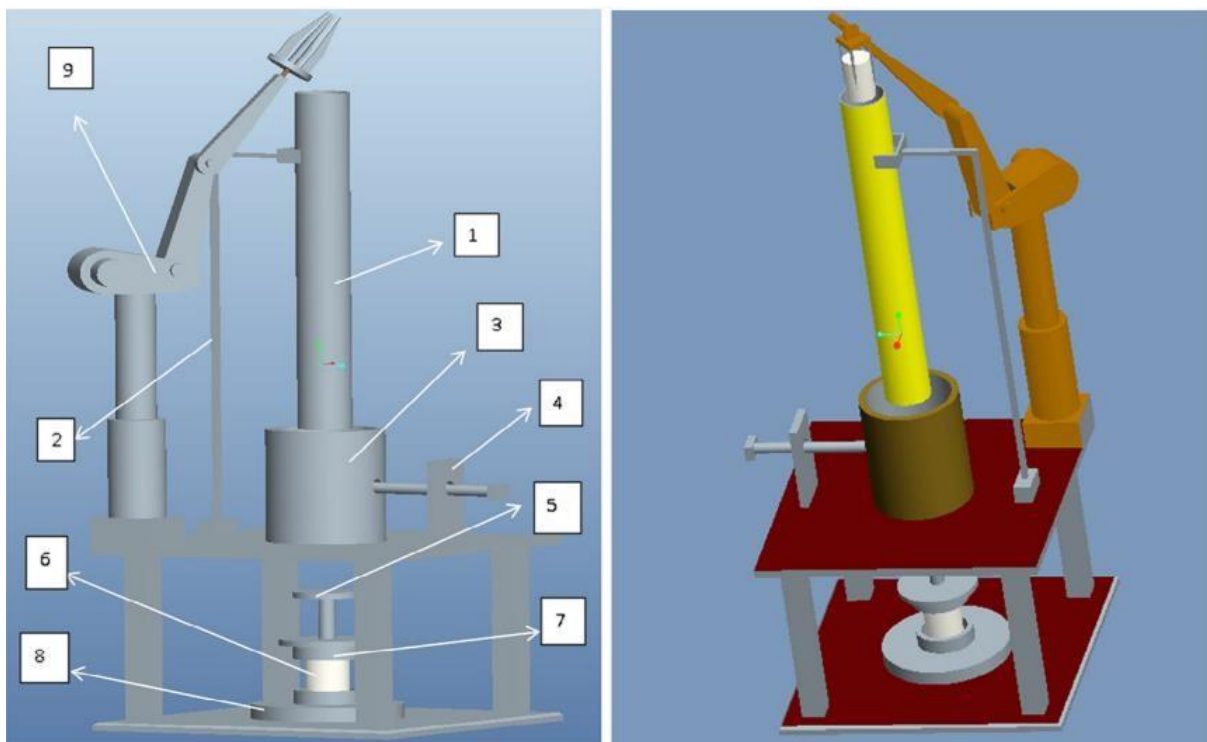


**Figure 2-9: Testing apparatus containing a guided tube, bracing piece, cylindrical barrier block, limiting rod, dental plaster cup base plate and a manipulator (Zhang et al. 2017)**

### 2.3.3 Pendulum method

Another model called Charpy pendulum was developed by Germanneau et al (2017) and was used to produce multiple impacts on human specimens (Figure 2-10).

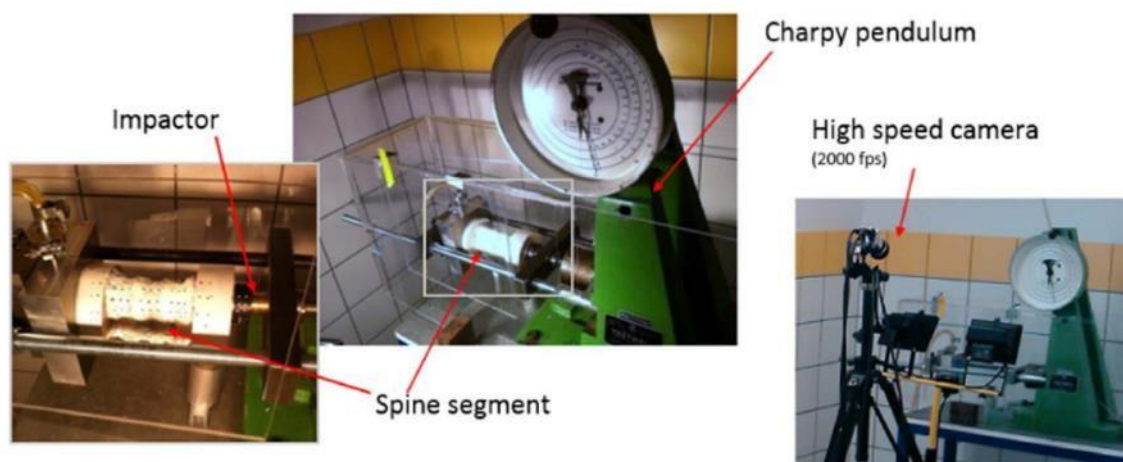


**Figure 2-10: Method of testing using a hammer, high speed camera and impactor (Germanneau et al. 2017)**

The above model was designed with the capability to apply an axial impact on seven vertebrae and had a slider that was designed to be struck by a hammer and then transfer the energy to the vertebrae to create the burst fractures. These researchers have discussed that to be able to create a fracture at a certain vertebra, it had to be weakened by creating a hole in its vertebral body. This model was coupled with a high-speed camera that would take images at a frequency of 2000 Hz. To analyse the fracture produced, an X-ray tomography and optical method with a tracking mark was used to detect the deformation and nature of burst fracture. This study found that the burst fracture was produced by a loading force of  $4020 \text{ N} \pm 1900 \text{ N}$ .

Some of the other testing methods included the combination of creating injuries on the facet, laminae or vertebral body of the specimen (Germanneau et al. 2012), and hammering, guided drop weights (Jones et al. 2011) to promote the burst fracture of the thoracolumbar (Fakurnejad et al. 2014; Germanneau et al. 2017). However, the induction of injuries by facetectomy, laminectomy and osteotomy are not preferable because they don't necessarily

---

represent the real appearance of clinical burst fracture (Germaneau et al. 2017) Different studies had different aims, but the common point was burst fractures at the thoracolumbar with the intention of assessing how it could be fixed. Many of the studies intended to create similar burst fractures at a certain vertebral of the thoracolumbar such as Shono, McAfee and Cunningham (1994) who used the method of drop weight to create identical burst fracture at L1, while others had the main aim of understanding how to fix the fracture. Creating identical thoracolumbar burst fractures requires that all the specimen be in the same or closest conditions as possible and have the same free vertebrae while testing. Some researchers produced this type of fracture by grouping human specimen cadavers based on the gender of the donors and the portion of the spine that was aimed to be tested (Shono, McAfee & Cunningham 1994). One example is in the research of Shono, McAfee and Cunningham (1994) who grouped six vertebrae from sixteen male and eight female spines ranging from T10 to L4. These vertebrae were transfixed with a K wire to ensure the alignment of the vertebrae bodies centre. The rest of vertebrae were left free between two pots. Normally radiographic testing is required before starting the test to ensure the specimen being tested are in a good condition or determine any conditions that would affect the results from the tests (Zhang et al. 2017). Based on the literature on high speed impact with the aid of radiographic abnormality check, specimen can be disseminated prior to testing and remove the ones that are unfit. Literature has also shown that bone mineral density of vertebrae needs to be measured prior to producing the burst fracture to explore any presence of osteoporosis. As discussed earlier, if the aim is to produce identical burst fracture at a certain vertebra, it must be free in all the specimen with its adjacent discs while other extremities are fixed in the impact loading apparatus. Some testing were performed by applying a high speed impact, however other machines were programmed to run and compress the upper and lower end of the fixture vertically until the heights between them were reduced to a certain percentage of its original in a certain amount of time (Shono, McAfee & Cunningham 1994). When testing, a PC is required to record the results while the frequency of recording must be determined depending on the test and the instrument being used (Yoganandan et al. 2013). The loading level vary from test to test, however if the fracture didn't happen at the initial test, the weights can be incremented by a certain amount until it happens.



---

Another study was conducted with the aim of creating a burst fracture of the vertebral body at L1 using human cadaveric specimen from young men aged between 33 and 35 (Fredrickson, B et al. 1992). The method applied was like the method used by Shono, McAfee and Cunningham 1994. In this study, the segment ranging from T10 to L4 was axially compressed by loading test but since only L1 that was intended to be fractured, it was exposed while all other three vertebrae at the extremities were mounted in potting materials.

All tests in this (Shono, McAfee and Cunningham 1994) study presented burst fractures at L1 using an average compressive load of 7199 N and energy of 260 Nm. In the author's evaluation, they compared the change in vertebral height and biomechanical properties to the percentage of canal compromise. They used a CT scan to determine the density and geometry of the vertebra, bone mineral density at the mid-pedicle level and the confirmation of L1 burst fracture. The geometric measurements were vertebra body width, depth, anterior height, mid-height, posterior height, canal width, depth, area, and pedicle width. This study found that the severity of the fracture based on the canal compromise was between 4 and 46% with a mean value of 25%, mean value of 0.88 anterior and 0.83 posterior for vertebral height before and after fracture. The compressive load was applied uniformly. There was a significant correlation between vertebral body depth and percentage loss of posterior vertebra body height. Based on this article, this correlation is important to assess the risk of burst fracture of the vertebral body based on its geometry. The vertebral geometry and the correlation can assist in assessing the level of fracture when CT scan is not present. Subsequently, this has formed one of the evaluation metrics in the results section of this report; however, the loading force and energy would not be compared with current study due to the differences in loading mode.

#### 2.3.4 Hybrid cadaveric simulation

Apart from these high impact machines, there was another test that used a hybrid cadaveric simulation, shown in (Figure 2-11).

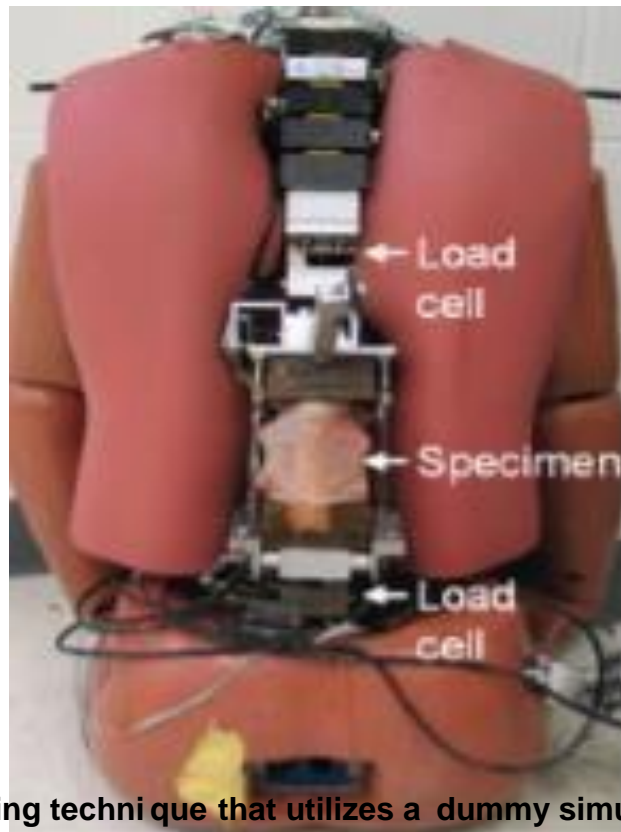


**Figure 2-11: testing technique that utilizes a dummy simulating a real -life fall from a height. it possesses load cells, specimen, and wires to hold the pieces together, trunk and pelvis (Ivancic, Paul C 2013).**

The authors of this paper tried to simulate a real-life development of thoracolumbar burst fracture from a height by using a hybrid cadaveric model (Ivancic, P. C. 2013) (Figure 2-11). As in many other papers reviewed here, this simulation used human specimens with segments of three vertebrae at a time which ranged from T9 to L5. Their approach consisted of a simulation in real life where a dummy had to be dropped from a height of 2.2 m at a speed of 6.6 m/s. The dummy had load cells on the top and bottom to measure the loads. Only the segments L3 to L5 were considered during the test. The specimen had a trunk, arms and pelvis but didn't have legs. A digital camera recorded the kinematics at 500 frames/s. The result was evaluated with the aid of radiography, fluoroscopy and anatomical dissection. This dummy had a total mass of 47.9 kg with the upper torso presenting 31.7 kg while the pelvis measured 15.2 kg. The outcome of this study indicated that the experiment was successful and produced a burst and split fracture, however the middle vertebrae was the one that was affected especially at the pedicle and endplate. The compression, endplate and pedicle's fracture led to the reduction of the specimen in height.

---

Another article researched different studies that aimed to induce thoracolumbar burst fractures in the compressive way by reviewing different testing methods applied previously. These methods included a drop tower, powered machine and a combination of clinical destabilization techniques such as facetectomy, osteotomy, laminectomy with drop tower and powered machines. One of the tests considered a cadaver with in vivo burst fracture. The drop tower used masses varying from 2.3 kg to 30.2 kg that were dropped from a height of 1 to 2 m with an edge angle varying from 0 to 15°. The specimens used were human spines and sheep (Fakurnejad et al. 2014). The testing techniques indicated burst fracture in the thoracolumbar region which matched with the previous study of Korovessis 2011 that had the aim of comparing transpedicular cancellous bone grafting and transpedicular calcium sulphate grafting while choosing if calcium sulphate cement could be used instead of autogenous cancellous bone used in the anterior body augmentation after the instrumentation of posterior short segment. This study has indicated that the most common type of fracture is the burst fracture and it occurs mainly in the thoracolumbar region, and it is caused by the failure of anterior and middle column due to axial loading. This article indicated that stable fractures can be treated predictably. This stability has been described as the ability of the spine to limit the displacement while undergoing loading therefore reducing the damage and pain caused by the changes in structure. This doesn't necessarily require surgical treatment. However, there are unstable burst fractures that are characterized by a loss of more than 50% of the anterior vertebral body heights, more than 20° of angulation or a compromise of more than 50% of spinal canal that is recommended to be treated surgically and they are mostly localized at the thoracolumbar region (Wood, Bohn & Mehbod 2005).

Another study investigated the effect of the level of loading on the spinal canal occlusion when the loading impact was applied in the same direction at the same energy but with a different rate of loading. In this study, T9 to L6 of bovine spines were tested considering three vertebrae at a time, namely T9-T11, T11-L1, L1-L3 and L3- L6, and the expectation was to obtain a burst fracture that leads to the increased severity of spinal cord injury because of vertebra fragments pushed into the spinal canal. Their review indicated that the vertebral body burst due to a high force applied on the top of the head causing either of the endplates of the vertebra to fracture and the enforcement of discs nucleus in the vertebra

---

body. But the main reason for bursting is the high rate of the nucleus materials entering the vertebra body and the low rate at which the contents of fats and marrows leave it.

The equipment used during this procedure included pressure transducers which measured the pressure of fluid circulating in the spinal canal, load cells to measure the impact load, computed tomography to observe the level of occlusion, the compressive machines and the drop weight. The results seen with computed tomography indicated a displacement of bone fragments in the spinal canal with a high impact loading rate, resulting in more bone fragments compared with that of a low rate, leading to a conclusion that the rate of loading plays a major role in thoracolumbar burst fracture. Labtech software was used to gather the data at the frequency rate of 350 Hz for the low rate impact and 450 Hz for high rate impact and stored on a PC. Based on these testing techniques, high rate impacts cause a burst fracture with bone fragments being pushed in the spinal canal while the low rate loading cause a compressive fracture with a small volume of bone pushed in the spinal canal. The mean time to failure was 400 ms with a spinal canal occlusion of 6.84% while the mean energy was 32.79 J for the low rate and the mean time of 20 ms presenting an occlusion of 47.62% with a bursting energy of 35.07 J (Tran et al. 1995). The aim was achieved in this study; however, there was a lack of understanding of the cut off load that would cause the burst fracture and no knowledge on how the viscosity would affect the results due to the variation of this property with age. Before testing, soft tissues were removed from the specimens paying attention to not damage the facet, disc and ligaments.

The literature has shown a great amount of study on reproducing burst fractures in the thoracolumbar region. However, there was no indication of testing a multilevel segment without inducing an injury or comparing the results Between T11-L1, T12-L2, and T11-L2.

The reviewed papers have developed a level of understanding that would be based on to prepare specimens and perform the testing for current study.

### 2.3.5 Flinders Hexapod

Hexapod robot is a biomedical testing machine that was created at Flinders University to test both human and animal specimens by applying forces or torque to deform them based

on the study intention. It has a maximum axial loading capability of 21 kN, a height of 180 mm and the maximum speed of 210 mm/s before an application of a load.

**Table 2-1: Table of specifications of hexapod robot testing system in all 6DOF (Boyin et al. 2011).**

Axis	Load Capacity	Stroke	Disp. Resolution	Max. Speed	Disp. Accuracy (RMS)			
					0.1 Hz	0.5 Hz	1 Hz	2 Hz
Ant/Posterior Shear ( $F_x$ )	4.8 kN	+150 mm	$\pm 0.3 \mu\text{m}$	480 mm/s	0.004 mm	0.014 mm	0.03 mm	0.10 mm
Lateral Shear ( $F_y$ )	5.1 kN	+150 mm	$\pm 0.3 \mu\text{m}$	540 mm/s	0.004 mm	0.014 mm	0.03 mm	0.10 mm
Axial Load ( $F_z$ )	21 kN	+90 mm	$\pm 0.25 \mu\text{m}$	210 mm/s	0.001 mm	0.007 mm	0.02 mm	0.07 mm
Lateral Bending ( $M_x$ )	2200 Nm	+25°	+0.001°	60°/s	0.004°	0.005°	0.015°	0.070°
Flex/Extension ( $M_y$ )	2500 Nm	+25°	+0.001°	63°/s	0.004°	0.005°	0.015°	0.070°
axial Torsion ( $M_z$ )	2000 Nm	+20°	$\pm 0.0005^\circ$	135°/s	0.002°	0.006°	0.018°	0.070°

The Table 2-1 above shows the specification of the hexapod in all 6DOF, however the aim of this project is high speed axial impact, therefore the datum for axial loading have to be considered for this study. It is important to mention that this force can be applied in either the compressive or extension direction (Ding et al. 2014). It is normally used to test sheep and human spines, knee joints and wrists, bones, soft tissues and some medical devices (Boyin et al. 2011; Fraysse et al. 2014). The force is generated by the actuators using the parameters that are set using computers. The hexapod is connected to two computers where one is used to set the parameters and the second controls the hexapod and collects the data. It has sensors that assist in the accuracy of the positional displacement (Ding et al. 2014).

This robot would be preferable for current testing however, its parameters discussed above are the limitation in using it as the main objective was to test at a high speed more than 3 m/s and a height of at least more than a half a metre.

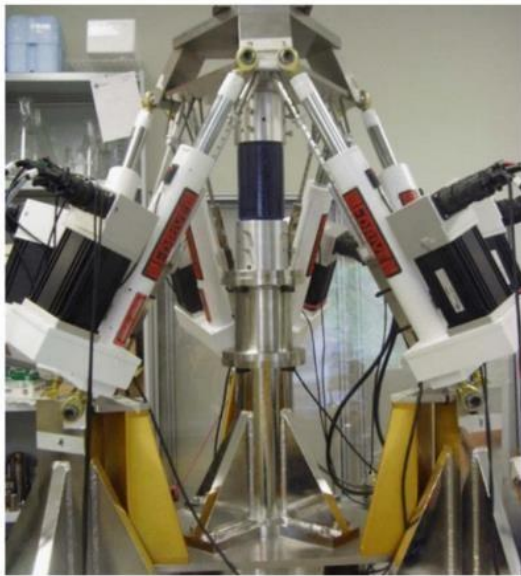


**Figure 2-12: Flinders hexapod 6 DOF robot. It is used to test specimens in six degrees of freedom. it can apply compressive or extensive forces (Boyin et al. 2011).**

### 2.3.6 Flinders drop tower

The initial aim of tests was to use a Hexapod machine; however, its parameters were not suitable to the model of this study. Luckily, a drop tower was being built at Flinders University for other purposes. When it was finished, it was found to better suited to the experiments required for the current study. This drop tower has a maximum height of one metre and the capability of supporting around 31 kg. The required height at testing could be adjusted at the intervals of 20 or 40 mm.

## 3. Aims

The main goals of the project were to investigate loading techniques to create reproducible thoracolumbar burst fractures and compare the results with the clinical cases reviewed in the literature review. In addition, this study would provide a recommendation on the thoracolumbar burst fracture treatment based on the observation of the results and potential of future work.

The planned number of specimens to be used was twenty-four sheep specimens that would be assessed to be free of defect before starting the tests.

---

### 3.1 Updated aims

Due to limitations discussed in section 2.3.5, the preliminary aims were modified with new objectives of reproducing Thoracolumbar Burst Fractures using a drop tower, test three groups of sheep specimens T12-L1, T13-L2, and then T12-L2 without any induction of injury in the specimens and compare the results in the three groups with the clinical cases from literature review and also provide a recommendation for future work.



---

## 4. Current testing methods

This section contains all the steps and procedures taken to conduct the experiment. It includes specimen preparation, potting, testing and data collection stages. It also defines the details why sheep specimens were used for this study.

### 4.1 Sheep specimens

Normally, human specimens would be ideal for this study; however, they were difficult to obtain due to their large cost, difficulty to find, need of ethics approval that would take some time to be granted and the limited time frame for the Thesis. Compared to the abovementioned human specimens, sheep specimens were found to be cheap, easy to find and have been proved by researchers to be a good model of study for human spines (Sheng et al. 2010). Furthermore, the literature had shown that sheep have close similarity with humans in the lower thoracic and upper lumbar regions in terms of range of motion (Wilke, H. J., Kettler & Claes 1997) and geometrical structure (Wilke, Hans-Joachim et al. 1997). These factors were the key considerations for making the decision to go with the sheep model for this study. Even though the sheep was considered, there are still some dissimilarities in the structure and mechanical properties. In humans, the thoracic section has twelve vertebrae while in the sheep model the spine is made of thirteen. This means that T12 in humans corresponds to T13 in sheep. It has also been proven that sheep bones are more compact and present higher fracture stress compared to human bones (Aerssens et al. 1998). Also based on the study of Aerssens et al (1998), human spine appears to show the lowest fracture stress than quadrupled meaning that axial impact of the sheep specimens may provide results that are slightly different from human specimens. These differences will be kept in mind while analysing the data.

### 4.2 Specimen preparation

All steps taken from soft tissue removal to cutting the specimens to the size required are specified in this section.



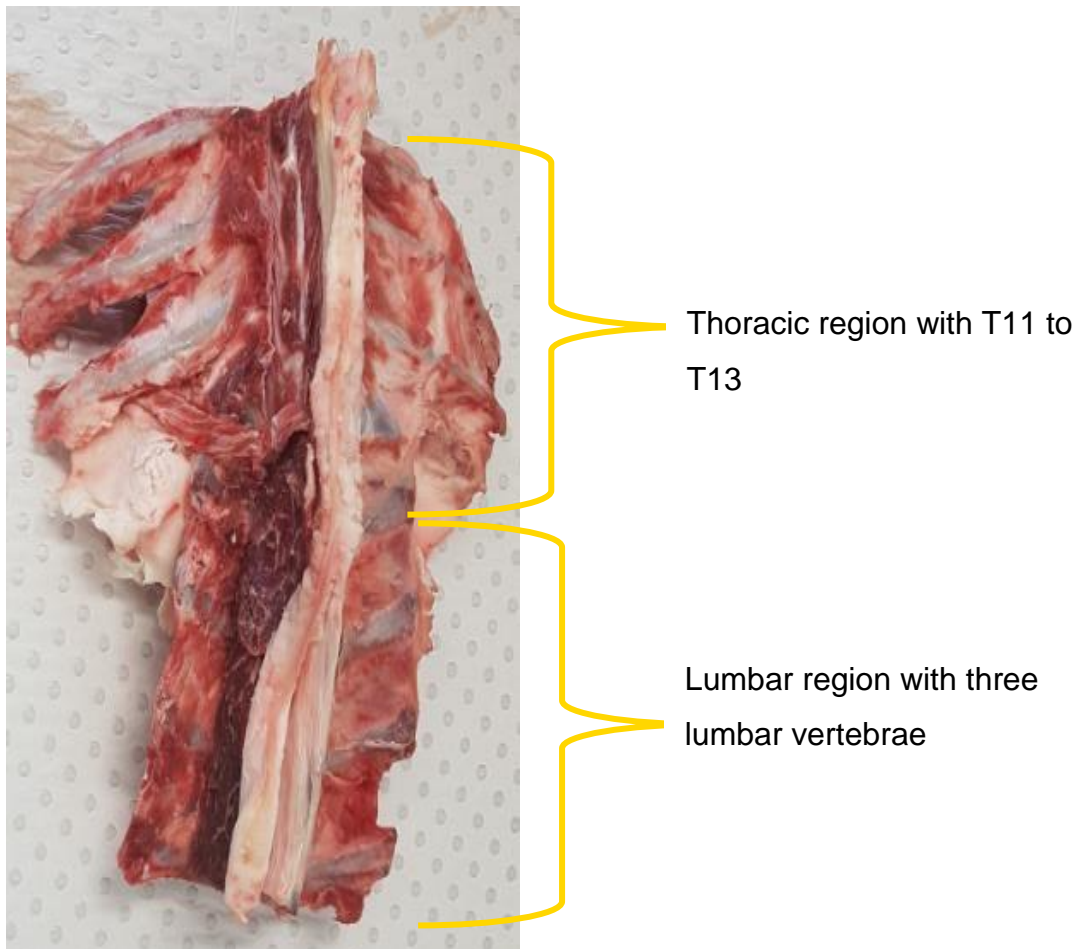


**Figure 4-1 - Fresh unclean thoracolumbar with Three thoracic and three lumbar vertebrae.**

Twenty-four specimens were collected from Austral meat and kept in a freezer in a biomechanical and implant laboratory at Flinders University, as shown in Figure 4-1. They were stored at a temperature of minus twenty degrees Celsius before they were used. The preparation of specimens involved defrosting them for three hours followed by a careful removal of soft tissues using size twenty blade, scalpels and forceps (Figure 4-2) while taking care not to damage the ligaments or bones.

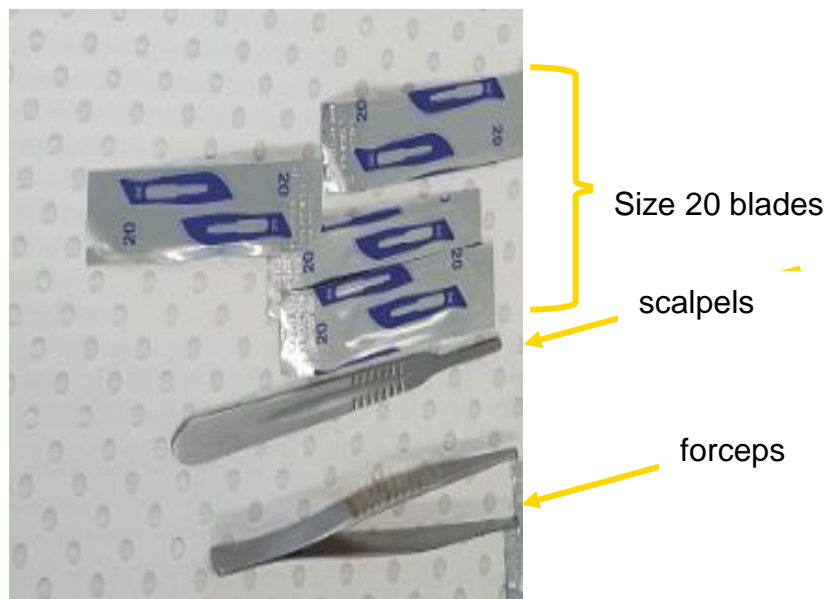


**Figure 4-2 - Equipment used to clean the specimens.**

After the removal of soft tissues, the specimens were then wrapped into paper towels, sprayed with normal saline to ensure they didn't dry out, placed in zipped plastic bags (Figure 4-3) and again placed them back in a freezer at same temperature of minus 20°C until they were ready to be tested.



**Figure 4-3 - Specimens with removed soft tissues, wrapped in paper towels, sprayed with normal saline and then zipped in plastic bags.**

Freezing the specimens before testing would not have made much difference compared with if they were tested before being frozen (Panjabi et al. 1994). When specimens were ready to be used, they were divided into three groups of eight specimens each. The first and third groups had segments of three vertebrae ranging from T12 to L1 and T13 to L2 respectively while the second group contained segments of multiple vertebrae ranging from T12 to L2. These specimens were then cut to the above-mentioned sizes using a bandsaw as shown in Figure 4-4.



**Figure 4-4 - Sheep specimen with removed soft tissues and cut at T12 L1 using a bandsaw.**

Before any potting was done, all the heights, anteroposterior (AP), and lateral measurements of the vertebrae and discs were taken for all the specimens using a calliper (Figure 4-5) and recorded in a spreadsheet.



**Figure 4-5 - measuring the heights and discs of the specimen with a calliper**

To ensure the accuracy, each of the measurements discussed above was taken three times and the average was taken as the final value.

### 4.3 Specimen potting

This step was performed by placing both ends of specimen into two aluminium cups and potted using polymethylmethacrylate (PMMA) powder and monomer agent liquid while leaving the vertebrae to be tested free between the cups. The procedure was done for all three groups of specimens. Note that the note that the free vertebrae of the multi-segment specimens were T13 and L1 while for the other two groups, they were T13, and L1 respectively. To secure the specimens into the cups and ensuring the PMMA didn't break while testing, three screws were used in each cup and screwed all the way through until they lightly clamped the specimen. Full procedure for the potting can be referred to from the Appendix A The potted specimens were left in the fume hood for fifteen to twenty minutes and sometimes longer to ensure they were properly dried, then taken for testing. Figure 4-6 and Figure 4-7 show one of the specimens in the bottom cup before and after the specimen was potted.

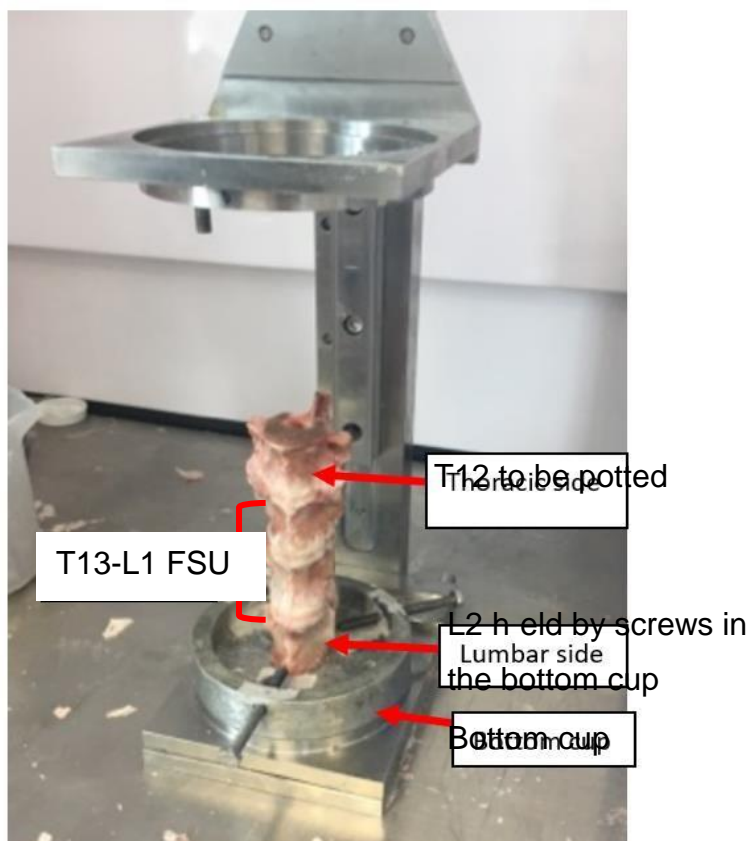


**Figure 4-6 - Specimen in the group of T13-L1 that is ready to be potted. It is held in the centre of the cup by three screws.**

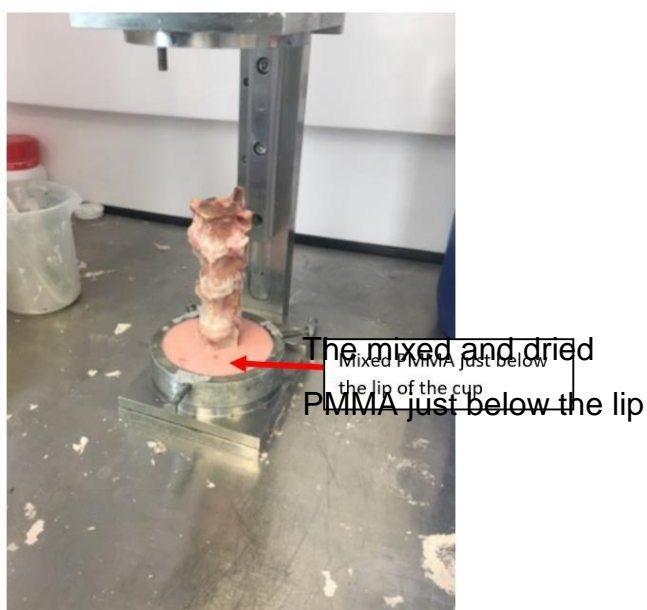


**Figure 4-7 - L2 of the specimen potted in the bottom cup using PMMA and monomer liquid.**



---

#### 4.4 Testing procedure

Testing was conducted into two sections where the first was pilot testing to investigate what the appropriate weight and height would be to generate reproducible burst fractures while the second section was the final tests after finding the needed parameters. Before any of the specimens was impacted, specimens were mounted on an adaptor plate and secured on an 'xy table' on the base of the drop tower vertically in line with the impact load cell using clamps (Figure 4-8). The alignment with the load cell was to avoid any flexing of the specimen that would damage it.

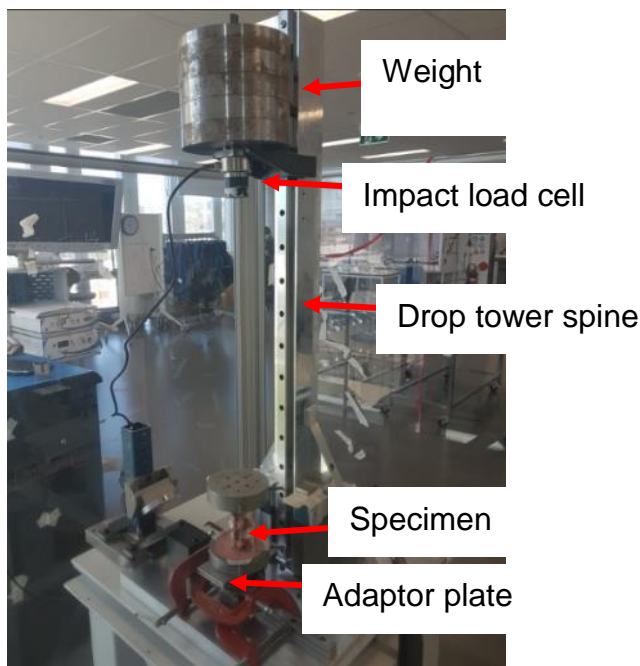


**Figure 4-8 - Specimen mount on the base of the drop tower and aligned with the impactor load cell.**

The xy table assisted in the alignment of the specimen and the impactor of the drop tower. A weight of 28.5 kg was then loaded on a mallet above the impact load cell and secured with another mallet and a nut. The distance between the top cup and the impact load cell varied between 49 and 55 cm depending on the height of the specimen between the cups.

After all the measurements were taken, the impactor load cell was connected to PC and some screen guards placed between the operator and the drop tower for safety. An extended string was then used to pull a trigger, dropping the mass on top of the top cup. Three operators were required in this instance; one to pull the trigger, the second person to

---

video the tests with a smart phone; and the third operator to collect the data using software. After each test, some pictures were taken using a smart phone in addition to the tested specimens being X-rayed to check the extend of the fracture and analyse if the burst fracture had occurred or not. After this step, specimens were dissected to check if there were any fragments pushed in the spinal canal. However, some of them didn't need to be dissected as the fragments were seen on the spinal cord right after the BF. The observation was recorded, and the dissected specimens were kept in a freezer for future reference during this project. The data was collected using the labview data acquisition software running on a computer connected to the impact load cell and analysed with Matlab software. The data was set to be collected at the frequency rate of 20 KHz. The full procedure taken to set up the software was provided by the Engineering Services team and can be referred to in the Appendix B.

X-ray images were taken after each specimen's test by an experienced PhD student who is licensed to use the X-ray machine at Flinders University. Two images of both lateral and AP (anterior-posterior) were taken once the potted specimen was placed on a bench under the X-ray machine in a perpendicular position.

#### 4.4.1 Pilot testing

Seventeen specimens were used for pilot test while varying the drop mass in three groups. 23.5 kg were used on four specimens while 26 and 28.5 kg were used on six and seven specimens respectively. The observations indicated that 28.5 kg at the height of 0.5 m was more promising in producing reproducible BF (Figure 4-9). These parameters resulted in the energy of around 140 joules and drop speed of around 3.2 m/s. As seen earlier in the literature review, other studies have used speeds between 3 and 6m/s and energy varying between 35 to 160 joules. This led to the conclusion that a 28.5 kg drop mass at 0.5 m height was reasonable for current testing to reliably reproduce Burst Fractures.



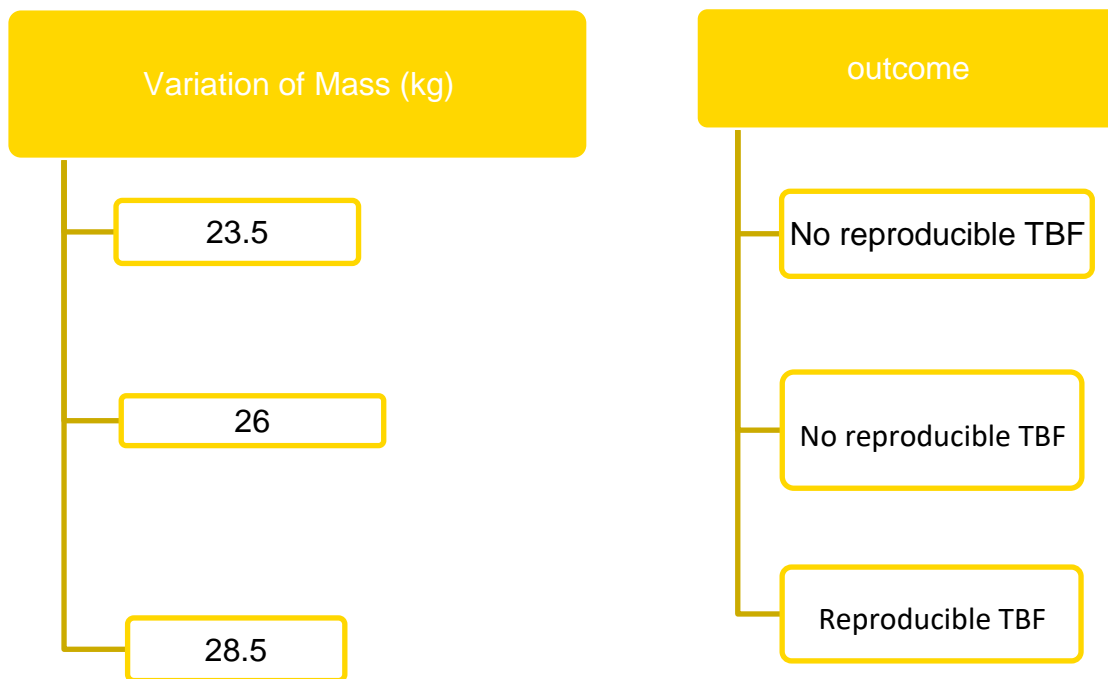


**Figure 4-9 - Variation in pilot testing and the outcome. An impact mass of 28.5kg showed a higher chance of producing a reproducible burst fracture.**

#### 4.4.2 Final tests

The planned total number of specimens for final testing was twenty-four sheep specimens divided into three groups of eight each (Figure 4-10).

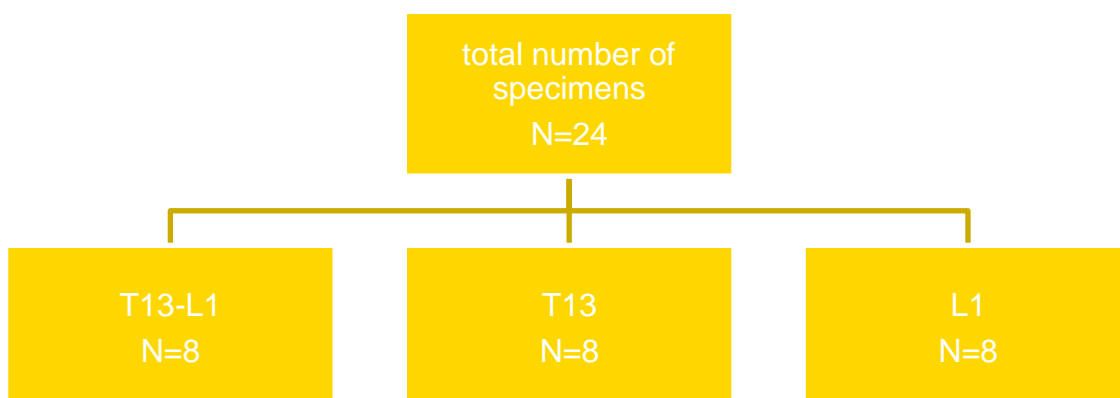


**Figure 4-10 - Total number of required specimens and its subdivision.**

As discussed in Section 4.4.1, the energy of 140 Joules was decided to be used to produce TCBF. This was achieved by using the weight of 28.5 kg at a height of 0.5 m; however,

---

heights of specimens varied between 0.49 and 0.55 m which led to the impact of some specimens with a 28.5 kg weight and others with 31 kg for keeping energy consistent.

#### 4.4.3 X-ray imaging

After each specimen was tested, a lateral and anteroposterior x-ray image was taken to analyse the nature of created thoracolumbar burst fractures. This was performed by placing the fractured specimen either in the lateral or anteroposterior position on top of a table and projecting the x-ray in vertical position.

#### 4.4.4 Statistical analysis

To validate the results, statistical analysis of all three groups was performed using a univariate ANOVA for stress per unit energy, Post-hoc multiple comparisons using a Bonferroni correction on alpha, and a post-hoc power using G\*power software.

This concludes the experiment method description with the following chapter detailing the results of the final tests, their analysis and discussion.

## 5. Results

This section encompasses the results from the geometrical measurements of the specimens, which includes the height, lateral and AP widths of both vertebral body and disc, figures of burst fractures resulting from high speed impact and from X-ray images of tested specimens as well as the Matlab graphs indicating the forces used to create the Thoracolumbar Burst Fractures.

### 5.1 Geometrical measurement results of all three specimen groups

As discussed in the method, each geometrical measurement was taken three times and then the average calculated to ensure the accuracy; however, in this section only the tables of average values are presented. The measured parts of the specimens were the discs and vertebrae that were not meant to be potted. Each of Table 5-1 to Table 5-3 indicate the average geometrical measurements of individual groups of the specimens and the mean values and standard deviation of all of all specimens.

Note descriptions of the notations in tables bellow: T13/L1 (H) represent the measurements of heights of T13 and L1 vertebrae respectively, Lat/AP represent lateral and

anteroposterior measurements of the vertebrae respectively while T12-T13 (H) and T13-L1 (H) represent the measurements of heights of discs. All the measurements are displayed in millimetres

**Table 5-1 Mean and SD values of T13 free vertebrae in mm.**

Specimen number	22	23	24	25	31	39	40	41	Mean	SD
T13(H)	29.8	30.9	27.6	29.3	26.5	30.9	28.9	27.7	29.0	1.6
Lat	25.5	30.5	20.7	30.0	28.7	29.5	27.9	27.9	27.6	3.2
AP	19.3	24.1	26.5	20.3	21.0	22.0	20.1	21.5	21.8	2.4
T12-T13(H)	4.3	5.1	2.7	4.3	4.5	3.4	3.4	3.7	3.9	0.8
LAT	22.2	23.9	22.5	22.6	24.7	25.5	23.9	24.5	23.7	1.2
AP	23.0	23.2	23.1	12.9	14.3	15.9	16.0	13.5	17.7	4.6
T13-L1(H)	4.2	4.3	3.4	4.1	4.2	3.5	3.6	3.4	3.8	0.4
LAT	23.3	26.5	17.6	26.1	24.3	26.4	25.8	24.8	24.4	3.0
AP	21.7	22.6	23.7	21.3	19.8	21.4	19.5	20.4	21.3	1.4

**Table 5-2 Average geometric measurements of T13-L1 free in mm.**

Specimen number	18	19	20	21	32	33	34	38	Mean	SD	
T13(H)		27.9	25.0	28.9	29.9	31.8	33.0	28.0	28.4	29.1	2.5
Lat		27.7	25.4	27.1	24.8	28.0	29.6	25.9	28.8	27.2	1.7
AP		21.5	21.3	20.1	18.5	19.4	23.0	20.3	22.3	20.8	1.5
L1(H)		28.5	32.7	32.9	32.7	32.1	34.2	29.9	31.1	31.8	1.8
LAT		26.8	25.2	25.8	24.2	26.6	29.6	24.9	29.5	26.6	2.0
AP		22.1	19.6	19.5	18.6	20.2	22.0	20.2	22.4	20.6	1.4
T12-T13(H)		3.6	3.7	4.2	4.0	4.0	4.4	4.0	3.0	3.9	0.4
LAT		22.5	22.4	22.9	22.8	25.2	26.8	21.9	23.8	23.5	1.7
AP		24.5	21.9	21.0	22.3	16.0	11.3	13.6	15.9	18.3	4.7
T13-L1(H)		3.8	3.9	3.4	4.5	4.3	4.7	4.5	3.3	4.0	0.5
LAT		22.8	24.4	23.5	23.8	25.1	27.9	21.9	26.8	24.5	2.0
AP		21.8	21.1	21.4	20.1	20.8	22.2	19.7	20.3	20.9	0.9
L1-L2(H)		3.9	4.1	3.4	4.8	4.7	3.9	4.4	3.9	4.1	0.5
LAT		22.9	24.8	24.7	23.8	25.8	29.7	23.1	26.5	25.2	2.2
AP		23.4	22.5	21.2	20.6	22.9	25.2	21.2	22.4	22.4	1.5

Table 5-3 - Average geometric measurements of specimens with L1 free in mm.

Specimen number	26	27	28	29	30	35	36	37	Mean	SD
L1(H)	30.1	32.1	32.9	26.5	30.2	28.1	30.0	29.5	29.9	2.0
LAT	27.8	19.6	20.2	18.5	20.7	27.3	27.2	25.3	23.3	3.9
AP	22.4	22.3	26.8	26.0	28.0	20.4	21.3	19.0	23.3	3.3
T13-L1(H)	4.8	3.8	4.3	4.0	3.6	3.7	4.3	3.9	4.1	0.4
LAT	25.0	19.2	19.6	17.2	19.7	25.4	24.3	24.6	21.9	3.3
AP	24.3	22.1	24.8	24.7	24.2	20.4	22.9	20.6	23.0	1.8
L1-L2()	3.9	4.2	3.5	3.7	3.3	4.1	3.8	3.7	3.8	0.3
LAT	26.0	20.1	19.3	20.6	20.0	24.6	25.4	24.3	22.5	2.8
AP	25.1	22.3	24.2	24.5	25.4	23.4	22.3	21.8	23.6	1.4

The results obtained in the above tables were compared with the dimensions in literature review where the mean  $\pm$  SD values were  $30.3 \pm 2.5$  mm,  $33 \pm 1.8$  and  $36.2 \pm 0.8$  for T12, T13 and L1 respectively (Mageed et al. 2013). Current dimensions had shown that previous study presented 5.35% higher in L1 and 4% in T13. Therefore, this study deems that this difference is minimal, and consequently, the results of both studies can be compared.

## 5.2 Force and energy required to produce burst fractures.

As was stated earlier in the pilot testing section, the energy required to produce Thoracolumbar Burst Fractures was determined to be 140 joules; however, there was slight alterations due to the heights of specimens and limited level of adjustment of the drop tower. To insure the energy was close to 140 joules as possible, some adjustments were made by increasing or decreasing the weight to counter the modification of drop height. The maximum weight applied was 31 kg at a height of 49.5 cm while the minimum was 28.5 kg at the height of 54 cm (Table 5-4).

As it will be seen in the following section, the overall forces that produced burst fractures varied from 3072 to  $5505 \pm 910$  N for T13, 2621 to  $6506 \pm 1337$  N for T12-L2, and 2525 to  $6278 \pm 1382$  N for T13 – L2. However, some of specimens from same groups were found to have similar forces. The required forces were calculated by taking the maximum force minus the threshold as shown in the plot (Figure 5-1).

By analysing the forces group by group, it was obvious that the lowest and highest forces were from the group of T12-L2 while the lowest was seen in the T13-L2 group. As it was shown in Table 5-4, T12-L1 had the lowest maximum and the highest minimum force followed by T12-L2. Also, its standard deviation was the smallest followed by the SD of

T12-L2. This indicates a greater consistency in the forces that created the fractures in T13 free vertebra. The higher variation in the group of T12-L2 might be a result of instability while testing caused by its height and it has the highest number of intervertebral discs which absorbs energies differently.

Table 5-4 Table of energies and forces used to produce FSUs fractures.

<b>Group</b>	<b>T1 2-L1</b>		<b>T12-L2</b>		<b>T13-L2</b>	
<b>Specimen number</b>	Force (N)	Energy (J)	Force (N)	Energy (J)	Force (N)	Energy (J)
<b>1</b>	4273*	138	4614*	144	2525	135
<b>2</b>	3072	134	4769*	128	4614*	135
<b>3</b>	4609*	140	3956*	128	4603*	135
<b>4</b>	3344*	137	3956*	128	2369*	138
<b>5</b>	4760*	138	2621*	130	2406*	135
<b>6</b>	5505	140	6506*	139	6278	141
<b>7</b>	5503*	140	6502*	139	3354*	138
<b>8</b>	5024*	140	5506*	142	3357*	141
<b>Mean</b>	4511	138	4804	135	3688	137
<b>SD</b>	910	2	1337	7	1382	3

Note: the numbers with an asterisk (\*) represent forces that created burst fractures in each group.

Table 5-4 showed a significant variation of forces across specimens in the same group. The minimum force needed for fracture was in the T13-L2 group while the maximum was in T12-L2 group, with the maximum force being almost three times the minimum. Even with this latter group having the highest force to create Thoracolumbar Burst Fracture, its mean value

---

was lower than the mean value of T12-L1 while the SD was higher than the other two groups (Table 5-4). This indicated an inconsistency in the force readings for this group. The mean value was higher in the T12-L1 group while the SD was very similar in both the T12L1 and T13-L2 group. This indicates that the quality of results obtained in the single FSUs is higher than those for the group of multilevel FSUs. However, the adjustment of the weight based on the variation of the height has maintained the consistency of energy as it can be seen in Table 5-4.

### **5.3 Impact of free vertebrae's geometry on fracture forces**

To examine if a higher force was generated in a specimen with higher geometrical values or vice versa, the mean values of each specimen in each group was compared with the mean values of the geometrical measurements for the same specimen in Table 5-1 to Table 5-3 the comparison indicated that some of the geometrical mean values were higher while a low force was generated for the same specimen and vice versa. This was an indication that forces were independent of the geometrical dimensions of specimens. The mean values considered were the measurements of the vertebrae and intervertebral discs of each specimen.

### **5.4 Fracture results of all FSUs and observation**

This section shows the picture of one of the fractured specimens, its x-ray image and the MATLAB plots of the corresponding forces. A full record of the rest of specimens is presented in the Appendix C.

It was seen that some of the specimens did not show burst fractures while some of the forces plot indicated some noise in the measurements. The noise might have been caused by the blocks that were used for the masses not being firmly tightened and rebound impact caused by the bounce after the initial impact.

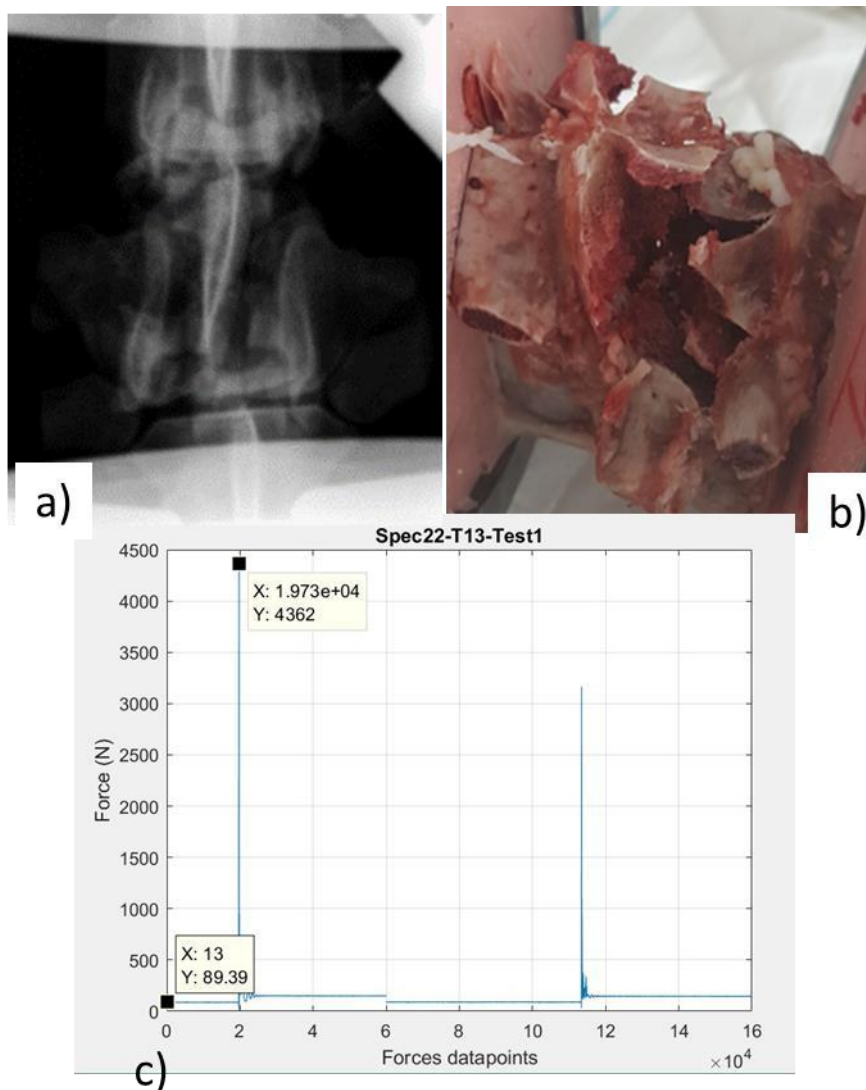


**Figure 5-1 a) represents the burst fracture x-ray image of T12-L1, b) the burst fracture and c) the MATLAB plot showing the corresponding forces applied on impact.**

A visual observation of the fractured specimens was then done for all the test results of the three groups (T12-L1, T12-L2 and T13-L2). This included analysing the images taken after each test, watching a slow motion of the videos taken with a smart phone, and analysing the X-ray images of the tested specimens. Lastly, a force graph for each specimen was generated and grouped in one figure to facilitate the analysis. This is illustrated in Figure 5-1.

---

#### 5.4.1 Fracture results of T12-L1

In this part, only T13 was exposed between two cups. The goal was to create reproducible burst fractures at T13 and to analyse the force needed for its reproduction.

In this group, the tests resulted in a similar burst fracture created in six specimens, while the other two fractured at the discs. Of these two, both showed flexion fractures with one of these presenting a fracture at both the superior endplate of L1 and inferior endplate of T12 leaving T13 intact in the middle. The other specimen fractured at the top endplate of T13 and showed a slight opening at the top endplate of L1. The nature of the fractures indicated that there might have been some type of flexion while testing. However, there is no large difference in forces even though the specimen that fractured at two endplates showed the lowest force for the group. These two specimens did not show any presence of bone fragments on the spinal cord; even the X-ray images didn't show much damage on the FSUs. All other six specimens produced reproducible burst fractures and had shown small number of bone fragments pushed against the spinal cord. The slow-motion videos taken with a smart phone indicated that the fractures were being initiated at the lower endplate of T13 and spread in the vertebra body. Four of the specimens with TLBF had vertebra bodies and spinous process crushed completely while the other two specimens had shown anteroposterior split and shear of the spinous process.

#### 5.4.2 Fractures of T13-L2

As in the T13 FSU group, half of T13 and L2 vertebrae were potted in two cups leaving L1, T13-L1 and L1-L2 discs free between. This group had burst fractures at L1 in five specimens with one of them having double fractures. This specimen burst fractured in the vertebral body and snapped at the lower endplate of T13. These five specimens were damaged such that some bone fragments could be seen against the spinal cord. The other three specimens produced similar fracture at T13-L1 disc with no appearance of bursting. Two of them initiated the fractures at the lower endplate of T13 and extended the fractures in the un-potted half vertebrae of T13 while the other one fractured at the upper endplate of L1 with no appearance of severe damage. The specimens that presented burst fractures of vertebra bodies showed fractures of the spinous process as well. These fractures were confirmed by the x-ray images; however, one of the specimens had the top half snapped off during testing therefore its X-ray was not taken even though it showed a few splits in the



---

vertebra body. Two of the specimens that didn't burst showed lower forces compared to the others; however, the third one had the highest force in this group.

#### 5.4.3 Group of multilevel free vertebrae (T12-L2)

The main objective of this section was to produce burst fractures in multilevel FSUs, made up of two vertebrae and three intervertebral discs free between two cups, and determine what vertebra would fracture, the nature of that fracture, the area of initiation, and the force required to cause it to fail. The FSU used was made of T13 and L1 vertebrae, T12-T13, T13-L1, and L1-L2 intervertebral discs. Using the same procedure as in the previous two groups, the potting process made sure only half of T12 and L2 were potted.

After testing the T12-L2 group, it was observed that all specimens provided reproducible burst fractures. Six of them had similar fractures at T13 initiated at its lower endplate extending upward into vertebral body. The other two specimens burst fractured at L1.

Contrarily to the other six, these fractures were initiated at the upper endplate of L1 with no to minimal damage on the disc or on the spinous process. Forces used to create burst fractures were higher compared with the forces in the rest of specimens in this group. This might have been caused by age differences. It has been discussed that in humans, the fracture toughness and strain reduces about 10% per decade (Osterhoff et al. 2016). Considering that the last three specimens were ordered differently from the first five, this would mean that they differed in their ages leading to this difference of fracture forces. By analysing this group of specimens separately from the other two groups, it can be concluded that the fracture rate of T13 and L1 vertebrae is 3:1. While the forces required to produce burst fractures at L1 were higher in T13-L2 compared with T12-L1.

#### 5.4.4 Visual examination of fractures

All three groups showed reproducible burst fractures in most of the specimens with a small number of exceptions in the T12-L1 and T13-L2 group. Both these groups produced a more consistent fracture loading force compared to the T12-L2 group, however T12-L1 showed more specimens with burst fractures and corresponding higher loadings than in T13-L2. In the group of T12-L2, there were more fractures at T13 than at L1 which agrees with the

---

findings in literature that discuss that the tendency to fracture is higher in the upper region of the spine than in the lower region (Hongo et al. 1999); however, higher force was generated in the burst fractures at L1. The burst fractures in this group were very similar to those produced in the single T12-L1 and T13-L2. As discussed earlier, most of burst fractures would initiate at the lower end plates. This correlates with the discussion of Zhang et al 2017 who observed that with a high-speed loading, there is a generation of high pressure in the intravertebral disc which results in the fracture of vertebral cortex. Secondly, this paper discussed that the superior layer is weaker than the inferior layer which again correlates with the results obtained in this study.

#### 5.4.5 Classification of burst fractures based on the observation and X-ray images

Based on the classification of Denis (Baker 2014), all the specimens tested in group T12L2 produced type A burst fractures, where the fracture resulted from compression; six specimens in group T12-L1 resulted in type A while the others were classified as type B and C each. T13-L2 produced type A burst fractures only (Baker 2014). Considering the discussion on the severity of each type, group T13 produced two fractures in the type B and C category, meaning that it produced more fractures with severe complications compare to the other groups.

### 5.5 Comparison of the result in all three groups and the literature

In this section, a comparison will be conducted based on the visual examination of fractures, forces produced and statistical comparison of stress on energy for all three groups and then validated using the literature review.

#### 5.5.1 Forces comparison

In Table 5-4, the forces have been shown together with energies of each specimen. The difference between these groups indicate that the mean value of T12-L2 is 293 N higher than T12-L1 and 1116 N higher than T13- L2. This means that the mean value of L1 is the lowest in all groups with T12-L2, being the highest. However, the SD of T12-L1 is lower compared to the other groups Table 5-4). This implies that there was not a big variation between the forces within this group. These differences are also illustrated in Figure 5-2 that shows the plot of these mean values.

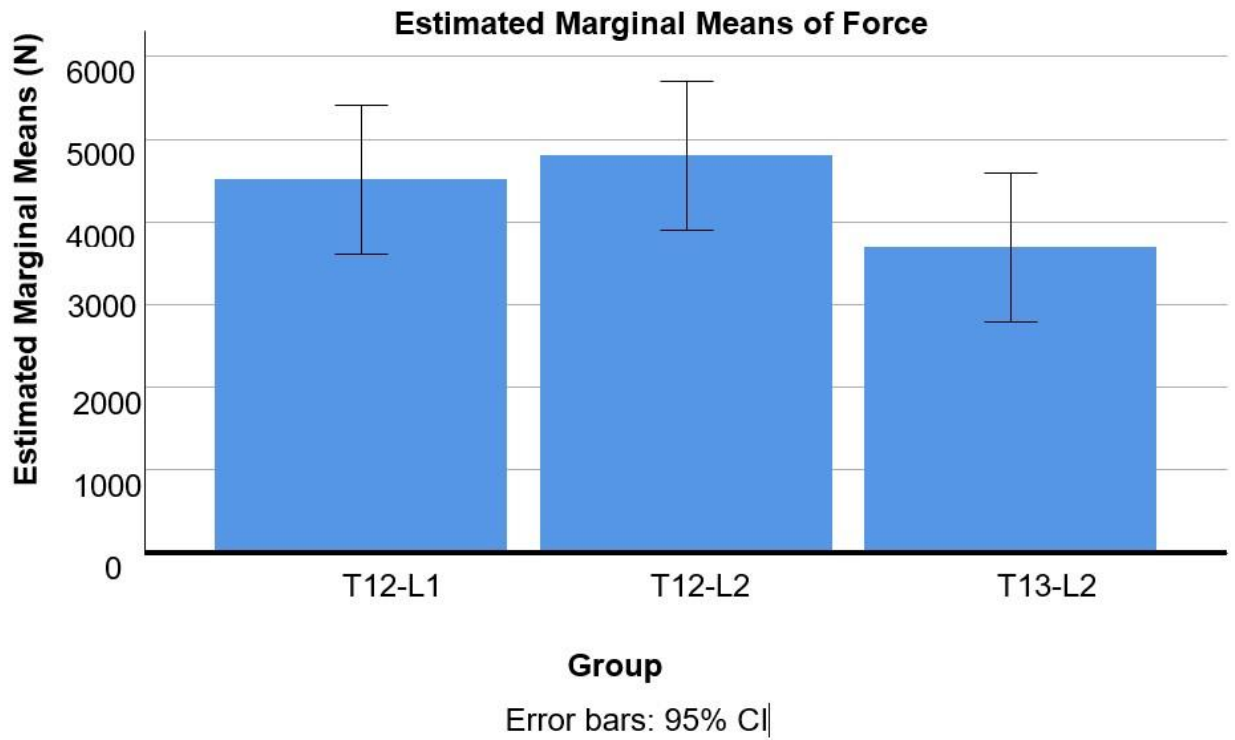


Figure 5-2 Comparison of mean value forces based on eight specimens in each group.

Also, the groups were compared using marginal mean values of forces divided by energy.

This has also shown similar results as the comparison of mean forces (Figure 5-3)

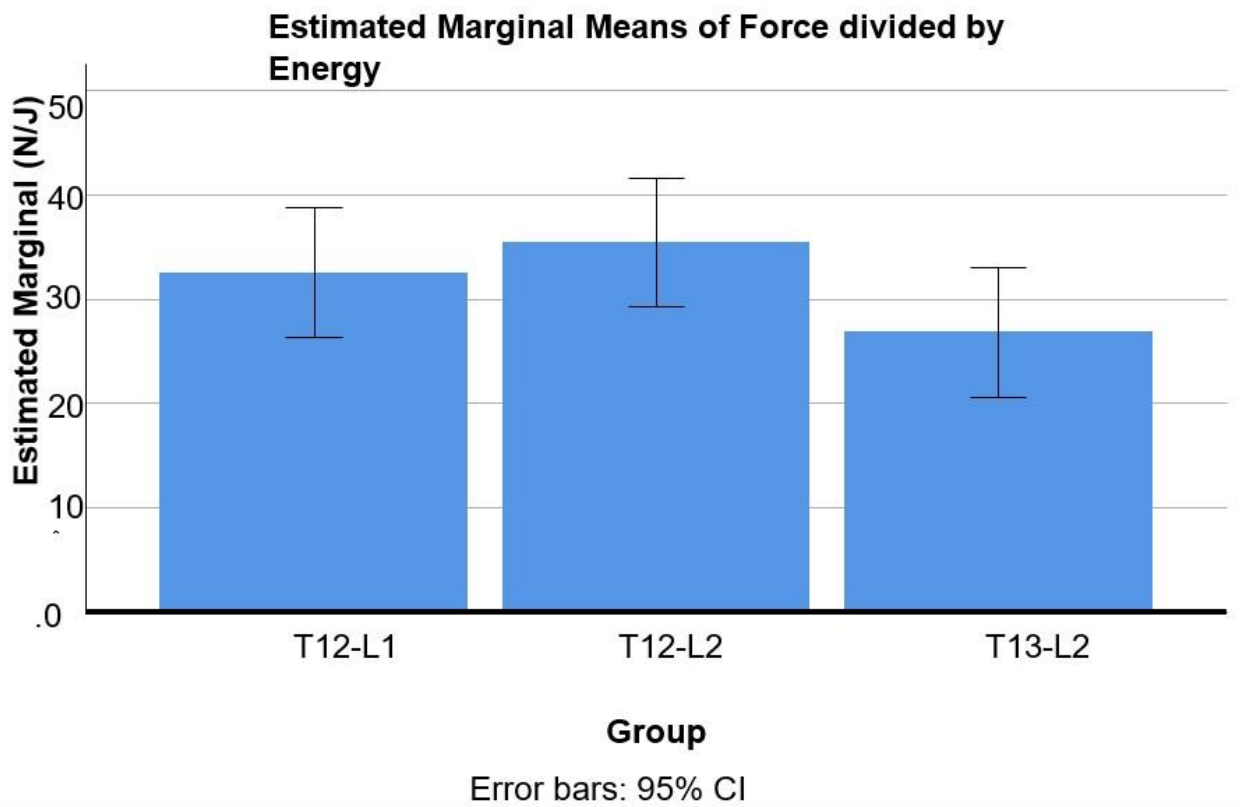
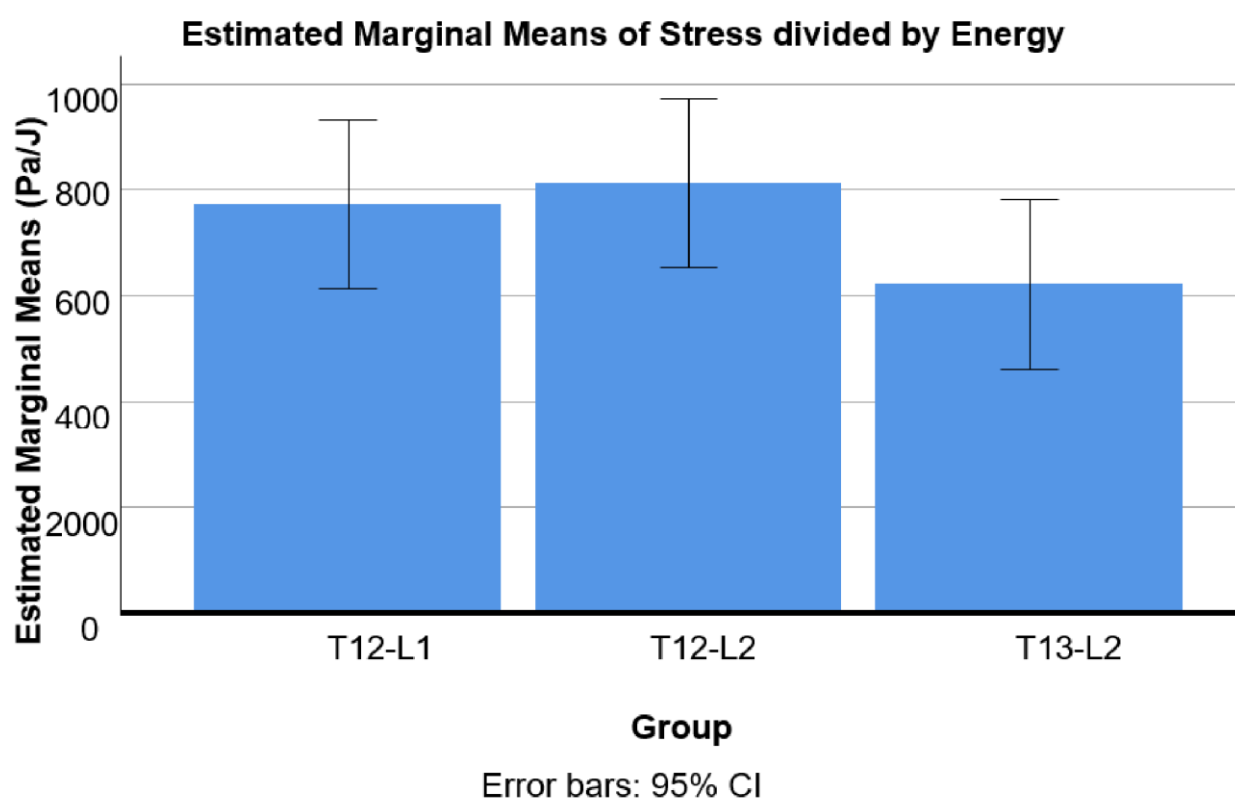


Figure 5-3 Comparison of forces by dividing the mean values of forces by mean values of energies.



**Figure 5-4 Comparison of T13, T13-L1 and L1 based on the mean values of stresses divided by the mean values of energies.**

### 5.5.2 Statistical comparison

To determine whether there were any differences between all three groups, a univariate ANOVA was performed on the dependent outcome measures of stress per unit energy having an independent factor of group (T12-L1, T12-L2 and T13-L2). Post-hoc multiple comparisons using a Bonferroni correction on alpha were performed when significant main effects were present. A post-hoc power analysis was conducted using G\*POWER, a power analysis software program using a type II error of 0.2, and a type I error of 0.05 (Erdfelder, Faul & Buchner 1996), based on the overall effect of the three groups. The results from this analysis have indicated that there was no significant effect of group on stress per unit energy ( $p = 0.205$ ). According to the power analysis, 25 specimens in each group would be required to detect the present differences between groups as significant if the standard deviation was to remain without changing.

---

## 6. Discussion

As was mentioned earlier, the aim of this study was to investigate loading techniques to create thoracolumbar burst fractures and compare the obtained results with clinical cases reviewed from the literature.

### 6.1.1 Comparison of the results with the Literature

The current study produced burst fractures using the energy of  $138 \text{ J} \pm 2 \text{ J}$ , for T12 -L1 group,  $135 \text{ J} \pm 7 \text{ J}$  for T12-L2 group and  $137 \text{ J} \pm 3 \text{ J}$ . The mean forces were  $4511 \text{ N} \pm 910 \text{ N}$ , for T12-L1, group,  $4804 \text{ N} \pm 1337 \text{ N}$  for the T12-L2 group and  $3688 \text{ N} \pm 1382 \text{ N}$  for T13L2 group. The results from literature have indicated that several other related studies were conducted using different specimen models, different energy levels and induced injuries according to the location aimed for its production Cotterill et al. (1987). With the study done by Cotterill et al (1987), a young calf was used with a mass of 32 kg dropped from a height of 1.55 m, which resulted in an energy of almost 486 Joules. Comparing this result with results from this current study, it shows that their energy was about 3.5 times higher. Note that Cotterill et al (1987) had also induced an injury on the disc and vertebra body of L1 prior to impact to allow its fracture. The induction of injury makes sense, because they managed to create reproducible burst fractures at L1 only; however, the above study has not discussed the forces used to create this fracture. Furthermore, the study by Zhang et al (2017) and Shono , McAfee and Cunningham (1994) showed the forces of  $4020 \text{ N} \pm 1900 \text{ N}$  while another study conducted with compressive load tests on T10 to L1 of human specimens without any induction of injury showed a fracture load force of 2809 N (Langrana et al. 2002). Many reviewed studies indicated that the specimens used to test thoracolumbar junction were humans and calves (Ching et al. 1995; Fredrickson, BE et al. 1992), yet, in all the papers reviewed, there was none that used sheep model for this sort of study.

Considering the results obtained in section 5.4.1 to 5.4.3, reproducible Thoracolumbar burst fractures were obtained from all specimens of multilevel vertebrae, five in T13-L2 and six in T12-L1 groups. The T12-L2 group has shown that T13 vertebrae are more vulnerable to fracture compared to L1. This finding contradicted some claims that that most of the injuries occur at L1 (Ivancic, Paul C 2014; Panjabi et al. 1995). This also emphasised the force used to generate these fractures. It was obvious that both specimens in T12-L2 group which

---

had fractures at L1 used a higher force compared to the other six Table 5-4. This group had also the highest loading forces while the lowest was found in L1 group (Table 5-4).

Similarly, the highest and lowest mean values were obtained in the T12-L2 and T13-L2 group respectively. This means that a multilevel vertebra FSU requires more force to be fractured compared with the other two groups, which might be caused by additional discs absorbing more energy. By analysing the standard deviation, it was observed that T13 had a lower standard deviation of 9.1% while T12-L2 and T13-L2 groups had 13.37% and 13.82% respectively. This would be interpreted as having more consistent forces in T12-L1 group compared to the others. By comparing the mean values of forces in the three groups it is obvious that there are differences; however the statistical analysis ( $p > 0.05$ ) has shown that this difference is not significant (Erdfelder, Faul & Buchner 1996; Zhang et al. 2017). The Force divided by energy and stress divided by energy results also indicated the same conclusion of not having significant differences of forces to create TLBF as in all cases  $p$  was greater than 0.05. As it was discussed in section (6.1.1), some of the forces in the current study were higher compared with the forces reviewed in the literature. This would have been caused by several factors which include the difference in specimen models used, the age of sheep specimens, what they were fed and the environments they grew up in. Most of the human specimens were from elderly people, which would indicate that the human bones might be at the stage where they start to develop osteoporosis. However, the findings disagree with the study conducted in the lumbar segment of different species which claims the fracture stress to be 1.21 MPa in humans and 13.22 MPa for sheep (Aerssens et al. 1998). Their study hasn't discussed the level of lumbar vertebrae used.

By examining the fracture results, and comparing with the classification by Denis, it was determined that all eight specimens from the T12 -L2 group produced burst fractures, with six at T13 and two at L1 while the T12-L1 and T13-L2 groups only had six and five specimens burst fractured, respectively. All specimens with burst fractures presented some bone fragments on the spinal cord which means that in a real life, they would result in a neurological injury, the others that didn't burst had minimal impact on the spinal cord; however, one of them had a spinal cord twisted which could also cause neurological impairment. Fractures were being initiated at the specimen ends and then extending in the vertebral bodies. This again correlates with the study of Zhang et al 2017, who discussed

---

that a fast loading causes the pressure in the intervertebral disc to increase, causing its fracture. The generation of more burst fractures at T13 in the group of T12-L2 disagrees with the literature that L1 is the vertebra that is most vulnerable to a burst fracture when falling from a great height; however, by considering a single FSUs and matching them with the forces, it would be possible for L1 to fracture first as the forces are lower compared with T12-L1 single FSU forces. Overall, this study has shown that the T13 has a potential to fracture when falling or jumping from a high height, however, the results have shown that the force required to create burst fractures is slightly higher than in L1 when considered individually. By considering a segment with multilevel vertebrae, the force required to create a burst fracture is higher in L1. It was also determined that burst fractures showed some bone fragments on the spinal cord. This study has contributed to the research by showing that even if there are significant differences in the forces that create the burst fracture, by considering both T13 and L1 together, L1 requires higher force to fracture; however, when considered individually, T13 requires a higher force. The literature has not indicated any research that compared these three groups of vertebrae or that conducted the same study using a sheep model. Based on the obtained results and a close similarity to the results obtained from the literature review for studies that used human specimens, it is obvious that this is a good model for this type of study.

## 6.2 Limitations

This study was conducted successfully; however, several limitations were encountered affecting the process and the quality of the results. These included the lack of the right equipment. Initially the study was aiming to impact the specimens at an offset to create an AP flexion fracture, but this did not happen because of the loadcell that was limited to the axial impact only to overcome this, the test was designed to impact the specimens axially. The specimens were collected from a Butcher shop that acquires the sheep from different places around Australia. This affected the quality of the result due to variation of quality of sheep spines because of their growing up in different environments and being fed different food. The other significant problem was not knowing the actual ages of the sheep specimen used in the tests. It is known that young sheep have high bone density compared to older ones, therefore it was not easy to determine if the variation in the results was due to age or condition the sheep grew in. Also, the height of the drop tower was limited to one metre which restricted the study to a height lower than this height, to ensure the energy required



---

was obtained, the masses were varied as required. Furthermore, even though the sheep were tested axially, there was no mass guide meaning that there was no assurance that there were no flexions in some of the specimens. In addition, the scale of the adjustment of the impactor was 2 and 4 cm, this led to a lack of consistency in the clearance between the impactor load cell and the specimens since all the specimens did not have the same height and the height between them and the load cell would not necessarily match the drop tower. The other intention of this study was to observe the retropulsion of bone fragments in the spinal canal, however, there was no camera that would show the motion of these fragments. Lastly, it was difficult to find human specimen which was supposed to be the best model for this study. Therefore, it was not possible to compare the result from sheep with humans tested in the same conditions.

### 6.3 Recommendation for future research

This study should be developed further by testing with a six degree of freedom load cell. The use of external high-speed cameras to record the motion and changes in the deformation of the vertebra during burst fractures is recommended, with small cameras ideal, if inserted into the spinal canal to record the motion of fragments in it. This mode of high-speed impact can be used to study herniation, and it could be used on human specimens. This work was conducted by aiming the drop weight at the centre of the spinal canal. However, burst fractures happen when falling from different directions, therefore this study could be extended to striking different locations of the specimens and analysing the differences. The adjustment graduations of the scaling and the height on the drop tower should be increased to allow greater precision in the height between the specimen, the impact load cell and the mass drop height respectively. It would also be best if the test is done in young sheep of same age and, grew up in the same conditions and fed same food.

## 7. Conclusion

The aim of the study was to investigate the loading techniques to create reproducible thoracolumbar burst fractures and compare the results with clinical cases reviewed in the literature.

The results obtained have shown that the aims of the study were achieved by reproducing similar burst fractures in all specimens in the T12-L2 group, six in T12-L1, and five in the

---

T13-L2 specimen groups. The T12-L2 group produced six fractures at T13 and two fractures at L1. The forces that produced burst fractures in the T13-L2 group were higher compared with those of the T12-L1 group, while there was a similarity in the fractures created in single vertebrae groups and in the multilevel ones. It was observed that the specimens that produced burst fractures resulted in some bone fragments forced against the spinal cord, indicating a severe injury, where neurological complications would have occurred. The forces that were used to produce thoracolumbar burst fractures were different across the three groups but the T12-L1 group has shown the most consistent fracture force. However, the statistical analysis indicated no significant differences of forces in all three groups.

- There were some similarities in the fractures obtained in this study with clinical cases reviewed in the literature.
- Some of the forces that created Thoracolumbar Burst Fractures were higher compared to related studies conducted on human spines while others were in the same range.
- This project was achieved by reviewing some papers from the literature, using a flinders university drop tower and having a surgeon to check the existence of bone fragments in the spinal canal
- It would be interesting to conduct this study on human spines to check if it would give similar results and test both human and sheep specimens by impacting at different location and compare the results with current since this study has only impacted the specimens axially.
- Overall, this study has shown that there is no big difference in forces that would create burst fractures and in a real life where there is a multilevel vertebra, T13 is likely to fracture.

---

## 8. References

Aerssens, J, Boonen, S, Lowet, G & Dequeker, J 1998, 'Interspecies differences in bone composition, density, and quality: potential implications for in vivo bone research', *Endocrinology*, vol. 139, no. 2, pp. 663-70.

Alpantaki, K, Bano, A, Pasku, D, Mavrogenis, AF, Papagelopoulos, PJ, Sapkas, GS, Korres, DS & Katonis, P 2010, 'Thoracolumbar burst fractures: a systematic review of management', *Orthopedics*, vol. 33, no. 6, pp. 422-9.

Aras, EL, Bungler, C, Hansen, ES & Sogaard, R 2016, 'Cost-Effectiveness of Surgical Versus Conservative Treatment for Thoracolumbar Burst Fractures', *Spine (Phila Pa 1976)*, vol. 41, no. 4, pp. 337-43.

Baker, AD 2014, 'The three column spine and its significance in the classification of acute thoracolumbar spinal injuries', in *Classic Papers in Orthopaedics*, Springer, pp. 289-92.

Boyin, D, Stanley, RM, Cazzolato, BS & Costi, JJ 2011, 'Real-time FPGA control of a hexapod robot for 6DOF biomechanical testing', in *IECON 2011 - 37th Annual Conference of the IEEE Industrial Electronics Society*, pp. 252-7.

Ching, RP, Tencer, AF, Anderson, PA & Daly, CH 1995, 'Comparison of residual stability in thoracolumbar spine fractures using neutral zone measurements', *J Orthop Res*, vol. 13, no. 4, pp. 533-41.

Costi, JJ, Hearn, TC & Fazzalari, NL 2002, 'The effect of hydration on the stiffness of intervertebral discs in an ovine model', *Clinical Biomechanics*, vol. 17, no. 6, pp. 446-55.

Cotterill, PC, Kostuik, JP, Wilson, JA, Fernie, GR & Maki, BE 1987, 'Production of a reproducible spinal burst fracture for use in biomechanical testing', *J Orthop Res*, vol. 5, no. 3, pp. 462-5.

Di Marco, A, Russell, M & Masters, M 2003, 'Standards for wheelchair prescription', *Australian Occupational Therapy Journal*, vol. 50, no. 1, pp. 30-9.

Ding, B, Cazzolato, BS, Stanley, RM, Grainger, S & Costi, JJ 2014, 'Stiffness analysis and control of a Stewart platform-based manipulator with decoupled sensor-actuator locations for ultrahigh accuracy positioning under large external loads', *Journal of Dynamic Systems, Measurement, and Control*, vol. 136, no. 6, p. 061008.

El-Rich, M, Arnoux, P-J, Wagnac, E, Brunet, C & Aubin, C-E 2009, 'Finite element investigation of the loading rate effect on the spinal load-sharing changes under impact conditions', *Journal of Biomechanics*, vol. 42, no. 9, pp. 1252-62.

Erdfelder, E, Faul, F & Buchner, A 1996, 'GPOWER: A general power analysis program', *Behavior research methods, instruments, & computers*, vol. 28, no. 1, pp. 1-11.

---

Fakurnejad, S, Scheer, JK, Patwardhan, AG, Havey, RM, Voronov, LI & Smith, ZA 2014, 'Biomechanics of thoracolumbar burst fractures: methods of induction and treatments', *J Clin Neurosci*, vol. 21, no. 12, pp. 2059-64.

Fraysse, F, Costi, JJ, Stanley, RM, Ding, B, McGuire, D, Eng, K, Bain, GI & Thewlis, D 2014, 'A novel method to replicate the kinematics of the carpus using a six degree-of-freedom robot', *Journal of Biomechanics*, vol. 47, no. 5, pp. 1091-8.

Fredrickson, B, Edwards, W, Rauschnig, W, Bayley, J & Yuan, H 1992, '1992 Volvo Award in Experimental Studies Vertebral Burst Fractures: An Experimental, Morphologic, and Radiographic Study', *Spine*, vol. 17, no. 9, pp. 1012-21.

Fredrickson, BE, Edwards, WT, Rauschnig, W, Bayley, JC & Yuan, HA 1992, 'Vertebral burst fractures: an experimental, morphologic, and radiographic study', *Spine (Phila Pa 1976)*, vol. 17, no. 9, pp. 1012-21.

Germaneau, A, Saget, M, D'Houtaud, S, Doumalin, P, Dupre, JC, Hesser, F, Bremand, F, Maxy, P & Rigoard, P 2012, 'In vitro production and biomechanical experimental analysis of thoracolumbar burst fractures', *Comput Methods Biomech Biomed Engin*, vol. 15 Suppl 1, pp. 316-8.

Germaneau, A, Vendeuvre, T, Saget, M, Doumalin, P, Dupré, JC, Brémand, F, Hesser, F, Brèque, C, Maxy, P, Roulaud, M, Monlezun, O & Rigoard, P 2017, 'Development of an experimental model of burst fracture with damage characterization of the vertebral bodies under dynamic conditions', *Clinical Biomechanics*, vol. 49, no. Supplement C, pp. 139-44.

Hongo, M, Abe, E, Shimada, Y, Murai, H, Ishikawa, N & Sato, K 1999, 'Surface strain distribution on thoracic and lumbar vertebrae under axial compression: the role in burst fractures', *Spine*, vol. 24, no. 12, pp. 1197-202.

Ivancic, PC 2013, 'Hybrid cadaveric/surrogate model of thoracolumbar spine injury due to simulated fall from height', *Accident Analysis & Prevention*, vol. 59, pp. 185-91.

Ivancic, PC 2013, 'Hybrid cadaveric/surrogate model of thoracolumbar spine injury due to simulated fall from height', *Accid Anal Prev*, vol. 59, pp. 185-91.

— 2014, 'Biomechanics of Thoracolumbar Burst and Chance-Type Fractures during Fall from Height', *Global Spine J*, vol. 4, no. 3, pp. 161-8.

Ivancic, PC 2014, 'Biomechanics of thoracolumbar burst and chance-type fractures during fall from height', *Global spine journal*, vol. 4, no. 3, pp. 161-8.

Jones, HL, Crawley, AL, Noble, PC, Schoenfeld, AJ & Weiner, BK 2011, 'A novel method for the reproducible production of thoracolumbar burst fractures in human cadaveric specimens', *The Spine Journal*, vol. 11, no. 5, pp. 447-51.

---

Langrana, N, Harten Jr, R, Lin, D, Reiter, M & Lee, C 2002, 'Acute thoracolumbar burst fractures: a new view of loading mechanisms', *Spine*, vol. 27, no. 5, pp. 498-508.

Mageed, M, Berner, D, Jülke, H, Hohaus, C, Brehm, W & Gerlach, K 2013, 'Morphometrical dimensions of the sheep thoracolumbar vertebrae as seen on digitised CT images', *Laboratory Animal Research*, vol. 29, no. 3, pp. 138-47.

Nachemson, AL 1981, 'Disc pressure measurements', *Spine*, vol. 6, no. 1, pp. 93-7.

Oberkircher, L, Schmuck, M, Bergmann, M, Lechler, P, Ruchholtz, S & Krüger, A 2016, 'Creating reproducible thoracolumbar burst fractures in human specimens: an in vitro experiment', *Journal of Neurosurgery: Spine*, vol. 24, no. 4, pp. 580-5.

Osterhoff, G, Morgan, EF, Shefelbine, SJ, Karim, L, McNamara, LM & Augat, P 2016, 'Bone mechanical properties and changes with osteoporosis', *Injury*, vol. 47, pp. S11-S20.

Oxland, TR, Panjabi, MM & Lin, RM 1994, 'Axes of motion of thoracolumbar burst fractures', *J Spinal Disord*, vol. 7, no. 2, pp. 130-8.

Panjabi, MM, Kifune, M, Wen, L, Arand, M, Oxland, TR, Lin, R-M, Yoon, W-SS & Vasavada, A 1995, 'Dynamic canal encroachment during thoracolumbar burst fractures', *Journal of spinal disorders*, vol. 8, no. 1, pp. 3948.

Panjabi, MM, Oxland, TR, Lin, R-M & McGowen, TW 1994, 'Thoracolumbar burst fracture. A biomechanical investigation of its multidirectional flexibility', *Spine*, vol. 19, no. 5, pp. 578-85.

Pintar, FA, Yoganandan, N, Maiman, DJ, Scarboro, M & Rudd, RW 2012, 'Thoracolumbar Spine Fractures in Frontal Impact Crashes', *Annals of Advances in Automotive Medicine / Annual Scientific Conference*, vol. 56, pp. 277-83.

Shen, Yx, Zhang, P, Zhao, Jg, Xu, W, Fan, Zh, Lu, Zf & Li, Lb 2011, 'Pedicule screw instrumentation plus augmentation vertebroplasty using calcium sulfate for thoracolumbar burst fractures without neurologic deficits', *Orthopaedic Surgery*, vol. 3, no. 1, pp. 1-6.

Sheng, SR, Wang, XY, Xu, HZ, Zhu, GQ & Zhou, YF 2010, 'Anatomy of large animal spines and its comparison to the human spine: a systematic review', *Eur Spine J*, vol. 19, no. 1, pp. 46-56.

Shono, Y, McAfee, PC & Cunningham, BW 1994, 'Experimental study of thoracolumbar burst fractures. A radiographic and biomechanical analysis of anterior and posterior instrumentation systems', *Spine (Phila Pa 1976)*, vol. 19, no. 15, pp. 1711-22.

Tran, NT, Watson, NA, Tencer, AF, Ching, RP & Anderson, PA 1995, 'Mechanism of the Burst Fracture in the Thoracolumbar Spine: The Effect of Loading Rate', *Spine*, vol. 20, no. 18, pp. 1984-8.

---

Wilke, HJ, Kettler, A & Claes, LE 1997, 'Are sheep spines a valid biomechanical model for human spines?', *Spine (Phila Pa 1976)*, vol. 22, no. 20, pp. 2365-74.

Wilke, HJ, Kettler, A, Wenger, KH & Claes, LE 1997, 'Anatomy of the sheep spine and its comparison to the human spine', *The Anatomical Record*, vol. 247, no. 4, pp. 542-55.

Willen, J, Anderson, J, Toomoka, K & Singer, K 1990, 'The natural history of burst fractures at the thoracolumbar junction', *Journal of spinal disorders*, vol. 3, no. 1, pp. 39-46.

Wood, K, Bohn, D & Mehbod, A 2005, 'Anterior versus posterior treatment of stable thoracolumbar burst fractures without neurologic deficit: a prospective, randomized study', *Clinical Spine Surgery*, vol. 18, pp. S15S23.

Yoganandan, N, Arun, MWJ, Stemper, BD, Pintar, FA & Maiman, DJ 2013, 'Biomechanics of Human Thoracolumbar Spinal Column Trauma from Vertical Impact Loading', *Annals of Advances in Automotive Medicine*, vol. 57, pp. 155-66.

Zhang, X, Li, S, Zhao, X, Christiansen, BA, Chen, J, Fan, S & Zhao, F 2017, 'The mechanism of thoracolumbar burst fracture may be related to the basivertebral foramen', *Spine J*.

## Appendices

### Appendix A

#### Procedure for Potting the Specimens

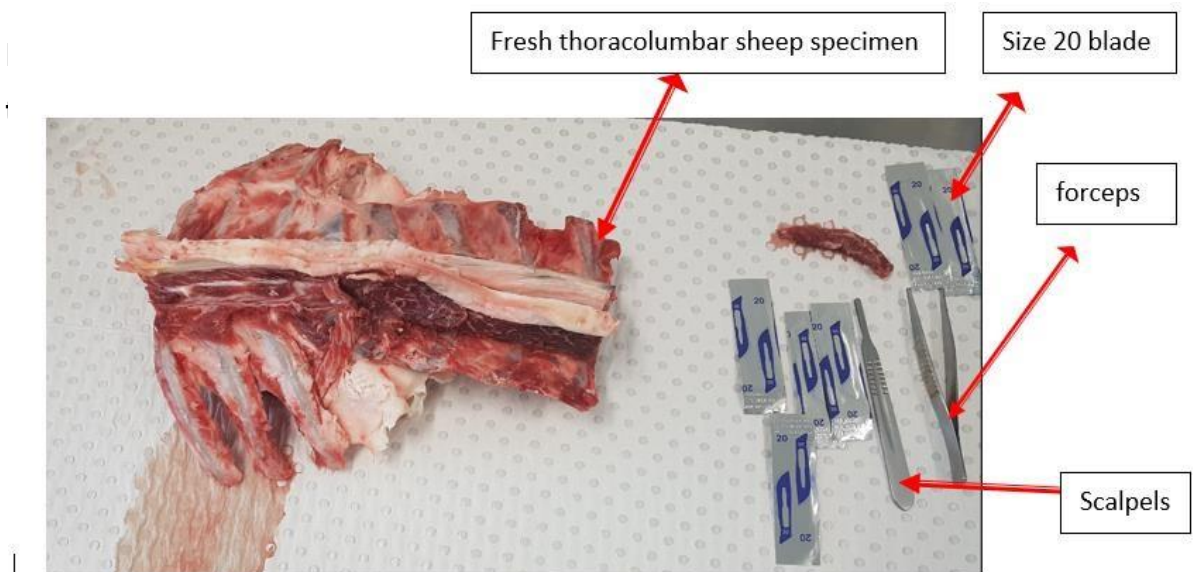
#### TESTING PROTOCOL USING A DROP TOWER

##### 1. PREPARATION OF THE SPECIMENS

###### 1.1. Removing soft tissues

1.1.1. Take the specimens out of the freezer and leave them on the bench in the cadaver room on an absorbent pad for two to three hours or leave them in a fridge overnight.

1.1.2. Once they are defrosted, remove soft tissues using scalpels, forceps and size twenty blades



1.2. Cut the specimens into segments of four vertebrae ranging from T11 to L2 using bandsaw (need someone from engineering services to do this)



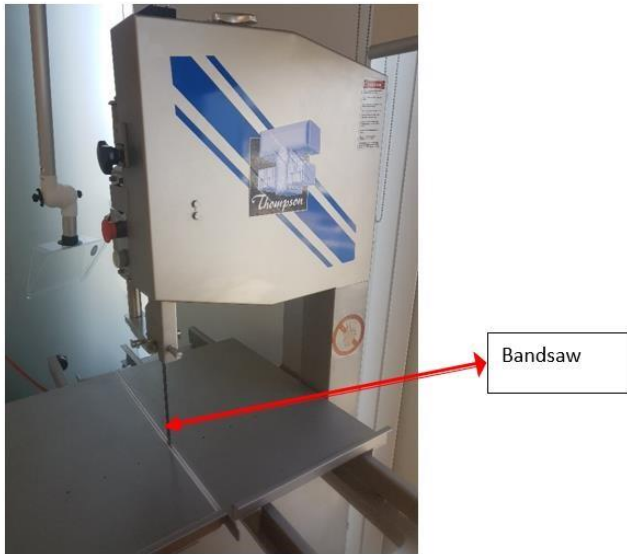


**Figure 8-2: Bandsaw used to cut the specimens to the required sizes**

- 1.3. Wrap the specimens into paper towels and spray them with normal saline to keep them hydrated



**Figure 8-3: Specimens sprayed with**



---

**normal saline, wrapped in paper towels in a zipped bag.**

1.4. Keep specimens into freezer at  $-20^{\circ}\text{C}$  until ready to be tested

2. Potting the specimens

2.1. Remove the specimens to be tested from freeze and leave them on work bench for 2 to 3 hours or put them in a fridge the night before day of testing.

2.2. Take the measurements of the height, lateral and anterior posterior of each vertebra (T12 and L1).

2.3. Take the measurement of the Height, lateral and anterior posterior of each disc (T11-T12, T12-L1, and L1-L2)

2.4. Clean the cups with alcohol

2.5. Cover the holes of the top and bottom cups with Kapton tape (These holes must be covered from inside) as shown in the picture below.

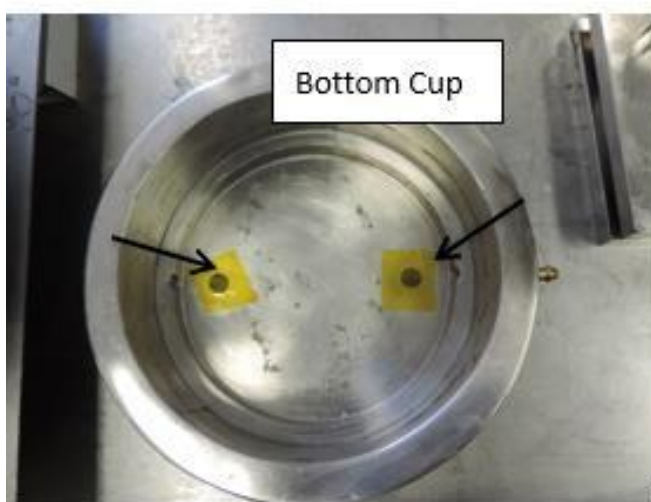
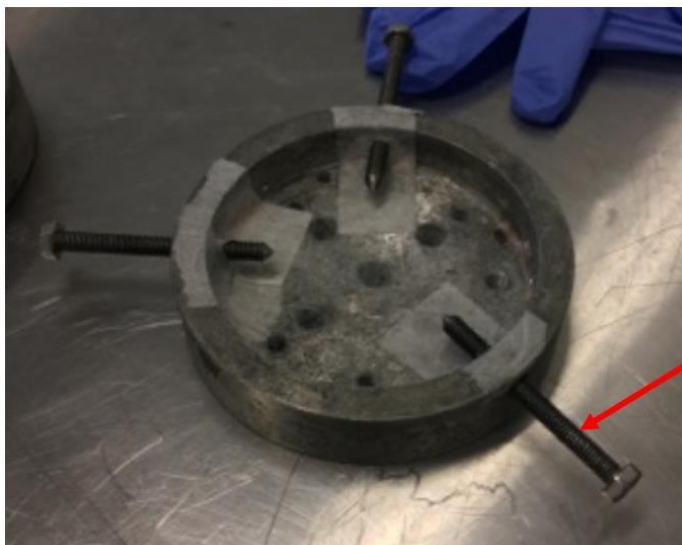


**Figure 8-4: Potting cup with the holes tapped with Kapton tape from inside.**

- 2.6. Put screws in three holes on sides of the cups and then grease them using the moly bond grease. The screws are to secure the PMMA into the cups. Greasing them allows their smooth removal after the testing (Note: If the screws are not degreased, they can't be removed). Also make sure the holes are tapped with self-adhesive tapes from inside before inserting the screws in.



Screw inserted in the side hole of the potting cup

**Figure 8-5: Potting cup with screws inserted in three holes from its sides**



Moly bond grease to grease the screws to allow an easy removal of the screws from the cups

---

**Figure 8-6: Molybond lubricant used to grease the screws before pouring the mixed PMMA in the potting cups.**

- 2.7. Take the cups and specimen into the fume hood. The specimen, cups and alignment rig must be in the fume hood during the process of potting.
- 2.8. Attach the bottom cup to the alignment plate and then the alignment plate to the base of the rig

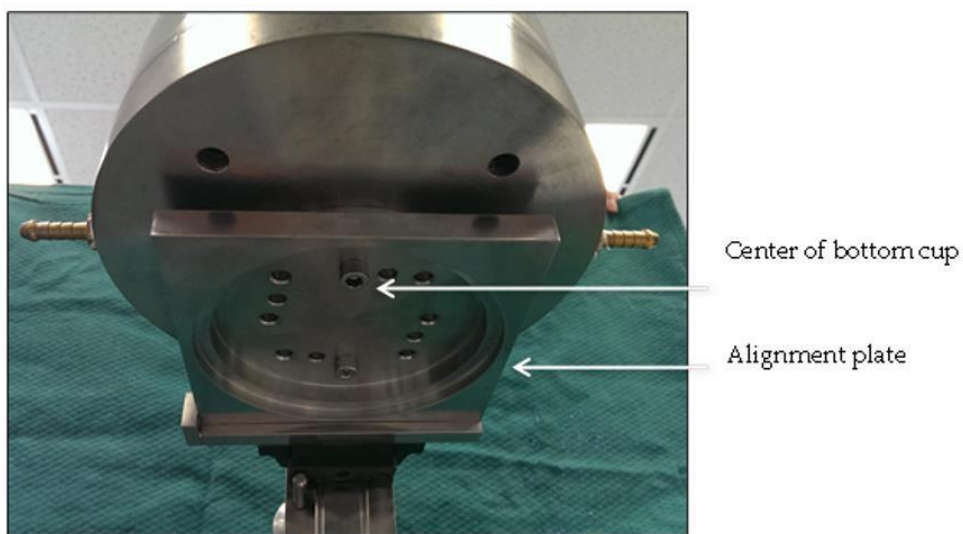


**Figure 8-7: bottom cup attached to the alignment plate**

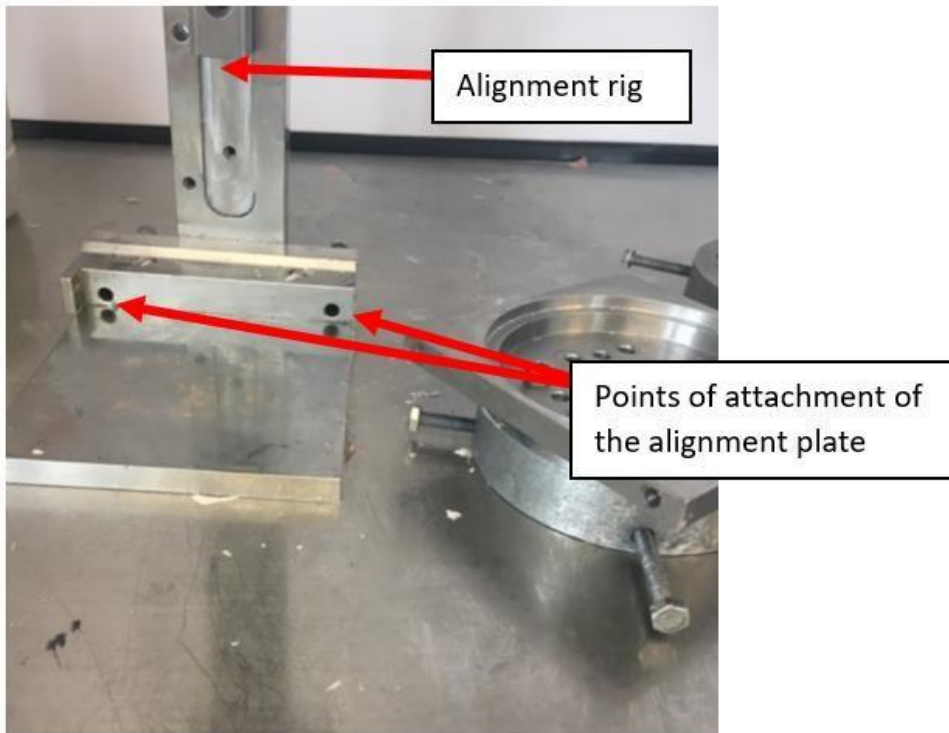


**Figure 8-8: Alignment rig displaying the location where the alignment plate is attached on its base. Note that the attachment screws are located at the back of the visible side.**

- 2.9. Place the specimen into the Centre of the bottom cup and make sure the lumbar side is on the bottom and the specimen is not rotated.

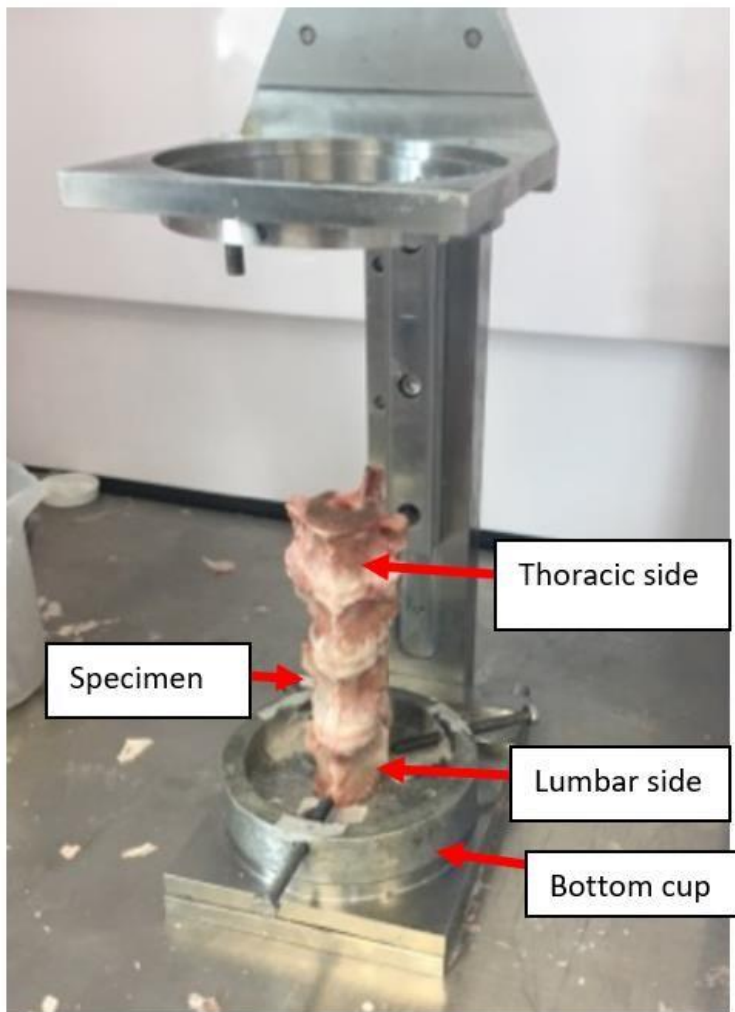


**Figure 8-9: picture showing how the specimen should be positioned in the potting cup.**

2.10. Measure 40 ml of monomer agent and 100 ml of PMMA powder using measuring cups, mix them in the mixing cup with the aid of mixing utensil Stir thoroughly and then pour the mix in the bottom cup. Ensure not to exceed the lip of the cup.

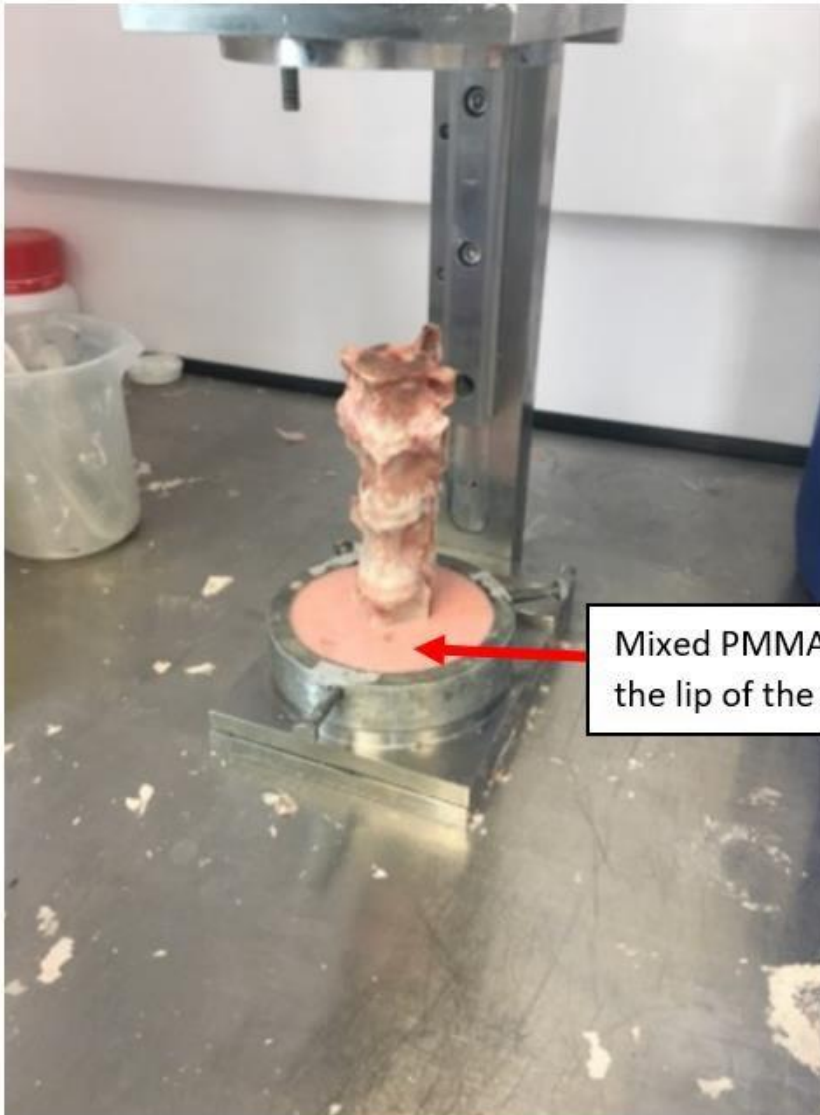


**Figure 8-10: this picture indicates the level of PMMA in the potting cup.**

- 2.11. Leave the potted specimen in the fume hood for about 30 minutes to allow the PMMA to harden
- 2.12. Once the PMMA has hardened, dismantle the alignment plate from the rig base and then detach the bottom cup.
- 2.13. Attach the top cup to the alignment plate and then to the base of the rig
- 2.14. Attach the bottom cup to the slide mount in the upside-down way and slowly slide it into the top cup and make sure the specimen is in the Centre of the top cup.
- 2.15. As did in the previous steps, mix PMMA and monomer agent and pour the mix in the top cup.

- 
- 2.16. Allow about 30 minutes for the PMMA mix to dry.
  - 2.17. Detach the cup from the alignment rig and measure the height of the specimen between the two cups.

### 3. TESTING PROCEDURE

- 3.1. Take the potted specimen in the Biomechanics Lab and get a licensed person to take an x-ray
- 3.2. Using a table next to the drop tower, Attach an adaptor plate on a small rail and then the bottom cup on the adaptor plate. This step can be done on the base of the drop tower as well, but you need to make sure the release mechanism of the drop tower is secured with a screw to avoid the drop of the weight which can result in injury.



**Figure 8-11: This picture indicates the adaptor plate attached on the small rail.**

- 3.3. Make sure the release mechanism with the bottom mallet are engaged and secured with a locking screw before conducting any work on the base of the drop tower.



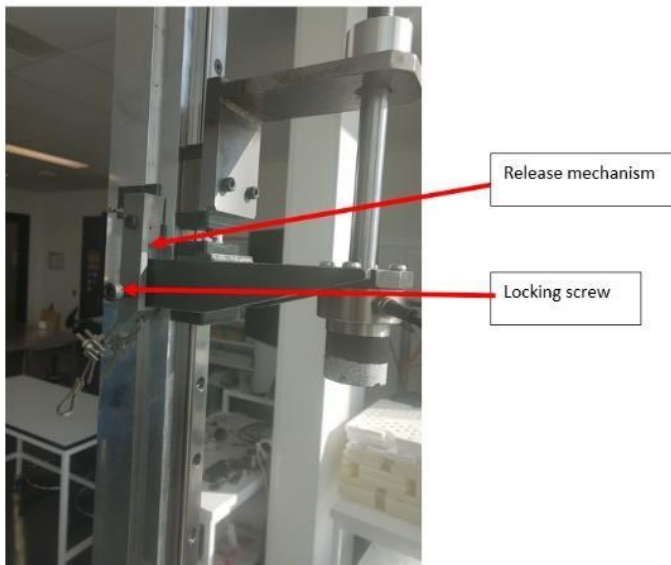
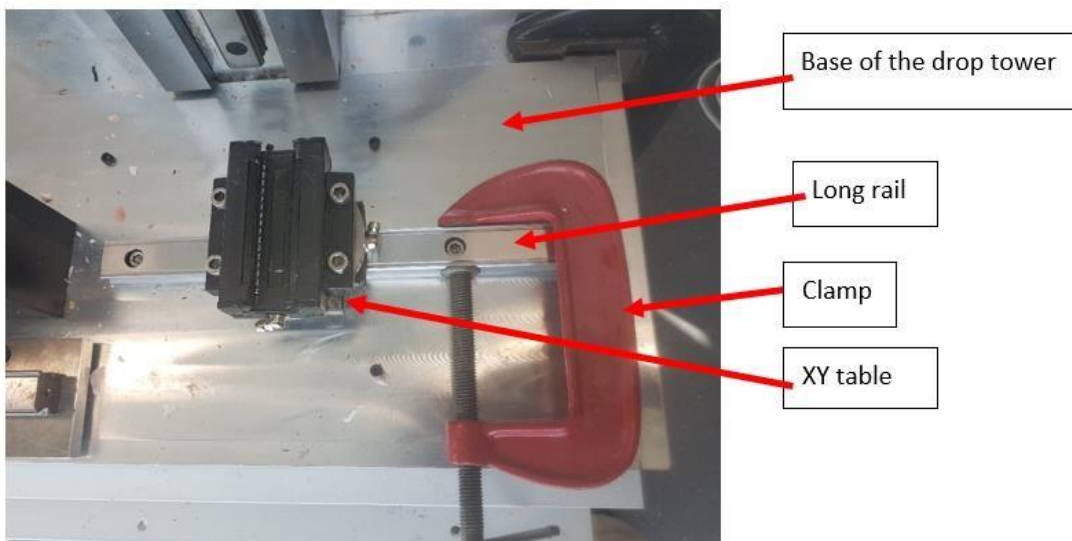


**Figure 8-13: Locking screw with a release mechanism. the locking screw prevents the unwanted release of the weight that could result in injuries or damage of the specimens.**

- 3.4. Mount the long rail and the XY table on the base of the drop tower aligned with the impact load cell. Make sure all the four holes of the rail are screwed in the base of the drop tower and use a clamp on the rail to stop the bearing from falling off the rail.





---

**Figure 8-14: Long rail attached on the base of the drop tower, XY table and clamp that stops the XY table from falling off the rail.**



**Figure 8-15: Small rail with the adaptor plate inserted into the top of XY table**

- 3.5. Slide the small rail mounted with the specimen in the bearing that is mounted on the long rail at the base of the drop tower. Secure the specimen vertically aligned with the impact load cell. Note that on the x-y table, the small rail must be on top.
- 3.6. Use four clamps, one on each side of the rail to avoid the sliding movements of the specimen while impacting



Two clamps on both sides of the small rail

One clamp on the front side of the long rail, the other clamp is behind the specimen and can not be seen

**Figure 8-16: Picture displaying the clamps that stop the sliding motion of the cups therefore stopping them from falling off the rails.**

- 3.7. Adjust the appropriate height between the top of top cup and the impact load cell. Measure this distance and record it in a data sheet (for current testing, this will be set to be 50 cm)
  
- 3.8. Load the mass on top of bottom mallet using a disc/block of 2.5 or 5 kg at a time until the required weight is achieved, attach the top mallet and then tighten them with a nut. If there is a gap between the top mallet and the threads for the nut, use a cylindrical rod adaptor to make sure the mallets and the mass don't wobble during the impact.

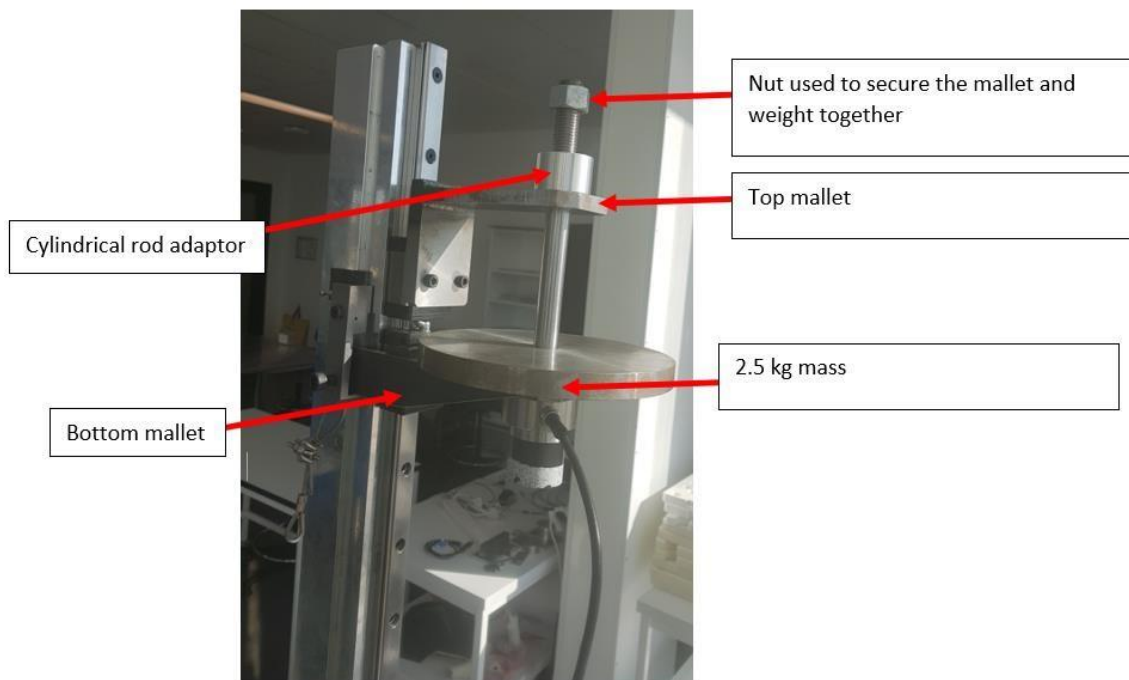


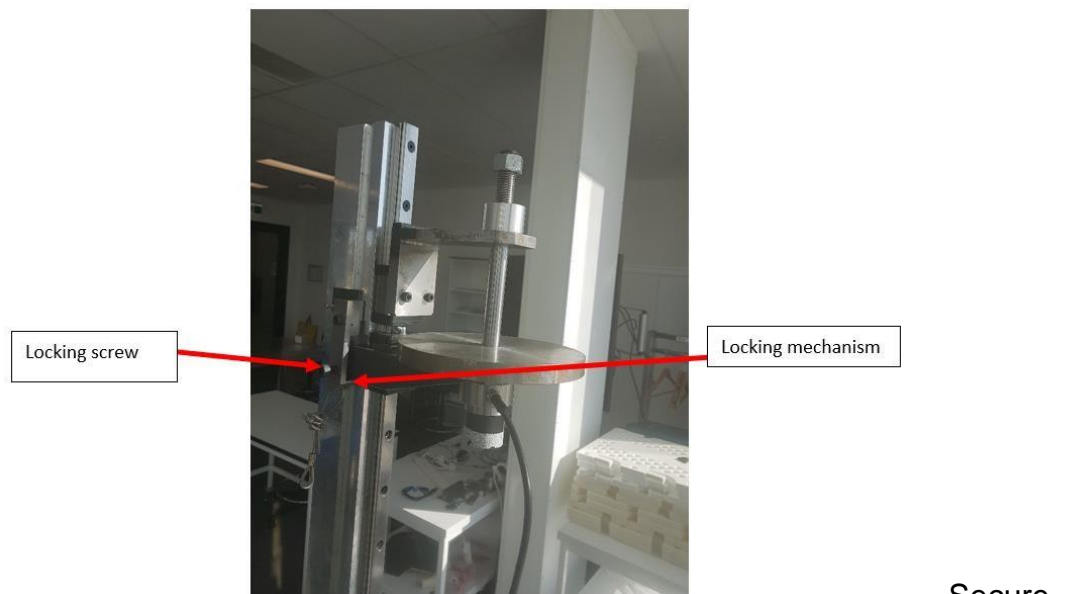
**Figure 8-17: This figure illustrates the location where the mass is loaded, the cylindrical load adaptor, the sample of mass and the nut that secures the weight on the top of the bottom mallet.**

- 3.9. Give a reference number to the specimen being tested to make sure the collected datum is not messed up.
- 3.10. Interface the impact load cell and the computer using the load cell cable.
- 3.11. If the computer is off, turn it on -> go to computer -> Windows (C)-> LABVIEW DATA ACQUISITION -> saved data-> Joseph-> open the impact practice project> make the modification needed -> save data with the specimen reference.
- 3.12. When ready to run the test, click the run button
- 3.13. Ensure that everyone is behind the drop tower guard before releasing the release mechanism to avoid any injuries.
- 3.14. Release the trigger to Impact the top cup using an extended cord (make sure to take a video and images during and right after the impact).
- 3.15. Click the stop button to stop the collection of the data-> remove the specimen from the x-y table-> detach the bottom cup from the adapter plate

---

->take another x-ray to be compared with the intact x-ray taken and other tested specimens.

- 3.16. Unpot the specimen, put in a plastic zip bag and back in a freezer until ready to be dissected for the assessment of the internal of the spinal canal.
- 3.17. Remove the weights and put them on the bench that is next to the computer



3.18.

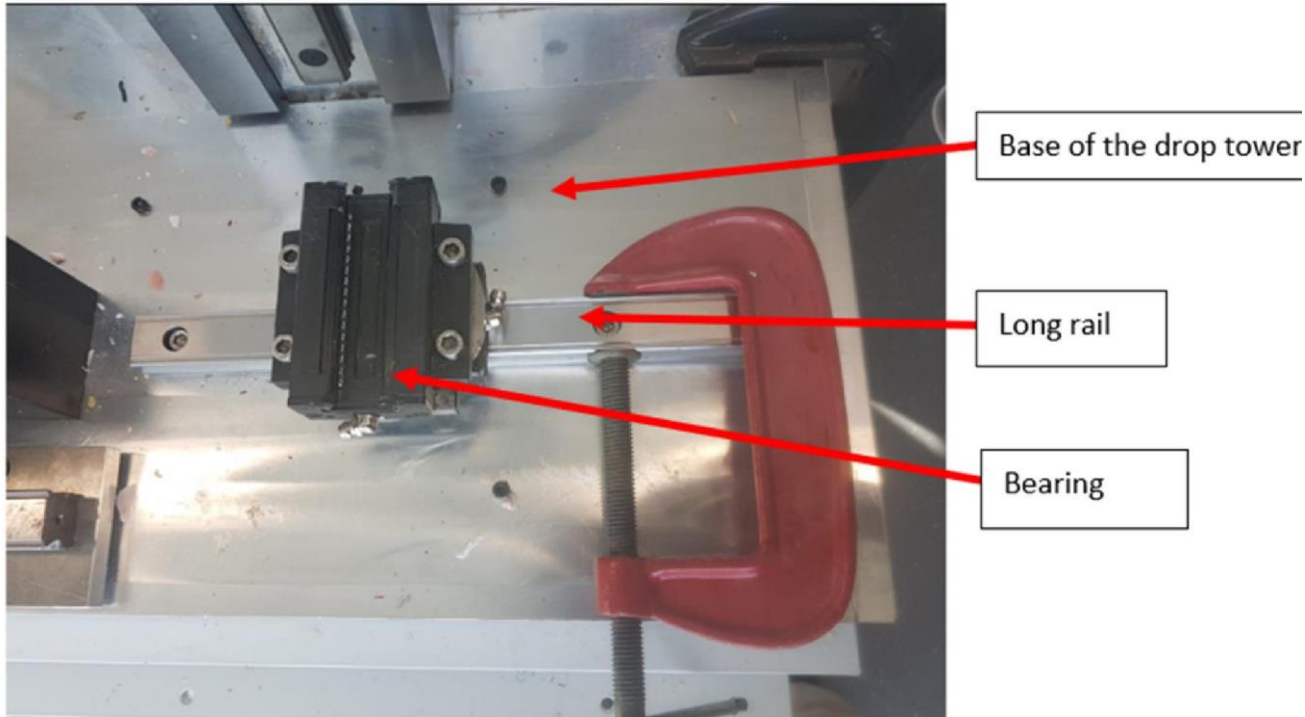
Secure

the release mechanism with a locking screw.

**Figure 8-18: This picture indicates the locking screw that prevent an unwanted release of the weight that can results in causing injury or damaging the specimen.**

- 3.19. Clean the base of the drop tower, the rail and bearing with alcohol

**Figure 8-19: This picture indicates the components and area that need to be cleaned with alcohol at the end of tests.**



- 3.20. Take the tested specimen in the Biomechanics lab where is the x-ray for the x-ray image to be taken.
- 3.21. Take the specimen in the cadaver room
- 3.22. Remove the specimen from the cups by unscrewing the screws using a spanner, and then inserting a driver in one of the bottom holes of the cup and hitting the driver's head with a mallet
- 3.23. At this stage, the specimen can be dissected to observe inside of the spinal canal or wrapped in a paper towel, placed in a zipped plastic bag and kept in a freezer at  $-20^{\circ}\text{C}$  until ready to dissect them.

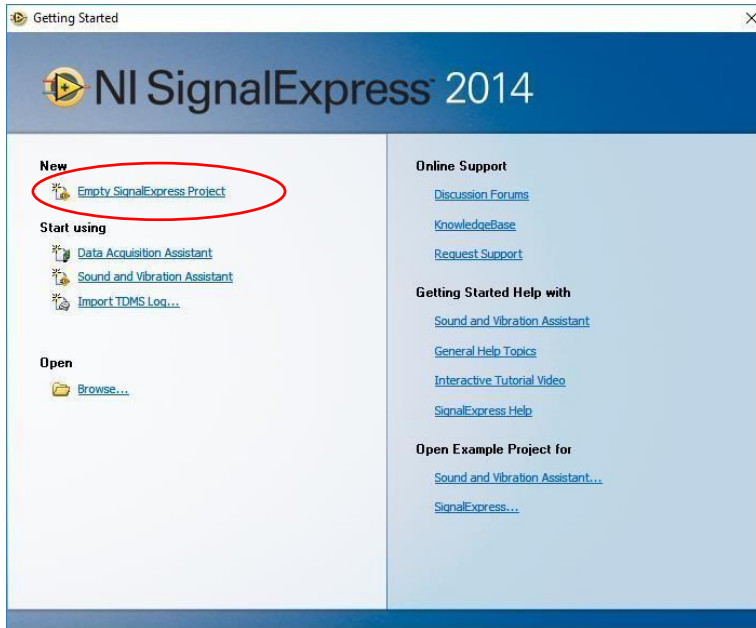
## Appendix B

### Data Acquisition using National Instruments: Signal Express

This guide will use acquiring strain gauge measurements as the aim of the task but can be replaced with any type of signal. It will also use a USB CDAQ chassis as the DAQ device.

Create a Project

1. Open Signal Express and select “New SignalExpress Project”



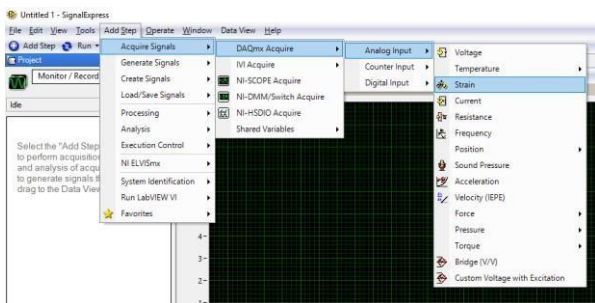
Add a Data Acquisition Step to the Project

1. Ensure your cDAQ chassis is powered, connected to the PC and the Required Modules are inserted

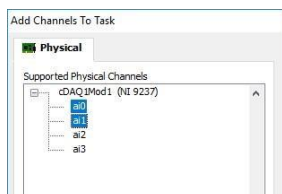
2. From the “Add Step”

Menu, select “Acquire Signals” ⑦ “DAQmx Acquire” ⑦

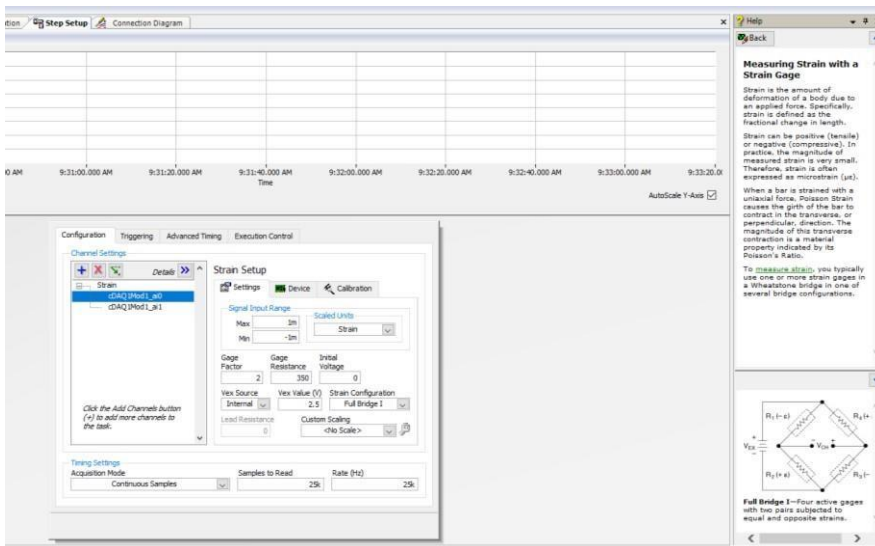
“Analog Input” ⑦ “Strain”



3. Select one or more channels from the list



- The screen will change to the “Step Setup” tab where you can change the parameters for each strain channel input. Multiple channels can be selected at once. Ensure that gauge resistance, gauge factor and strain configuration are correct



- Configure the timing settings according to the type of test to be conducted.

Nominal settings are Acquisition Mode: Continuous Samples, Rate: (slow if you are doing a long slow changing test, faster if you need to look at a more dynamic signal) and Samples to read (buffer size when continuous sampling) is generally the same size as the rate.

NOTE: the sampling rate entered may be coerced in the hardware to the nearest (faster) rate.

This is due to the max clock rate being divided down to a slower rate and there are a limited number of integer divisors. For more details, see NI Application Note - <http://digital.ni.com/public.nsf/allkb/593CC07F76B1405A862570DE005F6836>

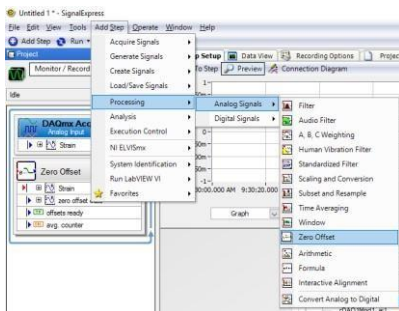
For the NI 7237 the max rate is 50kHz and the minimum is 1,612.9Hz



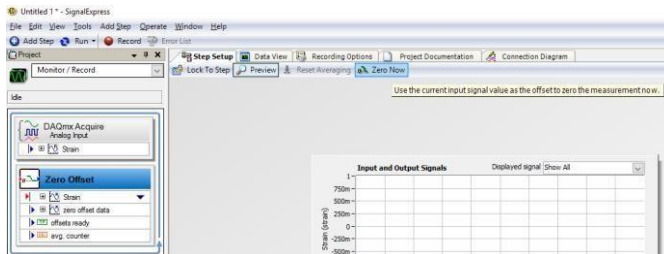
It is recommended to sample at 2kHz and then resample to a lower frequency if required.

## Remove Offset from signal

1. Add a “Zero Offset” step to the task from the “Add Step” ➤ “Processing” ➤ “Analog Signals” menu



2. When running the project, use the “Zero Now” button in the step setup to remove the offset from the signal.



## Optional Processing Steps

There are many other processing steps you can insert at this stage ie. Filtering, averaging and maths however it is recommended that for a normal data acquisition project that as little changes as possible are made to the signal before it is saved to file. The file can always be post filtered or manipulated but you can never get back the raw data once it has been saved.

## Resampling if Required

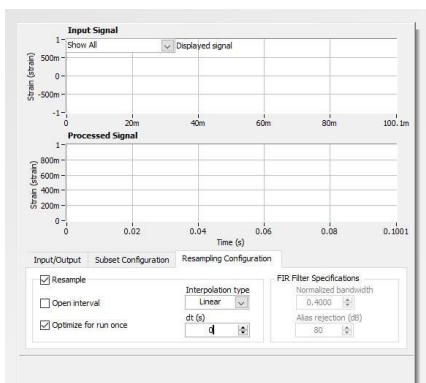


---

Resampling the signals is a good idea if the signal is slow moving and you want to save disk space by writing less data.

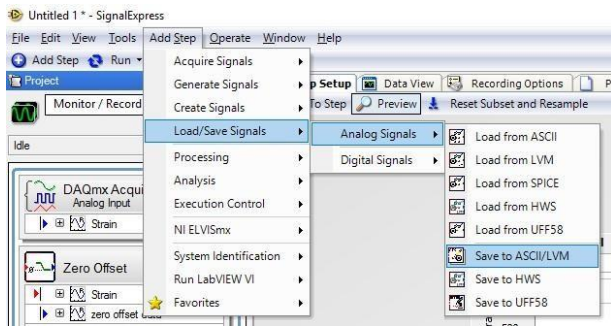
NOTE: This is important for long tests with the NI 9237 modules as 2kHz over multiple channels adds up quite quickly and MS Excel will start to have trouble with that amount of data.

1. Add a “Subset and Resample” step from the “Add Step” ⑦ “Processing” ⑦ “Analog Signals” menu.
2. In the “Subset Configuration” tab, deselect the Subset checkbox.
3. In the “Resampling Configuration” tab, ensure that the Resample box is checked.
4. Change the time between samples “dt (s)” field to the desired value ie. 0.01 for 100hz

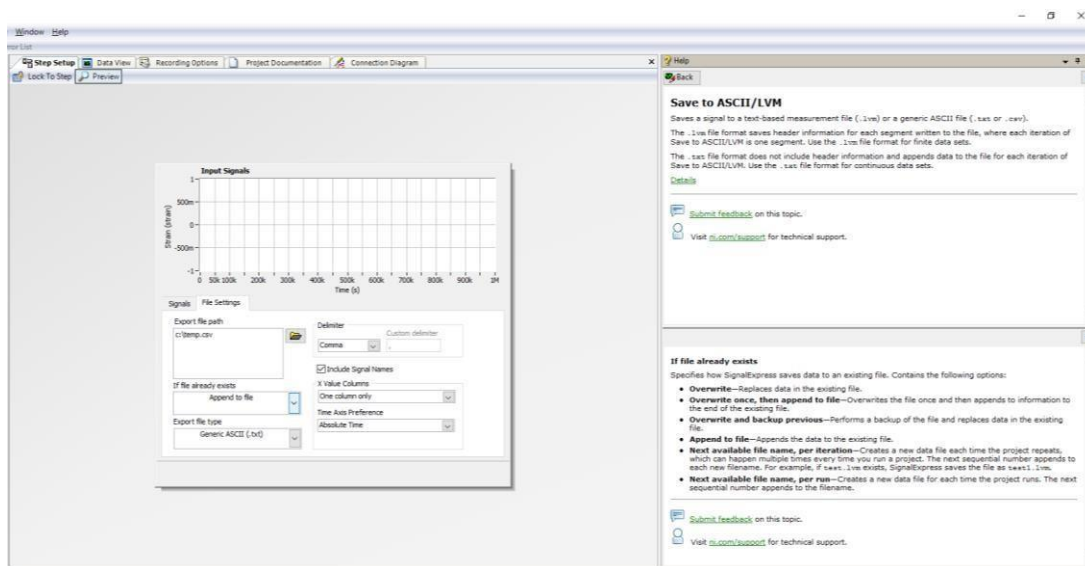


## Save To File

1. Add the “Save to ASCII/LVM” step to the project from the “Add Step” ⑦ “Load/Save Signals” ⑦ “Analog Signals” menu.

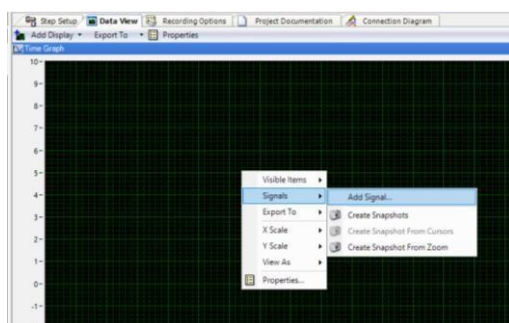


2. In the signals tab, ensure that the desired signals are selected.
3. Enter the path where you want to save the data in the “Export File Path” (include the .csv extension if you want excel to automatically open the file).
4. It is recommended to change the file exists option to “Append to File” or “Next available filename, per run”. This will stop accidental overwriting of files if the user forgets to change the file name for each test.
5. Set the delimiter to comma if you want a CSV file.
6. Check the “Include Signal Names” checkbox
7. Set the Time axis to “Absolute” (computer time) or “Relative” (starts at 0 and counts from when the task is run)

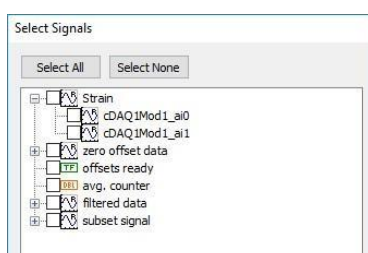


## Previewing the Data

1. Open the “Data View” tab
2. Right Click on the graph and select “Signals” ➤ “Add Signal”



3. Select the signals you want to preview. For Example, it may be useful to add the original signal and the zero offset signal to ensure that you have zeroed the signals properly before running the test.



4. When the task is run the data will be display on the graph.

---

## Save the Project

1. Save the project so all of the steps and the configuration can be used again.

## Running the Task

1. Ensure that the strain gauge/s are connected and you are ready to start the test.
2. Do any preload or setup of the specimen
3. Check the filename is correct for your test in the “Save to ASCII/LVM” step setup so you won’t overwrite an existing file.
4. Run the Task using the run button on the toolbar

NOTE: do not use the recording button – this generates unnecessary log files in the User drive on the network and will slow down the project (or crash on loading the project).



5. Ensure you are getting data in the “Step Setup” tab for the DAQmx Acquire step. (Or the “Data View” tab if you set that up.)
6. Go into the “Zero Offset” “Step Setup” tab and click the Zero Now button
7. Start your test
8. After your test has finished, click the Stop button on the toolbar.

You will now have a csv file with your acquired data.

---

IMPORTANT NOTE:

If you open a CSV file with MS Excel it will convert the ASCII timestamps and values to numbers, so they can be manipulated within Excel. **If you save the file from within Excel you will lose precision on your data.** The problem is that when excel saves a CSV file it doesn't save the numbers with the same precision as what signal express wrote.

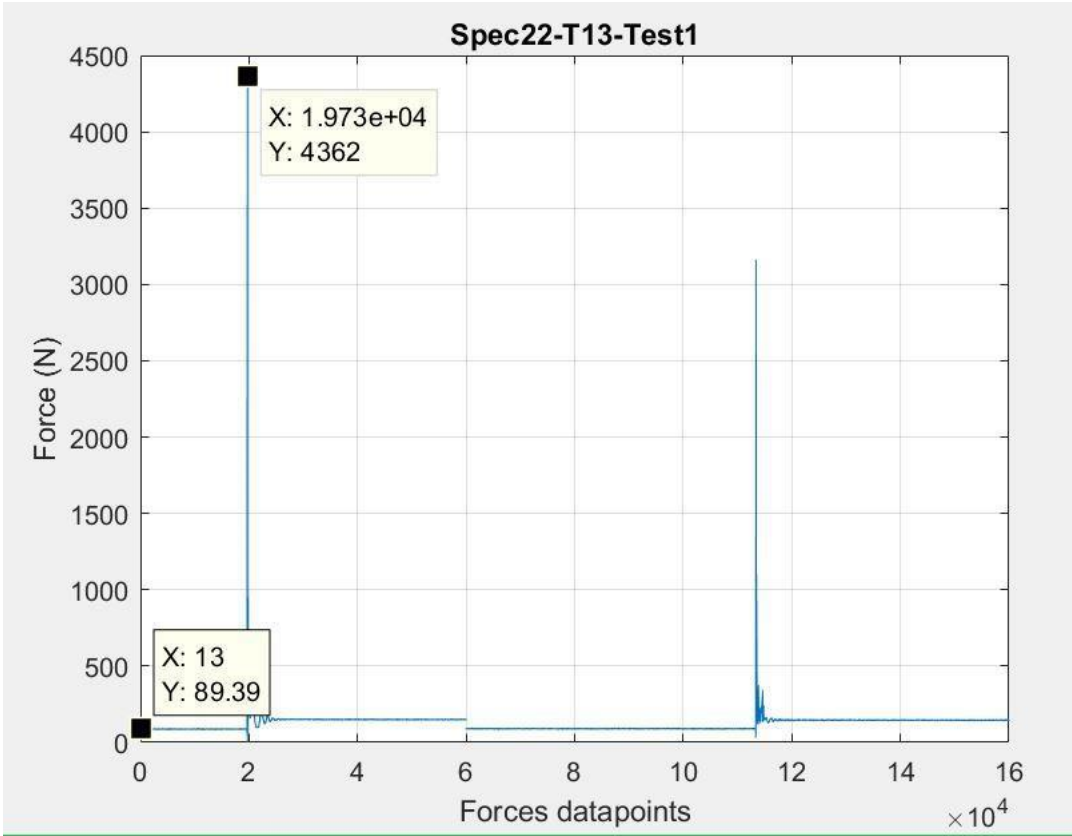
Make sure you either make a copy of the raw CSV before opening with Excel (safer) or use save as (not as safe) to avoid losing your data.

Appendix C

Fractures in T12-L1



b.





a. Burst fracture of T13 vertebra body. Vertebra body fractured into pieces



b. x-ray image shows the fractures of the specimen

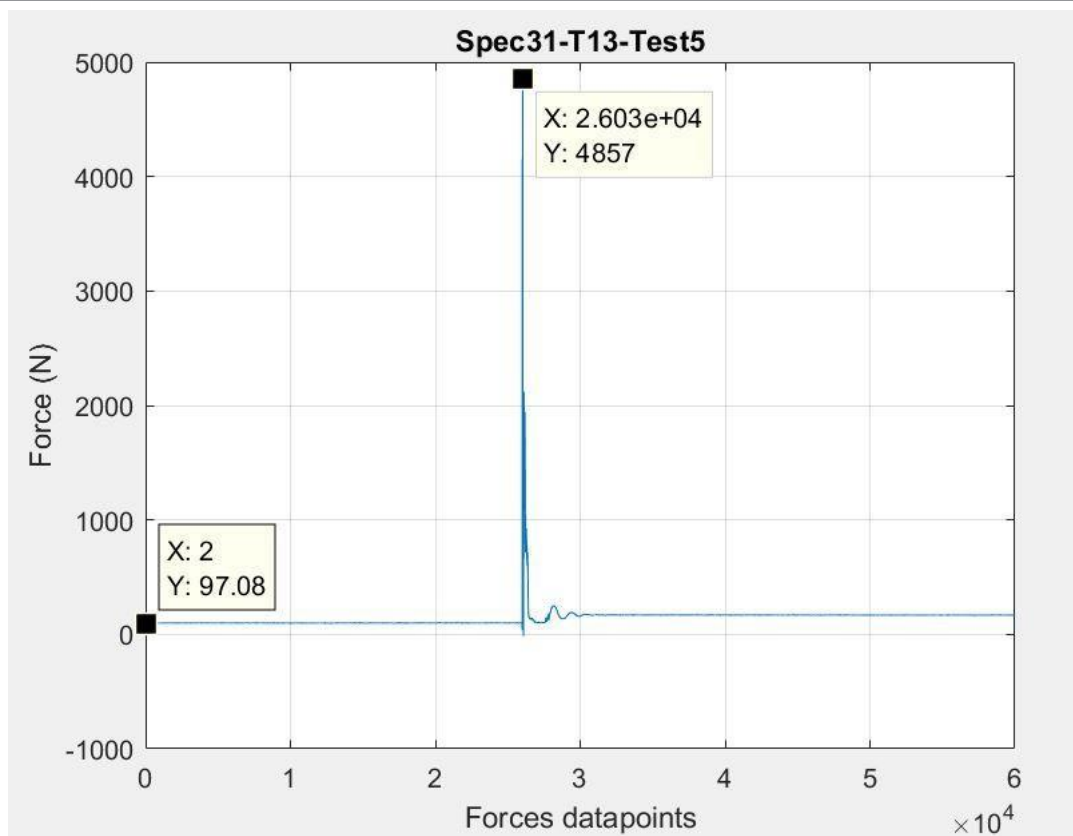


Figure 8-20 - figures a, b, and b represent the burst fracture, x-ray image and the force that produce the burst fracture.



a.



a.

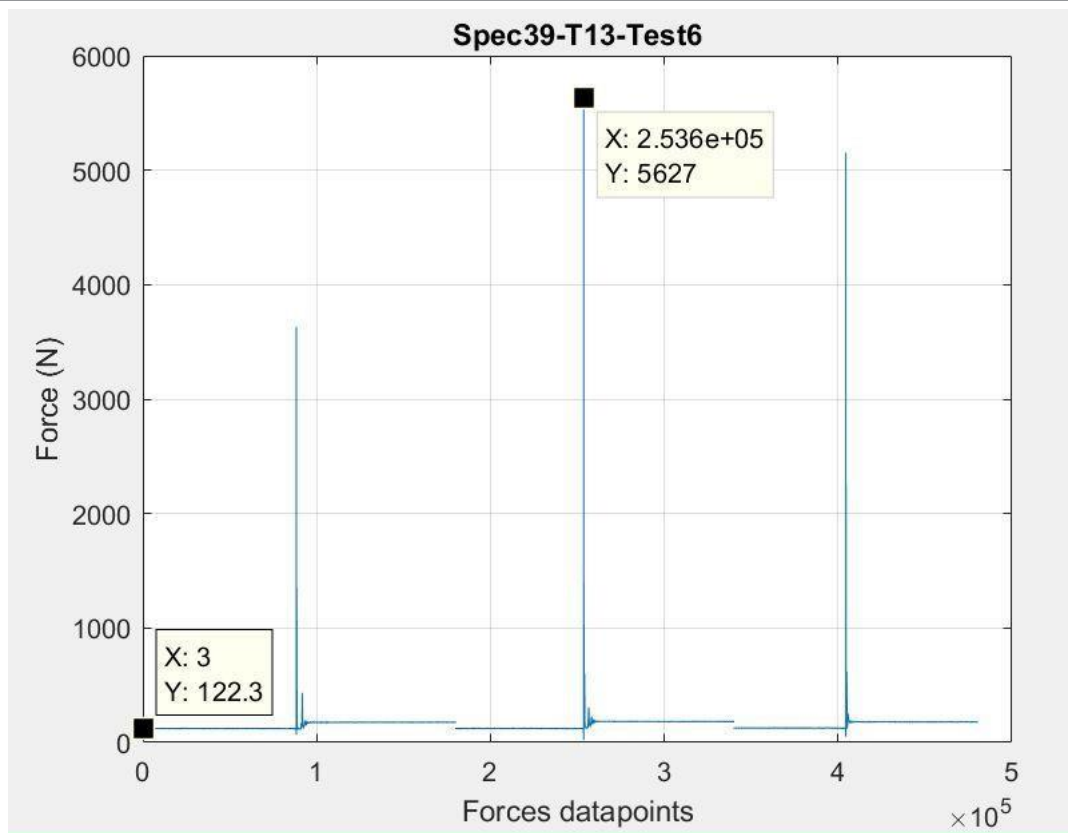
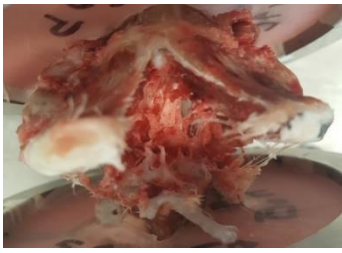


Figure 8-21 - a represent no burst fracture, b shows the image from x-ray and c the force generated to create the fracture.





a.



b.

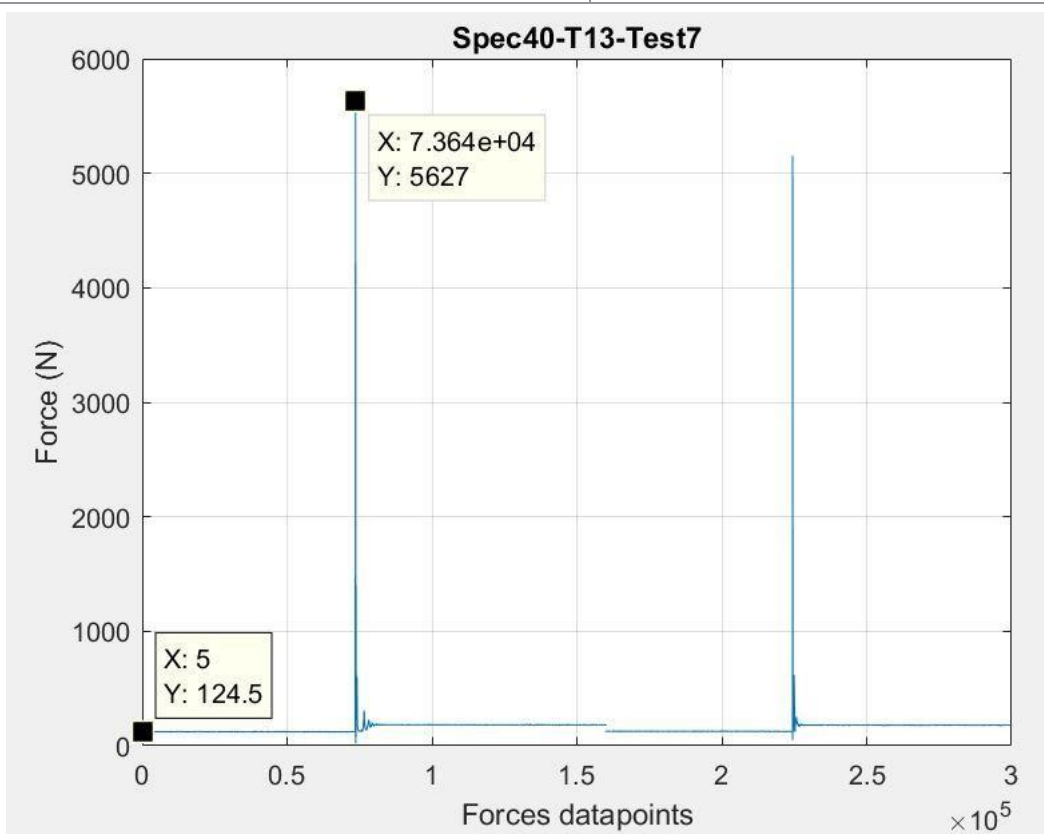
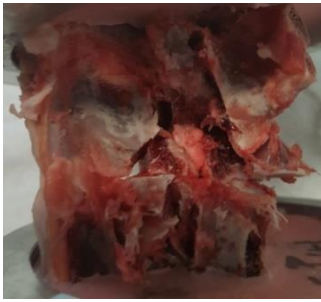


Figure 8-22 - burst fracture of the vertebra, x-ray image and force to create the fracture represented by a, b, and c respectively.



a.



b.

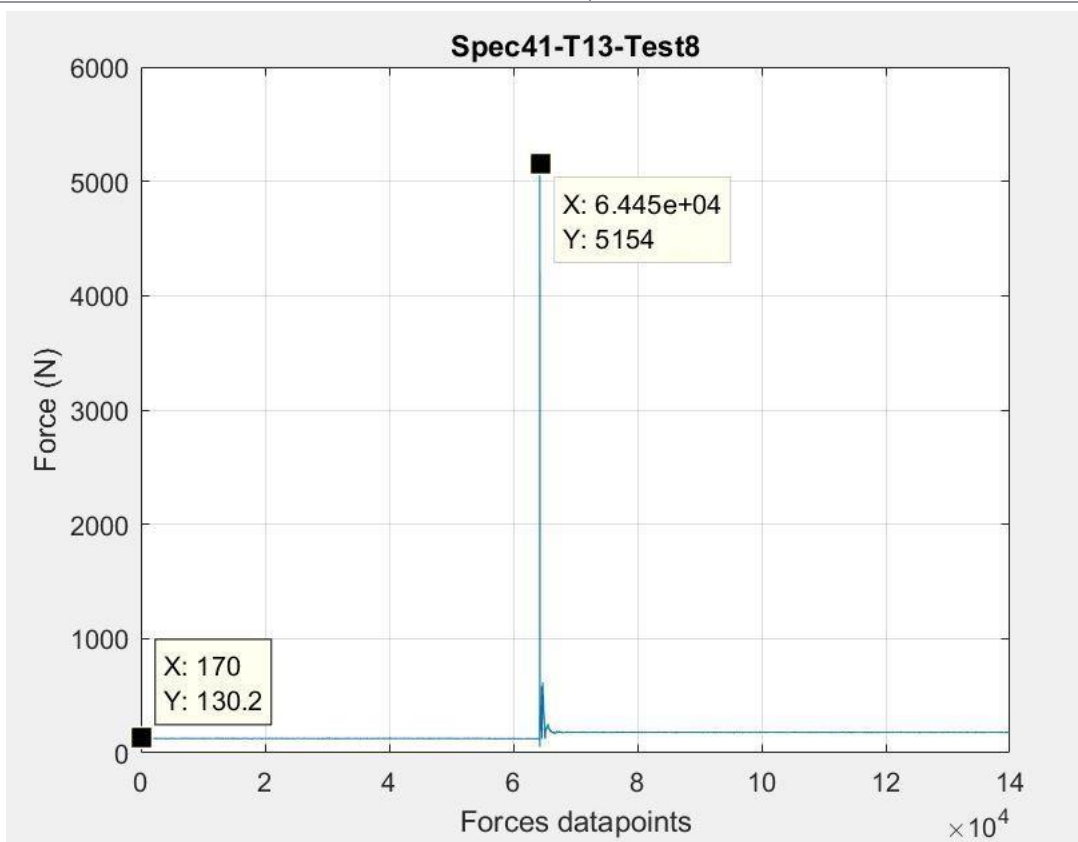


Figure 8-23 - Burst fracture, x-ray image of the fracture and the force that created to produce the burst fracture are represented by a, b, and c respectively.

### T13-L2 Fractures



a



b

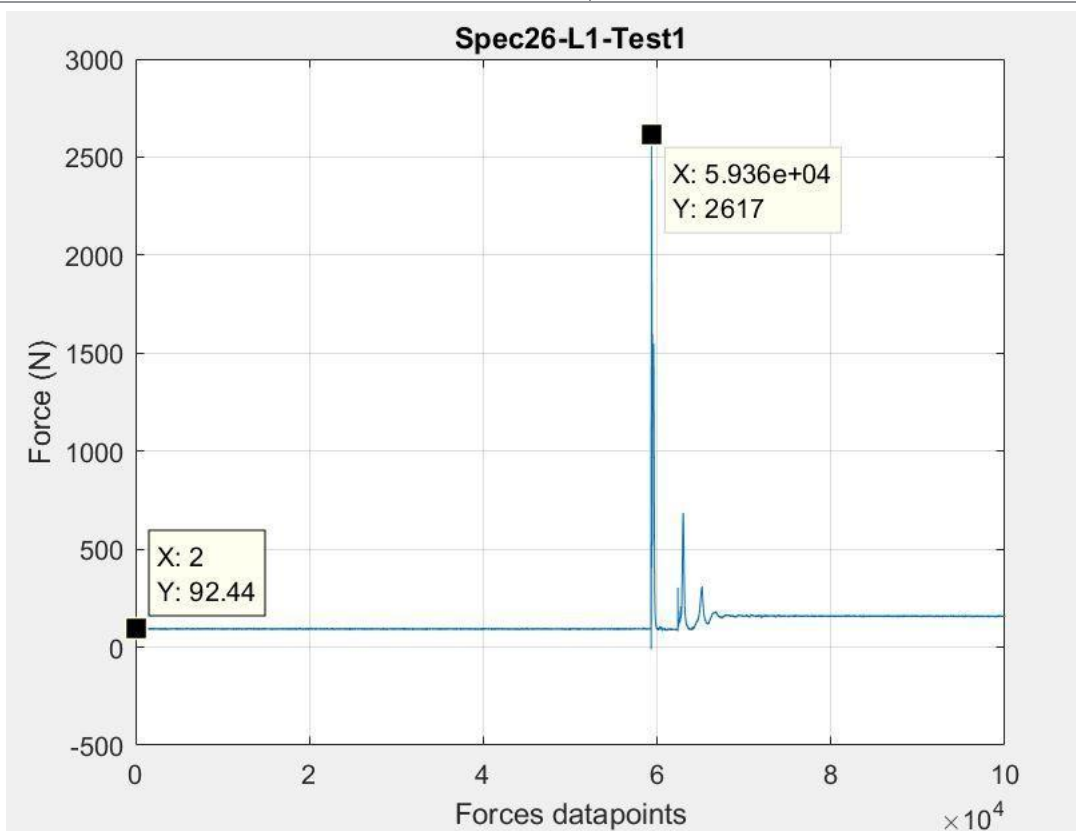


Figure 8-24 - The images in a, b and c represent the picture of the fracture, the xray to confirm it and the force that was produced during this fracture. there was a fracture at the upper endplate of L1 and a small part of T13 that was



a



b

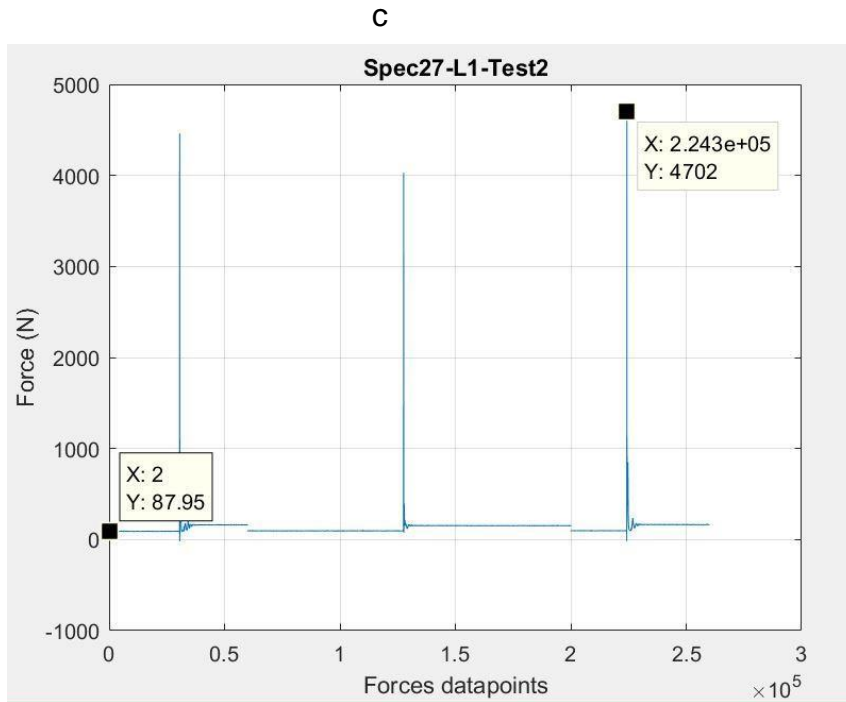


Figure 8-25 - a, b, and c represent the burst fracture of L1 with the disc remaining intact, the x-ray image that confirms this fracture, and the force of less than 300 N to create this burst fracture respectively.



a



b

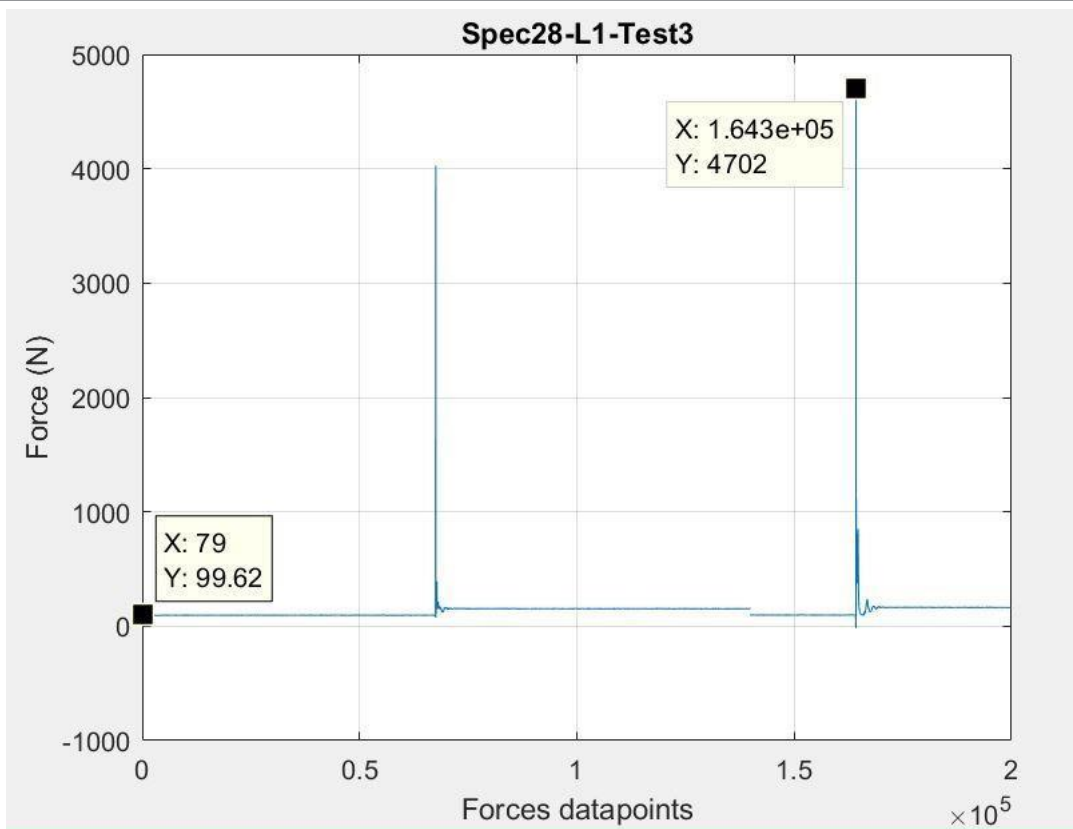
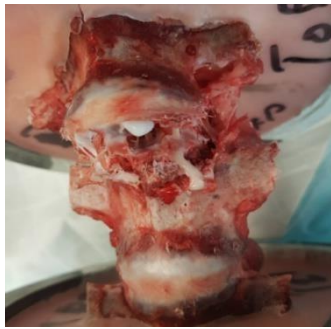


Figure 8-26 - a, b, and c represent the burst fracture initiated at lower endplate of L1, the x-ray image of the burst fractured vertebra and force of less than 600 N that produced this fracture.



a



b

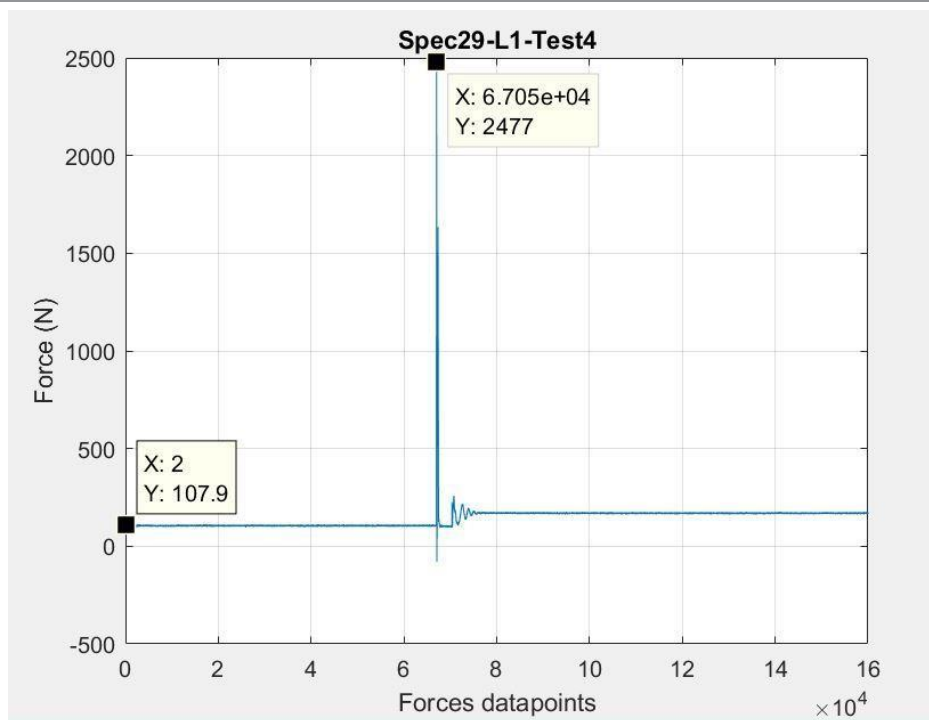


Figure 8-27 - a, b, and c represent the fracture of the top end plate of L1, the confirmation of this fracture by x-ray image and force of less than 300 N to create the fracture.



a



b

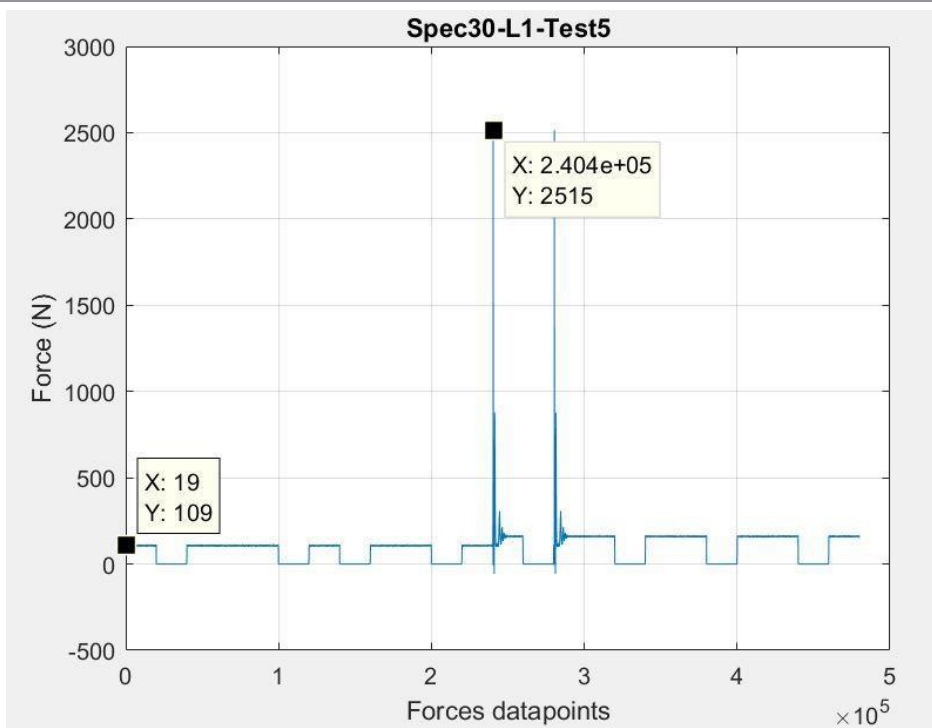


Figure 8-28 - burst fracture of the spinous process and shear fracture of L1 vertebra, x-ray image in b confirms the fracture and shows the force that produced the fracture.



a



b

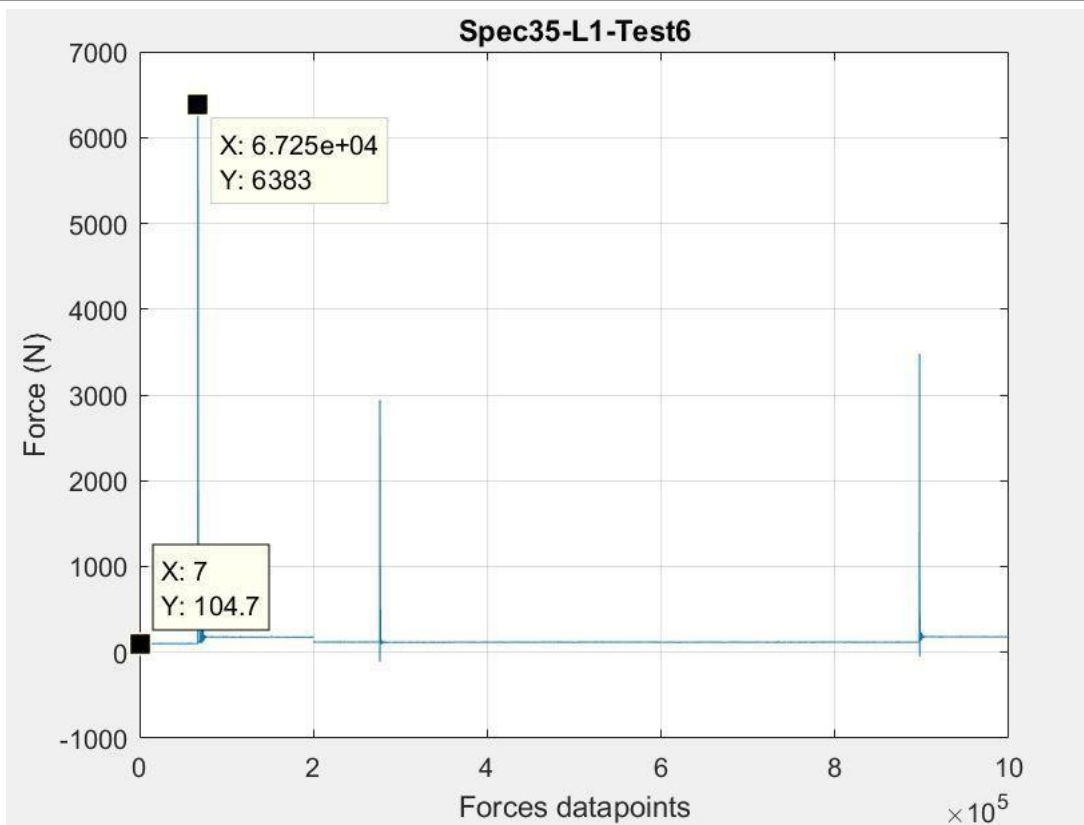


Figure 8-29 - a, b, and c represent the fracture of the lower endplate of T13, x-ray image confirming this fracture and the force of 700 N respectively





a



b

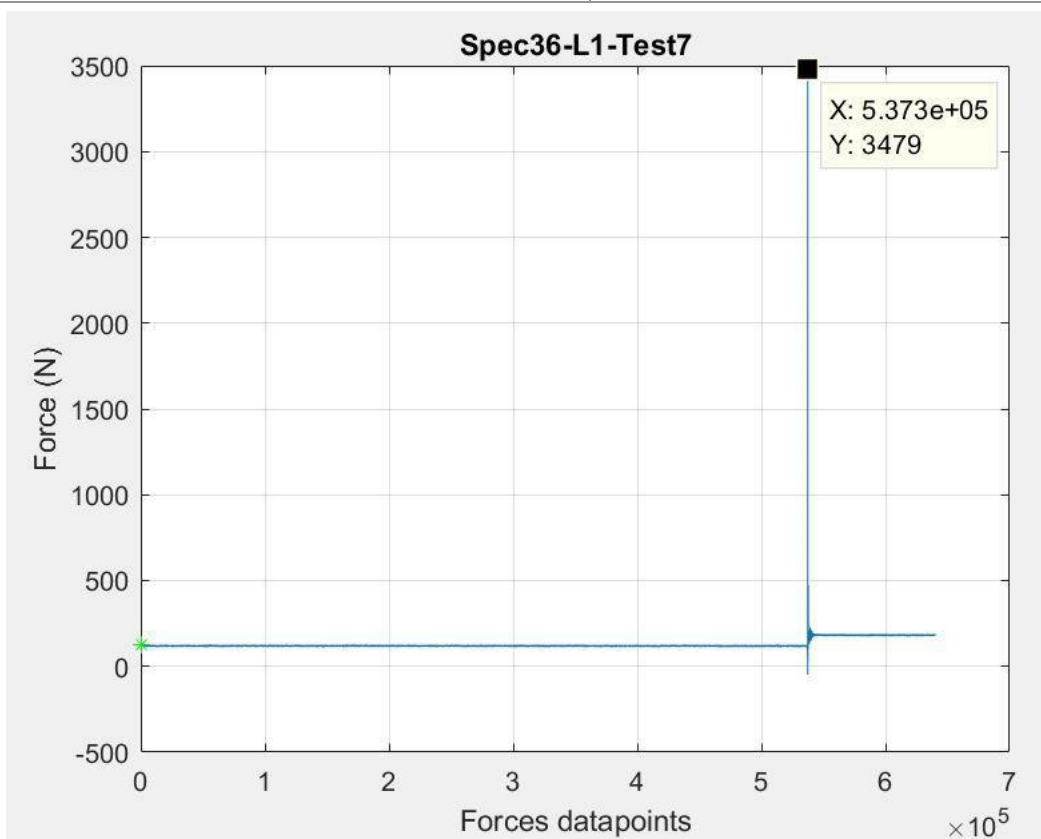


Figure 8-30 - a, b, and c represent a complete burst fracture of L1 and spinous process, the x-ray image confirming this fracture and showing a split of the vertebra body and a force of about 400 N that led to this fracture respectively.

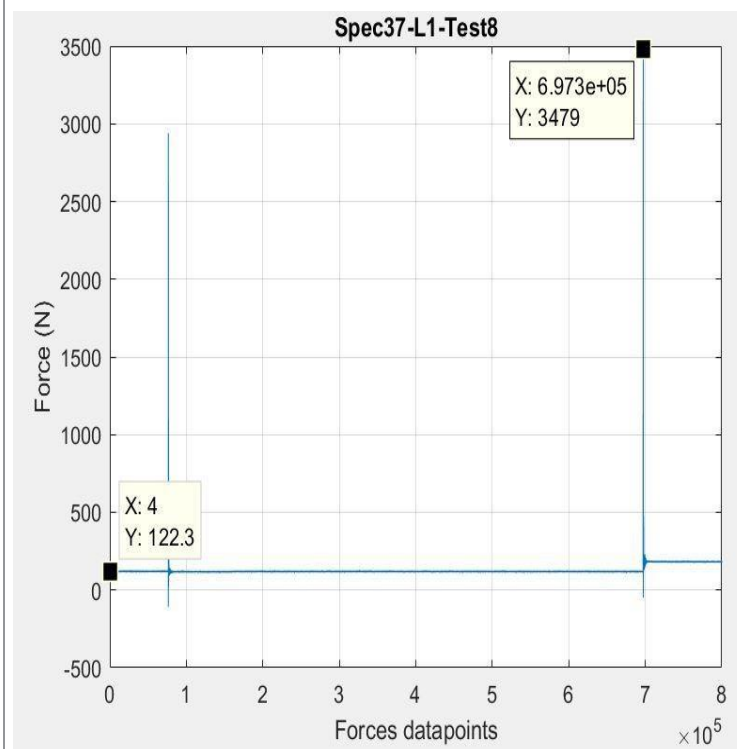
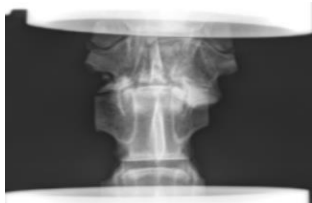


Figure 8-31 - a and b represent the burst fracture of L1 initiated at its upper endplate and split through the spinous process and the vertebra body, and the force of about 400 N to create the burst fracture.

Figures of group T12-L2



a



b

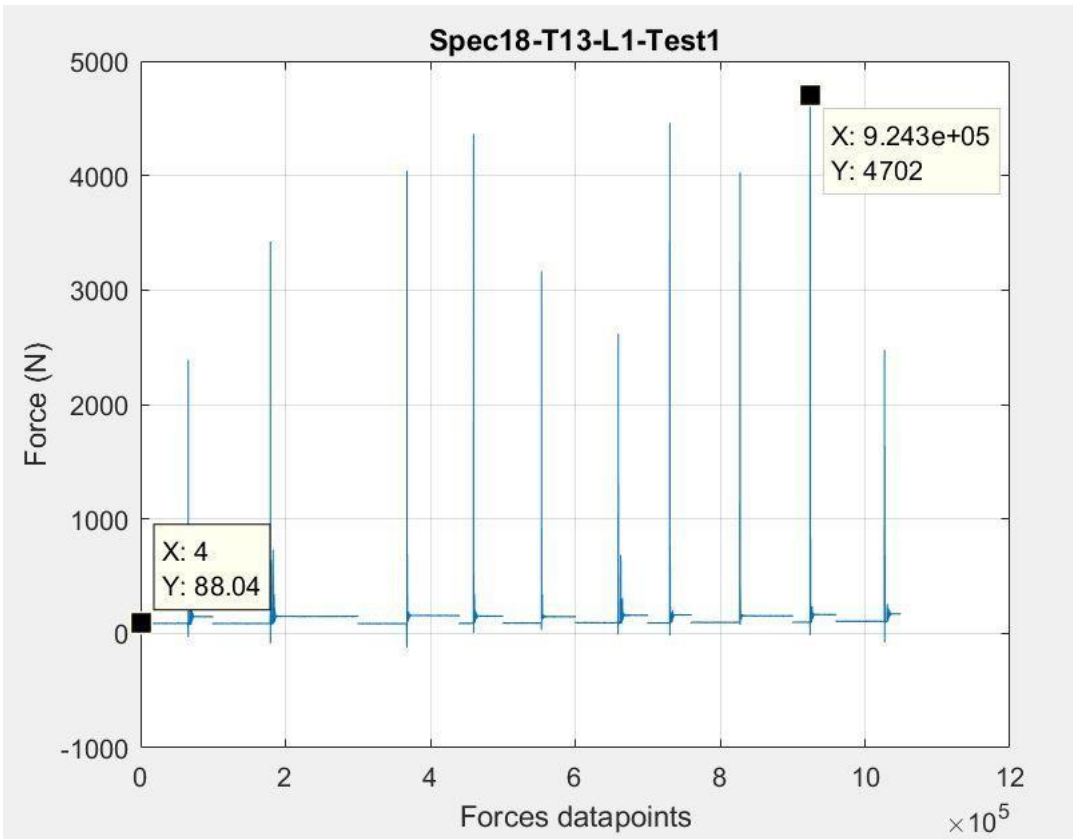


Figure 8-32 - image a represent the fracture of T13 with a split in the lateral view, the AP x-ray image in b doesn't seem to show the lateral view fracture and figure c represent the force generated during the fracture of vertebra.



a



b

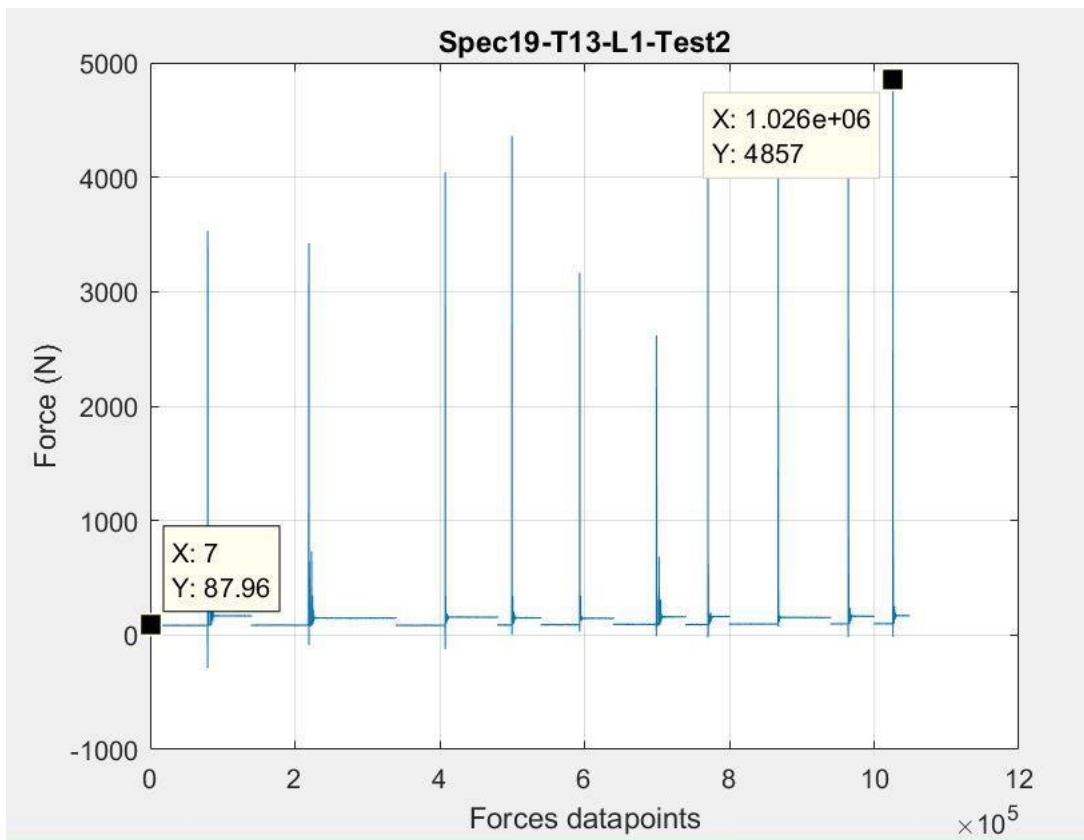


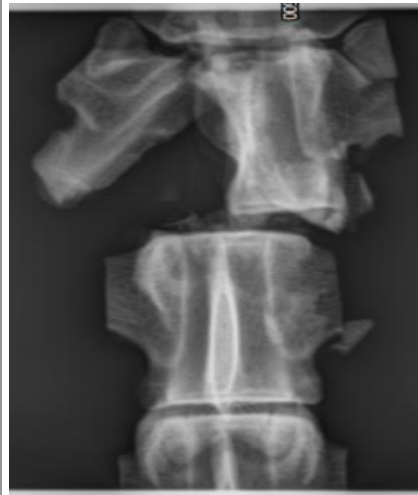
Figure 8-33 - a, b, and c represent the burst fracture of T13, its x-ray image and the force generated to create the fracture respectively. the AP of the x-ray does not appear to show the fracture of the vertebra body.



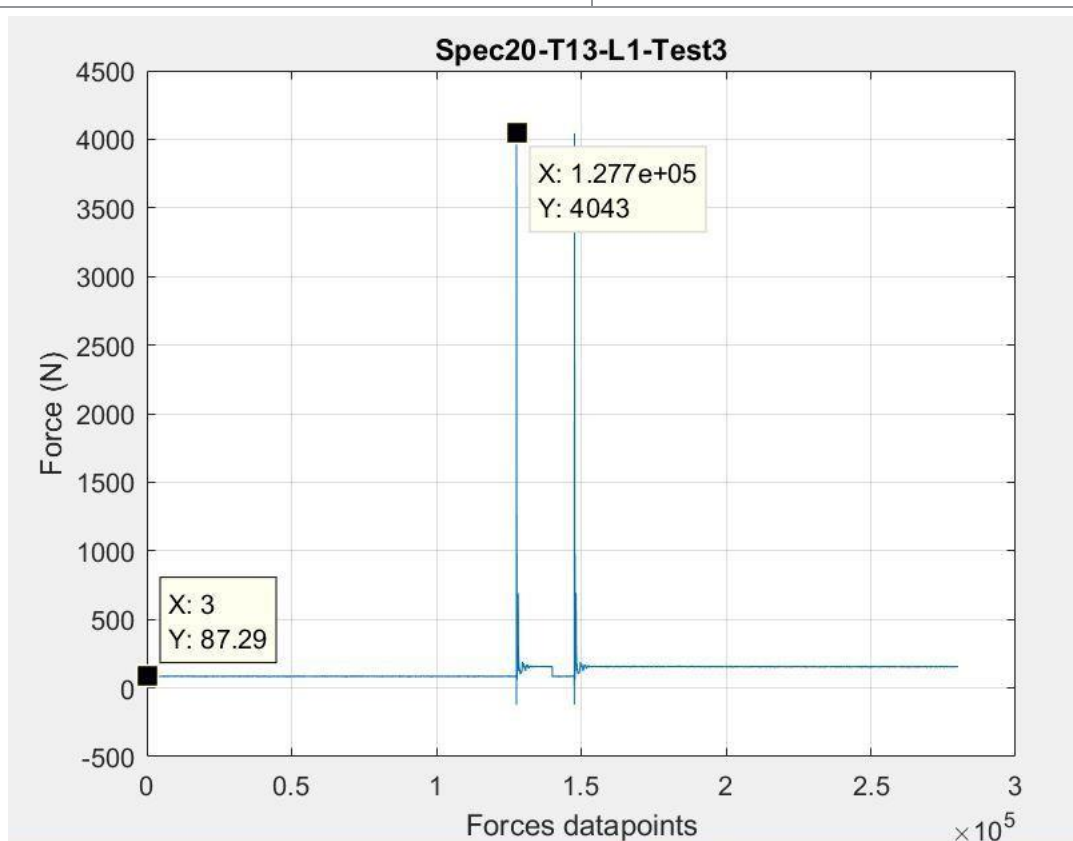
1



a



b



---

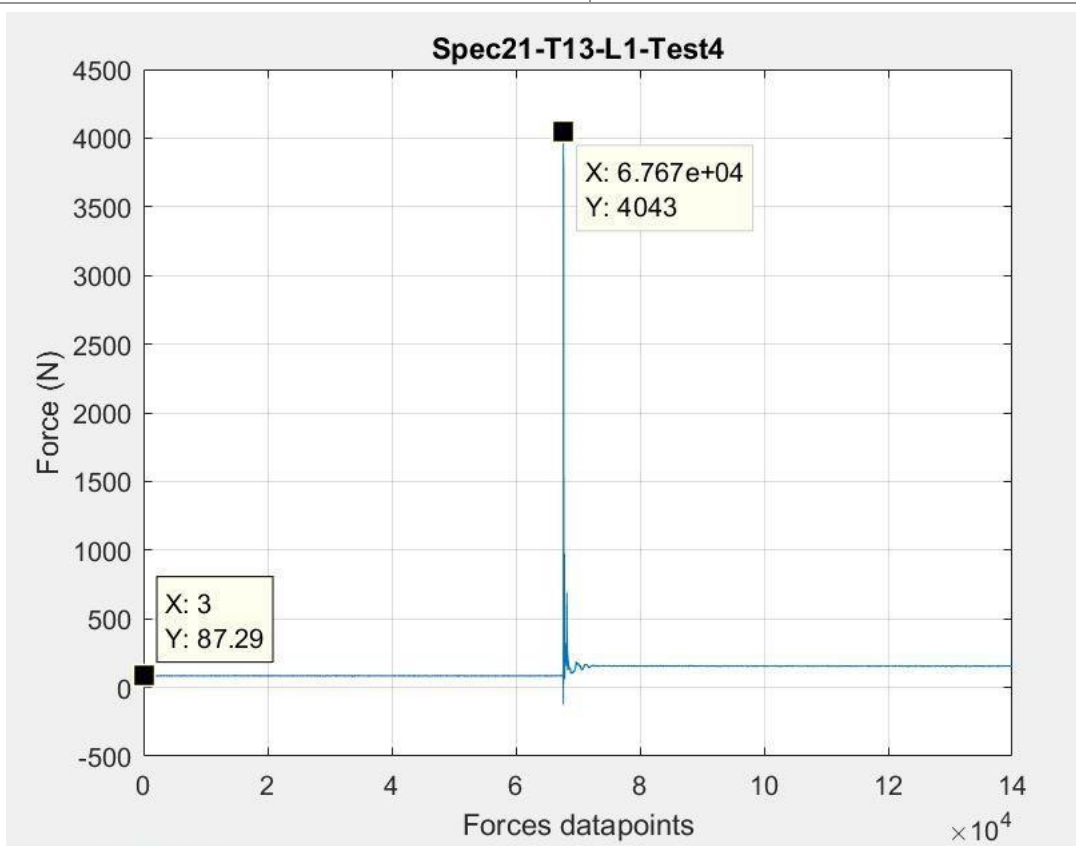
Figure 8-34 - a, b, and c represent a complete burst fracture of the vertebral body and spinous process, x-ray image that agrees with the fracture picture and the force of about 3956 N generated to create this fracture respectively.



a



a







a



b

Figure 8-35 - in this figure, a, b, and c represent respectively the fracture of the vertebra body and spinous process at T13, x-ray image confirming this fracture and the force of about 3956 N that created the fracture.

Figure 8-36 - a, b, and c represent respectively the burst fracture of T13 initiated at its lower endplate, it's x-ray image and a force of just less than 2621 N that created the burst fracture.



a



b

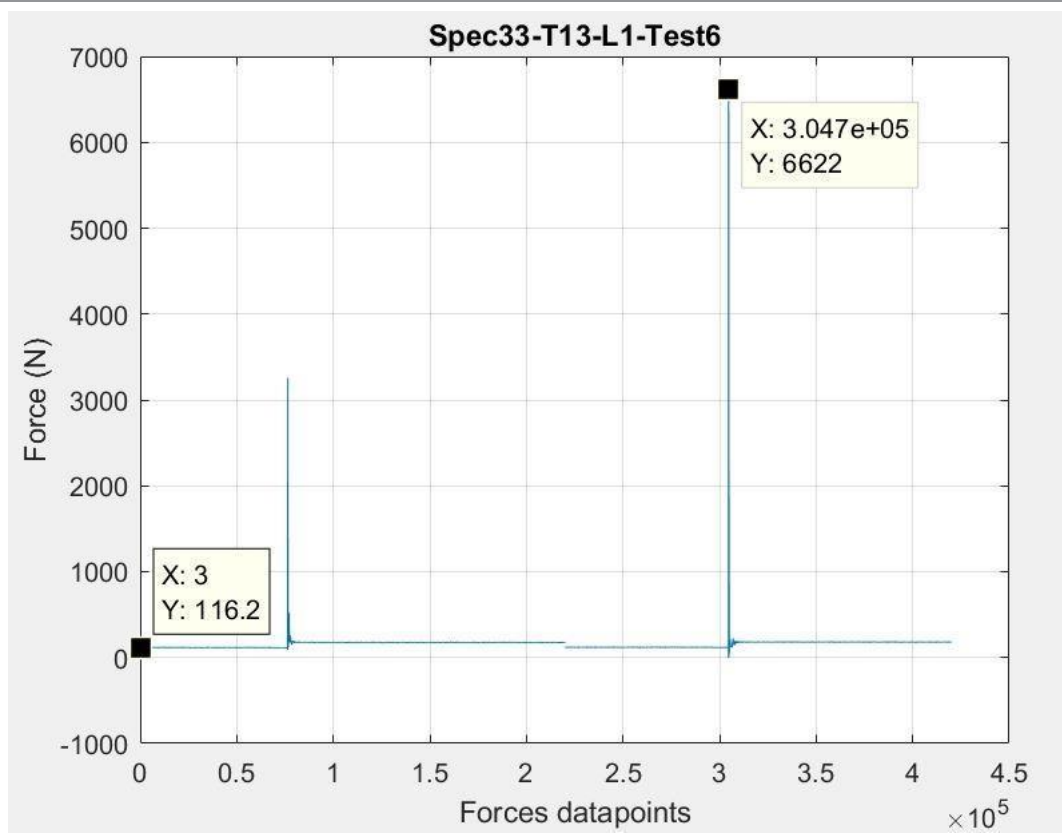


Figure 8-37 - a, b, and c indicate the burst fracture of T13 and herniation of T13-L1, x-ray image of the fracture and a force of around 6506 N respectively.



|





a



b

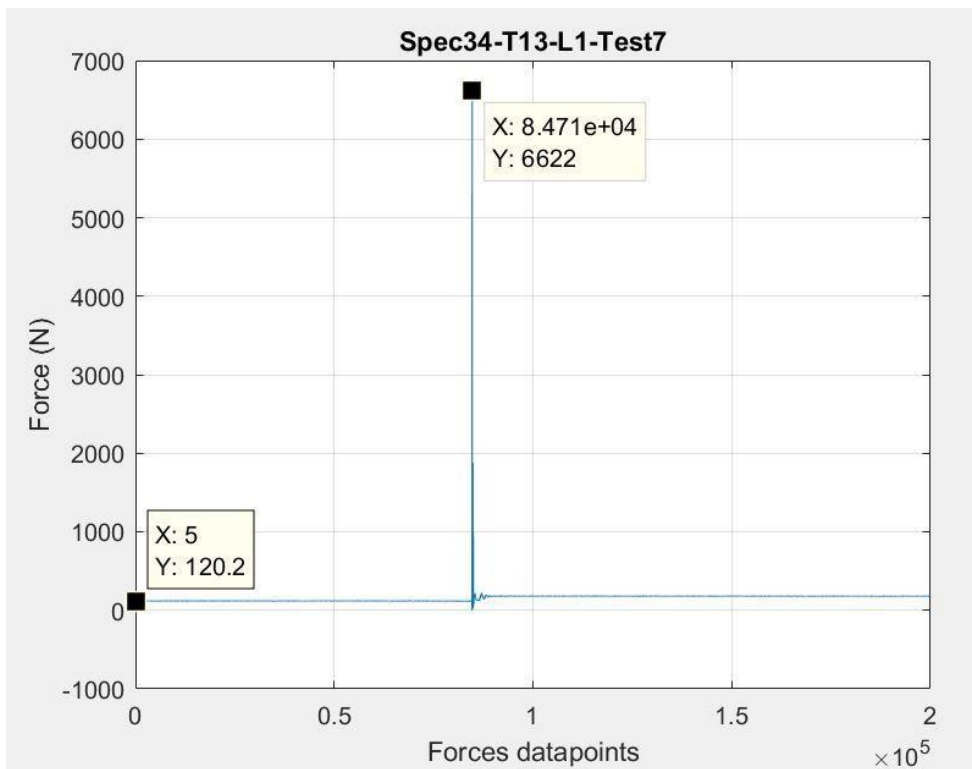


Figure 8-38 - Image a represent the burst fracture of L1 confirmed by the x-ray image b. the force of around 6502 N in graph c generated the burst fracture.



a



b

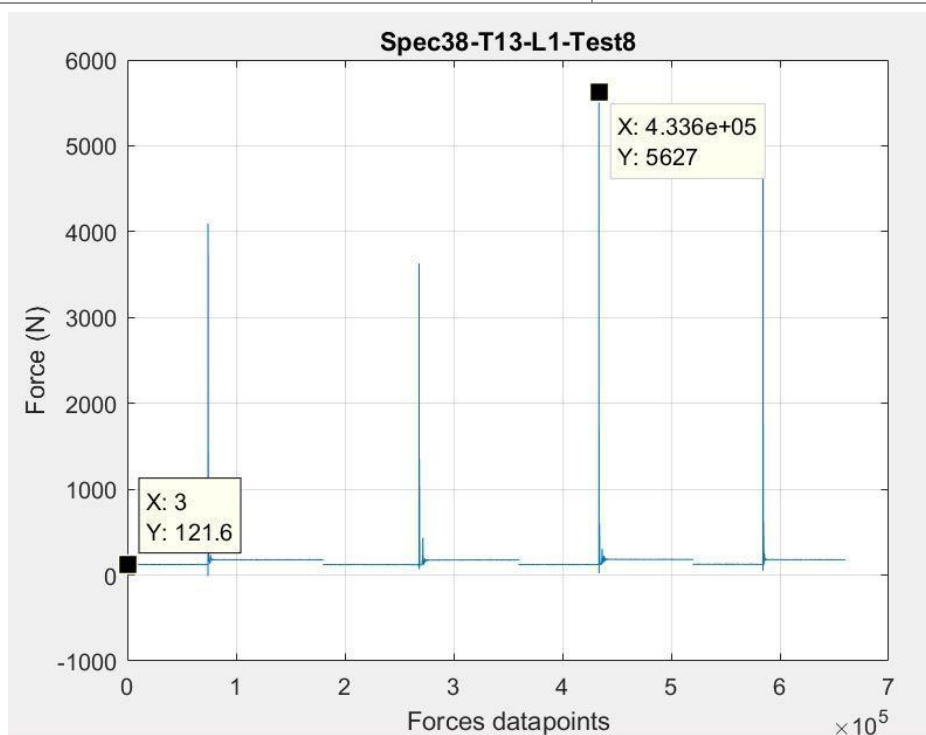
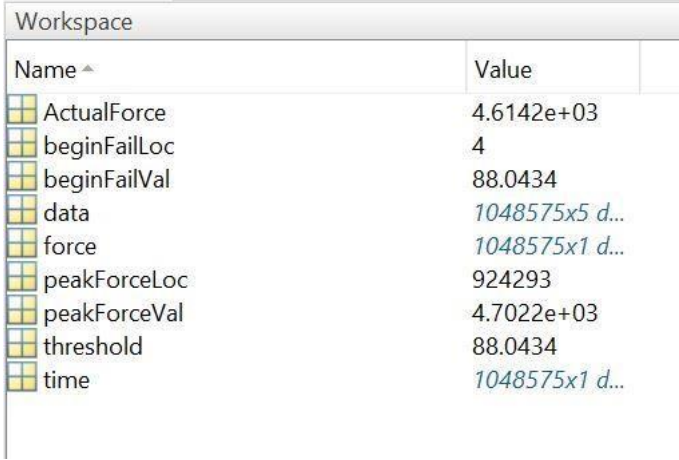


Figure 8-39 - burst fracture of L1 represented by a, b represents the x-ray image of the fracture and c represent the force of around 5506 N that created the fracture.

---

---

## Appendix D



The image shows a screenshot of the Matlab workspace window. The window title is 'Workspace'. It contains a table with two columns: 'Name' and 'Value'. The variables listed are ActualForce, beginFailLoc, beginFailVal, data, force, peakForceLoc, peakForceVal, threshold, and time. The values are: ActualForce (4.6142e+03), beginFailLoc (4), beginFailVal (88.0434), data (1048575x5 d...), force (1048575x1 d...), peakForceLoc (924293), peakForceVal (4.7022e+03), threshold (88.0434), and time (1048575x1 d...).

Name ^	Value
ActualForce	4.6142e+03
beginFailLoc	4
beginFailVal	88.0434
data	1048575x5 d...
force	1048575x1 d...
peakForceLoc	924293
peakForceVal	4.7022e+03
threshold	88.0434
time	1048575x1 d...

**Figure 8-40** Image of Matlab workspace indicating the maximum force, the force when the specimens started to fail, the threshold and the actual forces that created the fractures

